

AD_____

Award Number: W81XWH-07-1-0002

TITLE: Profiling Jet Fuel on Neurotoxic Components with Comprehensive Two-Dimensional GC

PRINCIPAL INVESTIGATOR: Henk C. Trap

CONTRACTING ORGANIZATION: TNO Defence, Safety and Security
Rijswijk, The Netherlands

REPORT DATE: November 2007

TYPE OF REPORT: Final

PREPARED FOR: U.S. Army Medical Research and Materiel Command
Fort Detrick, Maryland 21702-5012

DISTRIBUTION STATEMENT: Approved for Public Release;
Distribution Unlimited

The views, opinions and/or findings contained in this report are those of the author(s) and should not be construed as an official Department of the Army position, policy or decision unless so designated by other documentation.

REPORT DOCUMENTATION PAGE

*Form Approved
OMB No. 0704-0188*

Public reporting burden for this collection of information is estimated to average 1 hour per response, including the time for reviewing instructions, searching existing data sources, gathering and maintaining the data needed, and completing and reviewing this collection of information. Send comments regarding this burden estimate or any other aspect of this collection of information, including suggestions for reducing this burden to Department of Defense, Washington Headquarters Services, Directorate for Information Operations and Reports (0704-0188), 1215 Jefferson Davis Highway, Suite 1204, Arlington, VA 22202-4302. Respondents should be aware that notwithstanding any other provision of law, no person shall be subject to any penalty for failing to comply with a collection of information if it does not display a currently valid OMB control number. **PLEASE DO NOT RETURN YOUR FORM TO THE ABOVE ADDRESS.**

1. REPORT DATE (DD-MM-YYYY) 01-11-2007			2. REPORT TYPE Final		3. DATES COVERED (From - To) 10 OCT 2006 - 9 OCT 2007	
4. TITLE AND SUBTITLE Profiling Jet Fuel on Neurotoxic Components with Comprehensive Two-Dimensional GC			5a. CONTRACT NUMBER			
			5b. GRANT NUMBER W81XWH-07-1-0002			
			5c. PROGRAM ELEMENT NUMBER			
6. AUTHOR(S) Henk C. Trap E-Mail: henk.trap@tno.nl			5d. PROJECT NUMBER			
			5e. TASK NUMBER			
			5f. WORK UNIT NUMBER			
7. PERFORMING ORGANIZATION NAME(S) AND ADDRESS(ES) TNO Defence, Safety and Security Rijswijk, The Netherlands			8. PERFORMING ORGANIZATION REPORT NUMBER			
9. SPONSORING / MONITORING AGENCY NAME(S) AND ADDRESS(ES) U.S. Army Medical Research and Materiel Command Fort Detrick, Maryland 21702-5012			10. SPONSOR/MONITOR'S ACRONYM(S)			
			11. SPONSOR/MONITOR'S REPORT NUMBER(S)			
12. DISTRIBUTION / AVAILABILITY STATEMENT Approved for Public Release; Distribution Unlimited						
13. SUPPLEMENTARY NOTES						
14. ABSTRACT Exposure to jet-propulsion fuel 8 (JP-8) is probably the most occurring chemical exposure within the military. The discussion on the possible adverse health effects of such an exposure is ongoing. Methodology is needed to identify and quantify low concentrations of potentially toxic components in the complex JP-8 matrix. Comprehensive GC (GCxGC), in which continuous two-dimensional separation occurs, was shown to be highly suitable for this purpose. =In combination with time-of-flight mass-spectrometry up to 3,500 components in JP-8 could be chromatographically resolved, in most cases identified and (semi-)quantified. Differences in composition between JP-8 from various sources and with various ages were demonstrated. This technology was used to establish the evaporation profiles at -10 and 20 °C of 20 components that are considered to be potentially neurotoxic. Rough estimates of the external exposures of personnel were made from these evaporation profiles as well as preliminary toxicological evaluations.						
15. SUBJECT TERMS Jet fuel, JP-8, profiling, Comprehensive Gas chromatography, GC, *GC-ToF-MS, evaporation profiles, neurotoxicity, Toxic Load						
16. SECURITY CLASSIFICATION OF:			17. LIMITATION OF ABSTRACT UU	18. NUMBER OF PAGES 85	19a. NAME OF RESPONSIBLE PERSON USAMRMC	
a. REPORT U	b. ABSTRACT U	c. THIS PAGE U			19b. TELEPHONE NUMBER (include area code)	

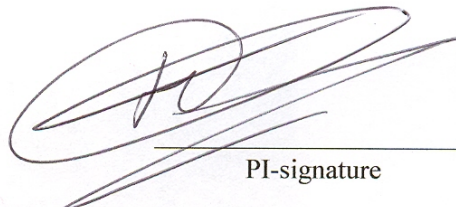
FOREWORD

Opinions, interpretations, conclusions and recommendations are those of the authors and are not necessarily endorsed by the US Army.

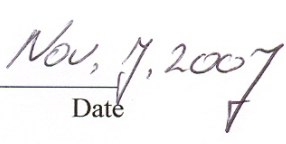
_____ Where copyrighted material is quoted, permission has been obtained to use such material.

_____ Where material from documents designated for limited distribution is quoted, permission has been obtained to use the material.

_____ Citations of commercial organizations and trade names in this report do not constitute an official Department of Army endorsement or approval of the products or services of these organizations.



PI-signature



Nov. 7, 2007

Date

ACKNOWLEDGEMENTS

The authors wish to thank Mr. Jeroen van der Meer for the construction of the vapor generation unit and analyzing the fuel and vapor samples. Drs. Marcel J. van der Schans and Daan Noort of TNO Defence, Security and Safety are acknowledged for valuable discussions.

SUMMARY

Jet-propulsion fuel 8 (JP-8) has become the standard fuel for military use in the USA, and is also widely used within NATO. JP-8 is a complex mixture of aromatic and aliphatic hydrocarbons. Due to its wide use of *ca.* 5 billion gallons a year, large numbers of military personnel are exposed either via inhalation of vapors and/or aerosols of JP-8 and/or percutaneously to the liquid fuel itself. Such exposures may occur during various activities, such as refueling of vehicles and aircraft and maintenance thereof.

The discussion on the possible health effects on exposed personnel is still ongoing. It seems likely that among the several thousands of components in JP-8 there will be toxic ones. In particular there is concern about a few hundred components that are suspected of being neurotoxic. Analysis of the concentrations of these compounds in JP-8 as well as in the vapors that originate thereof, is a first step in toxicological evaluation of exposure to JP-8.

Since jet fuels are specified on the basis of performance instead of composition, there may be significant differences in the contents of the individual components between jet fuels from various sources and batches. Furthermore, the composition may alter due to aging of the fuel.

Obviously, an analytical procedure is needed that is able to identify and quantify low concentrations of components in the highly complex jet fuel matrix.

In this study, the potential of comprehensive GC (GCxGC) for profiling JP-8 was investigated. Comprehensive GC is a relatively new chromatographic methodology in which a continuous two-dimensional separation takes place. This creates a unique resolving power and also increases the sensitivity of the analysis. The columns for first and second dimension chromatography were optimized with respect to resolution between the numerous components in JP-8. In combination with time-of-flight mass-spectrometry up to 3,500 components in JP-8 could be chromatographically resolved, in most cases identified and (semi-)quantified. Differences in composition between JP-8 from various sources and with various ages were demonstrated.

GCxGC was also used to establish the evaporation profiles at -10 and 20 °C of 20 selected components that are considered to be potentially neurotoxic. The evaporation profiles differ considerably for the two temperatures as was expected. Also differences in the evaporation profiles of JP-8 samples obtained from various sources were noted. Based on these results, rough estimates of the external exposures of personnel were made from these evaporation profiles as well as preliminary toxicological evaluations. So far it is unclear whether the observed differences in composition of jet fuels from various sources at various ages and in the evaporation profiles will have toxicological implications.

TABLE OF CONTENTS

	page
FOREWORD	4
ACKNOWLEDGEMENTS	5
SUMMARY	6
TABLE OF CONTENTS	7
LIST OF FIGURES	8
LIST OF TABLES	12
I. INTRODUCTION	13
II. EXPERIMENTAL PROCEDURES	19
II.1 Materials	19
II.2 Gas chromatographic configurations	19
II.3 JP-8 vapor generation experiments	24
II.4 Calibration and Quantification	24
III. RESULTS AND DISCUSSION	26
III.1 Chromatographic optimization	26
III.2 Categorization/classification of components in the 2D chromatograms	28
III.3 Concentration of neurotoxic components in Jet Fuel (JP-8) samples	32
III.4 On-line and Off-line JP-8 vapor analysis	34
III.5 Evaporating profile of the JP-8 samples	36
III.6 Toxic load estimate of the JP-8 samples	39
III.7 Suggestions for further research	41
IV. CONCLUSIONS	43
REFERENCES	44
ANNEX A: Statement of work for Cooperative Agreement W81XWH-07-1-0002	48
ANNEX B: Analytical reference standards	49
ANNEX C: 3D Plots of Jet Fuel analysis	50
ANNEX D: Evaporation profile of the KC135 JP-8 sample	52
ANNEX E: 2D Plot of the KC135 JP-8 sample	53
ANNEX F: Vapor concentration time courses of the neurotoxic components in JP-8 vapor at -10 °C.	54
ANNEX G: Vapor concentration time courses of the neurotoxic components in JP-8 vapor at +20 °C.	67
ANNEX H: Vapor concentration time courses at -10 °C, graphical representations.	69
ANNEX I: Vapor concentration time courses at +20 °C, graphical representations.	77
ANNEX J: Acronyms and abbreviations	85

LIST OF FIGURES

	Page
Figure 1; Schematic representation of the GCxGC system.	15
Figure 2; Schematic representation of the chromatographic process.	15
Figure 3; Schematic representation of a modulated chromatographic analysis of two not perfectly separated peaks.	16
Figure 4; Schematic representation of the process of transposing separate modulated analysis to a 2nd dimension data array.	17
Figure 5; Schematic representation of the 2D and 3D viewing options of modulated chromatograms.	18
Figure 6; Photograph of the inside of the GC (1), showing GCxGC components and connections.	20
Figure 7; An example of the possibilities of the deconvolution software.	21
Figure 8; Schematic representation of the configuration used for the vapor analysis.	22
Figure 9; Photograph of the inside of the GC (2), with on the right the 6-port valve.	23
Figure 10, Schematic representation of the off-line sampling configuration.	24
Figure 11, Optimized 2D gas chromatographic separation of jet fuel using a medium non-polar first dimension column and a polar second dimension column.	26
Figure 12; 3D Plot of the TIC of an optimized chromatographic separation of jet fuel using medium non-polar first dimension column and a polar second dimension column.	27
Figure 13; 2D gas chromatographic separation of jet fuel using a reversed column combination a polar first dimension column and a non-polar second dimension column.	28
Figure 14; Schematic representation of the various classes of components in the Dutch Jet Fuel sample no III.	29
Figure 15; Schematic representation of the various classes of components in the US KC135 Jet Fuel sample I	29
Figure 16; A 2D gas chromatographic separation of JP-8 sample I (KC135) where the masses 71, 85 and 99 are selected which are representative for the alkanes..	30
Figure 17; A 2D gas chromatographic separation of JP-8 sample I (KC135) where the masses 78 and 91 are selected which are representative for the aromatics.	31
Figure 18; On the left a modulated chromatogram of sample I using mass 83 and on the right the 2D plot of the same analysis.	32
Figure 19; The modulated chromatogram of the first vapor sample taken at 5 min after start of the evaporation of jet fuel sample I, the KC135 JP-8, at -10 °C.	34
Figure 20; The modulated chromatogram of the vapor at 80 hr after start of the evaporation of the jet fuel sample I, the KC135 JP-8, at -10 °C.	35

Figure 21; 3D plot of the modulated chromatogram (masses 78+91) of a vapor sample taken at 80 hr after start of the evaporation of the jet fuel sample I, the KC135 JP-8, at -10 °C.	35
Figure 22; Concentration time course of Benzene vapor during evaporation of JP-8 sample I (KC135 JP-8), at -10 °C.	37
Figure 23; Concentration time courses of Benzene vapor during evaporation of JP-8 samples I to IV at -10 °C.	37
Figure 24; 3D Plot of the TIC of a chromatographic separation of JP-8 using a reversed column combination.	50
Figure 25; 3D plot of the summed masses 71, 85 and 99 (representatives for alkanes) of a sample I (KC135 JP-8).	50
Figure 26; 3D plot (mass 83) of the vapor analysis, sample taken at 80 hr after start of the evaporation of the jet fuel sample I, the KC135 JP-8, at -10 °C.	51
Figure 27; Modulated chromatograms of vapor samples of the KC135 JP-8 sample(I).	52
Figure 28; A 2D plot of the vapor analysis, sample taken at 80 hr after start of the evaporation of the jet fuel sample I, the KC135 JP-8, at -10 °C.	53
Figure 29; Concentration time courses of benzene vapor during evaporation of JP-8 samples I to IV at -10 °C.	69
Figure 30; Concentration time courses of heptane vapor during evaporation of JP-8 samples I to IV at -10 °C.	69
Figure 31; Concentration time courses of toluene vapor during evaporation of JP-8 samples I to IV at -10 °C.	70
Figure 32; Concentration time courses of octane vapor during evaporation of JP-8 samples I to IV at -10 °C.	70
Figure 33; Concentration time courses of cycloheptane vapor during evaporation of JP-8 samples I to IV at -10 °C.	71
Figure 34; Concentration time courses of isopropylcyclopentane vapor during evaporation of JP-8 samples I to IV at -10 °C.	71
Figure 35; Concentration time courses of ethylbenzene vapor during evaporation of JP-8 samples I to IV at -10 °C.	72
Figure 36; The summed concentration time courses of p- and m-xylene vapor during evaporation of JP-8 samples I to IV at -10 °C.	72
Figure 37; Concentration time courses of o-xylene vapor during evaporation of JP-8 samples I to IV at -10 °C.	73
Figure 38; Concentration time courses of isopropylcyclohexane vapor during evaporation of JP-8 samples I to IV at -10 °C.	73
Figure 39; Concentration time courses of isopropylbenzene vapor during evaporation of JP-8 samples I to IV at -10 °C.	74

Figure 40; Concentration time courses of 2-ethyltoluene vapor during evaporation of JP-8 samples I to IV at -10 °C.	74
Figure 41; Concentration time courses of 1,2,3-trimethylbenzene vapor during evaporation of JP-8 samples I to IV at -10 °C.	75
Figure 42; Concentration time courses of 1,2-diethylbenzene vapor during evaporation of JP-8 samples I to IV at -10 °C.	75
Figure 43; Concentration time courses of naphthalene vapor during evaporation of JP-8 samples I to IV at -10 °C.	76
Figure 44; Concentration time courses of cyclohexane vapor during evaporation of JP-8 samples I and II at +20 °C.	77
Figure 45; Concentration time courses of benzene vapor during evaporation of JP-8 samples I and II at +20 °C.	77
Figure 46; Concentration time courses of heptane vapor during evaporation of JP-8 samples I and II at +20 °C.	78
Figure 47; Concentration time courses of toluene vapor during evaporation of JP-8 samples I and II at +20 °C.	78
Figure 48; Concentration time courses of octane vapor during evaporation of JP-8 samples I and II at +20 °C.	79
Figure 49; Concentration time courses of cycloheptane vapor during evaporation of JP-8 samples I and II at +20 °C.	79
Figure 50; Concentration time courses of isopropylcyclopentane vapor during evaporation of JP-8 samples I and II at +20 °C.	80
Figure 51; Concentration time courses of ethylbenzene vapor during evaporation of JP-8 samples I and II at +20 °C.	80
Figure 52; The summed concentration time courses of p- and m-xylene vapor during evaporation of JP-8 samples I and II at +20 °C.	81
Figure 53; Concentration time courses of o-xylene vapor during evaporation of JP-8 samples I and II at +20 °C.	81
Figure 54; Concentration time courses of isopropylcyclohexane vapor during evaporation of JP-8 samples I and II at +20 °C.	82
Figure 55; Concentration time courses of isopropylbenzene vapor during evaporation of JP-8 samples I and II at +20 °C.	82
Figure 56; Concentration time courses of 2-ethyltoluene vapor during evaporation of JP-8 samples I and II at +20 °C.	83
Figure 57; Concentration time courses of 1,2,3-trimethylbenzene vapor during evaporation of JP-8 samples I and II at +20 °C.	83
Figure 58; Concentration time courses of 1,2-diethylbenzene vapor during evaporation of JP-8 samples I and II at +20 °C.	84

Figure 59; Concentration time courses of naphthalene vapor during evaporation of JP-8 samples I and II at
+20 °C.

LIST OF TABLES

	Page	
Table 1;	Suspected neurotoxic components, selected for this study	19
Table 2;	Indication of the presence of sulfur containing components in two jet fuel samples.	30
Table 3;	Jet Fuel composition with respect to selected neurotoxic components	33
Table 4;	Calculated external exposure	40
Table 5;	Content of the Gasoline refinery standard ASTM/EPA	50
Table 6;	Content of the naphtene mixture ASTM-P-0034	50
Table 7;	Concentration time course of 9 neurotoxic components in JP-8 vapor at -10 °C,(Ia).	55
Table 8;	Concentration time course of 9 neurotoxic components in JP-8 vapor at -10 °C,(Ib).	56
Table 9;	Concentration time course of 8 neurotoxic components in JP-8 vapor at -10 °C,(Ia).	57
Table 10;	Concentration time course of 8 neurotoxic components in JP-8 vapor at -10 °C,(Ib).	58
Table 11;	Concentration time course of 9 neurotoxic components in JP-8 vapor at -10 °C,(IIa).	59
Table 12;	Concentration time course of 9 neurotoxic components in JP-8 vapor at -10 °C,(IIb).	60
Table 13;	Concentration time course of 8 neurotoxic components in JP-8 vapor at -10 °C,(IIa).	61
Table 14;	Concentration time course of 8 neurotoxic components in JP-8 vapor at -10 °C,(IIb).	62
Table 15;	Concentration time course of 9 neurotoxic components in JP-8 vapor at -10 °C,(IIIa).	63
Table 16;	Concentration time course of 8 neurotoxic components in JP-8 vapor at -10 °C,(IIIb).	64
Table 17;	Concentration time course of 9 neurotoxic components in JP-8 vapor at -10 °C,(IVa).	65
Table 18;	Concentration time course of 9 neurotoxic components in JP-8 vapor at -10 °C,(IVb).	66
Table 19;	Concentration time course of 8 neurotoxic components in JP-8 vapor at -10 °C,(IV).	67
Table 20;	Concentration time course of 9 neurotoxic components in JP-8 vapor at +20 °C,(I).	68
Table 21;	Concentration time course of 8 neurotoxic components in JP-8 vapor at +20 °C,(I).	68
Table 22;	Concentration time course of 9 neurotoxic components in JP-8 vapor at +20 °C,(II).	69
Table 23;	Concentration time course of 8 neurotoxic components in JP-8 vapor at +20 °C,(II).	69

I. INTRODUCTION

Jet-propulsion fuel 8 (JP-8) has become the standard fuel for military use in the USA, and is also widely used within NATO. JP-8 is a complex mixture of aromatic and aliphatic hydrocarbons. To this date, approximately 2,500 components have been identified in JP-8. Due to its wide use – *ca.* 5 billion gallons a year – large numbers of military personnel are exposed either via inhalation of vapors and/or aerosols of JP-8 or percutaneously to the liquid itself. Such exposures may occur during various activities, such as refueling of vehicles and aircraft and maintenance thereof.

Meanwhile the discussion on the possible health effects on exposed personnel continues. In the nineteen eighties the U.S. Navy proposed an interim permissible exposure level (PEL) for JP-8 vapor of 350 mg.m⁻³ (8-hr time-weighted average [TWA]), and a 15-min short-term exposure limit (STEL) of 1,800 mg.m⁻³. The Navy requested the National Research Council (NRC) to review the proposed values. The results of this review by the Committee on Toxicology's Subcommittee on Permissible Exposure Levels for Military Fuels were published in 1996 (NRC, 1996). The subcommittee found no reasons to change the PEL-value that was proposed by the Navy, but did suggest a lower STEL value of 1,000 mg.m⁻³, as an interim value, in order to avoid acute toxic effects on the central nervous system (CNS). Furthermore, advice was given to avoid respiratory and dermal exposure to JP-8 aerosols, and to perform some research to improve the ability to perform a health risk assessment for JP-8. According to this subcommittee the major adverse health effect resulting from inhalation of JP-8 vapor is on the CNS.

Some ten years ago, the U.S. Air Force requested the NRC to review the available data on health effects of JP-8. The NRC assigned this task to the Committee on Toxicology (COT), which in its turn appointed a Subcommittee on Jet-Propulsion Fuel 8. The report of this subcommittee was published in 2003 (NRC, 2003). The subcommittee concluded that the interim PEL of 350 mg.min⁻³ as proposed by the U.S. Air Force might be too high to avoid adverse effects on the CNS. However, no suggestions for an alternative PEL value were made because the subcommittee was not tasked to do that, and because additional studies are needed to be able to define a meaningful PEL value. In addition it was suggested to develop separate PEL values for vapors and aerosols of JP-8, since their toxicities are different. Furthermore, the subcommittee stated that the dermal route might contribute substantially to the overall exposure to JP-8, by contact with vapors, aerosols or liquid fuel. Interestingly, the American Conference of Governmental Industrial Hygienists (ACGIH) proposed a Threshold Limit Value (TLV) for kerosene and jet fuels of 200 mg.m⁻³ (ACGIH, 2002). Also, the subcommittee made some recommendations for additional inhalation toxicity studies in laboratory animals with JP-8 vapors, aerosols and mixtures thereof. And finally the U.S. Air Force was advised to minimize dermal exposure to JP-8 by using personal protective measures for personnel who are likely to come into (direct) contact with the jet fuel.

Since the publication of the 2003-NRC report several papers on the possible health effects of JP-8 have been published. Baldwin *et al.* (2007) repeatedly exposed rats to JP-8 aerosols up to 20 days and observed increased DOPAC levels in the hippocampus after 4 weeks of exposure. Behavioral effect were not seen until the 3rd or 4th week of exposure, which stresses the need to perform longitudinal studies. Fechter *et al.* demonstrated that exposure to JP-8 (2007a), and in particular to two of its constituents – toluene and ethylbenzene (2007b) – promotes noise-induced cochlear injury in rats, presumably via oxidative stress. This is an important observation, since the combination of JP-8 exposure and noise is frequently encountered in military activities.

The Neurotoxin Exposure Treatment Research Program (NETRP), which is part of the Military Operational Medicine Research Program (MOMRP) of the U.S. Army Medical Research and Materiel Command (USAMRMC) is aimed at understanding of environmental and military operational factors

potentially involved in neurodegenerative diseases, with particular emphasis on Parkinson's disease. This program also explores mechanisms of injury and identifies potential neuroprotectants and other preventive and treatment strategies. Within the NETRP there is, among others, an interest in the possible neurotoxic effect of exposure to JP-8. As stated above, this jet fuel is a highly complex mixture of numerous compounds. Some of the constituents are either proven or suspect neurotoxic compounds. The health and safety issue of JP-8 exposure is further complicated by the fact that jet fuels are specified on the basis of performance and not on composition. This means that jet fuels from different sources will have different compositions, including the (potentially) neurotoxic components. Furthermore, in order to be able to evaluate the health effects of actual respiratory or percutaneous exposures, insight into the concentration-time profiles of the (potentially) neurotoxic compounds as occurring from evaporating JP-8 is needed.

Obviously, a highly selective analytical methodology is needed to be able to identify the potentially neurotoxic components in JP-8. Furthermore, the methodology needs to be highly sensitive to quantify low levels of the neurotoxic components.

The technique which provides the most information in terms of identification and quantification of solvent mixtures is gas chromatography (GC) in combination with mass spectrometry (MS). Nevertheless, thorough analysis with GC-MS not always reveals all the required information on the composition of the investigated sample, in particular with extremely complex mixtures such as jet fuels.

Comprehensive GC or 'GCxGC', which can be considered as a continuous 2-dimensional chromatographic process, has increased the resolving power of traditional chromatography considerably. In combination with a fast time-of-flight MS (TOF-MS) and powerful data-acquisition systems more flexibility and capabilities to discriminate between classes of compounds in multi-components mixtures and to identify most of the components is obtained.

Our hypothesis is that using an 1D-analysis for the examination of evaporating jet fuels large abundant components will mask compounds which are present in much lower concentrations but are possibly of more toxicological importance. This would lead to an underestimation of the risk resulting from exposure to such a vapor. Using the 2D-analytical technique as proposed, it will be possible to identify and quantify the more relevant components in the complex matrix. The technique can be used to investigate the evaporation time profile of individual components in fuels which subsequently can be used to predicting the toxic load of jet fuels for chosen scenarios.

For a Comprehensive GC analysis a normal length separation column is used for pre-separation of the analytes and a very short very thin (internal diameter) separation column is used for a second dimension separation. Not only the dimensions of the columns are different but also the column phases are different, in this way a complete orthogonal separation is possible (but not always necessary). Both columns are connected to one another with an all glass press-fit connector and housed-in in a so-called modulator, see also Figure 1. This modulator modulates the eluted peaks from the first column into tiny fractions by using a combination of hot and cold jets. Through these jets a flow of heated air (hot) or cooled nitrogen(_{liq}) gas (cold) is directed on the first part of the second dimension column. These jets are switched on and off alternatively in a preset schedule in order to optimize the resolution between components in the mixture.

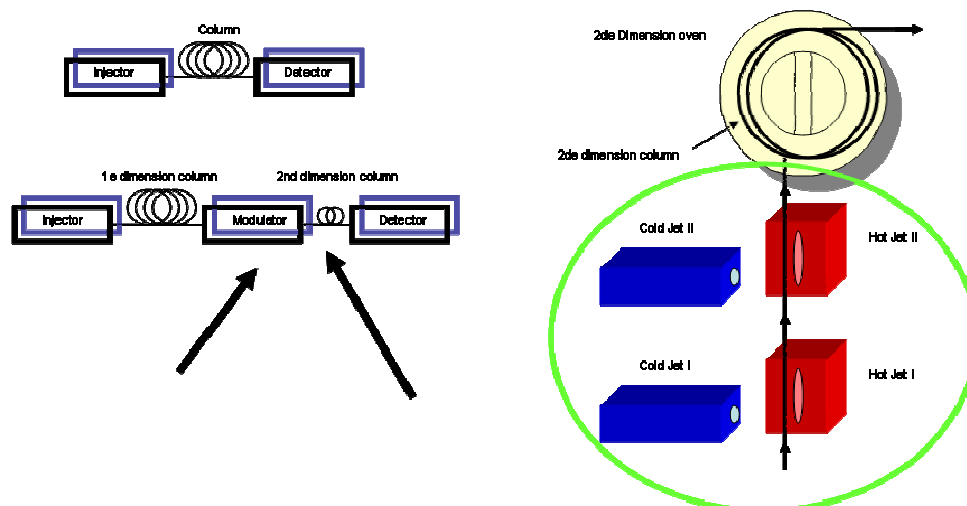


Figure 1. Schematic representation of the GCxGC system. On the left a standard GC configuration is extended with a ‘modulator’ and a 2nd dimension separation column. On the right a schematic representation of the modulator with the four jets and on top a small heated column oven for the 2nd dimension column.

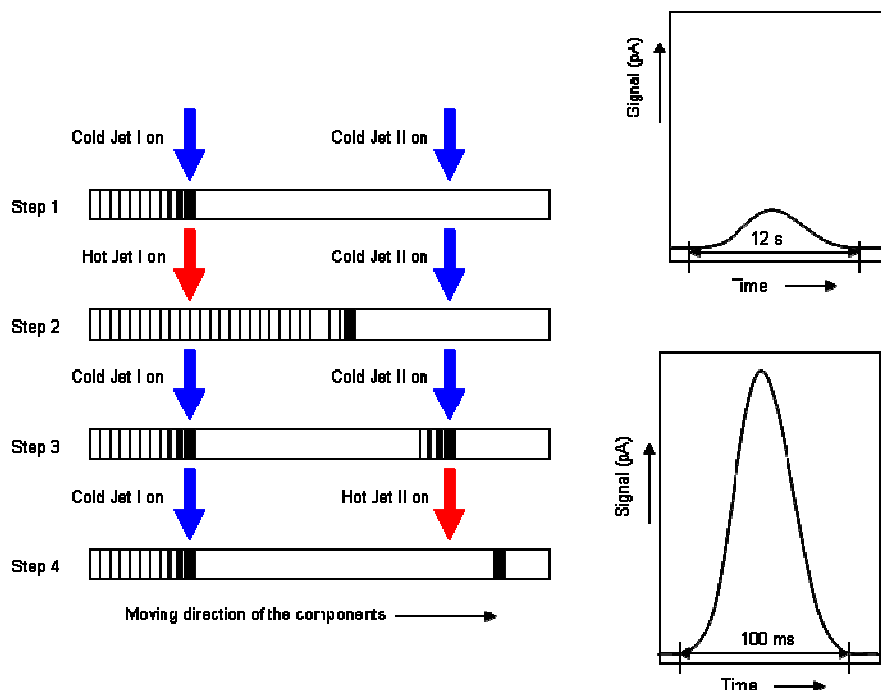


Figure 2. Schematic representation of the chromatographic process (on the left). On the right the effect of modulation on a chromatographic peak, not only is the peak width decreased from, e.g. 12 s to 100 ms, but the signal intensity is also increased.

Switching on the first cold jet freezes the chromatographic process in a small band of the first column at the connecting point (Step 1), see also Figure 2. Firing (or rapidly heating) the hot jet remobilizes (Step 2) the components trapped in this band into the second column. The 2nd cold jet is switched on simultaneously. Components which were not trapped directly during the initial phase are thereby trapped also in this second small band. Switching (Step 3) on this 2nd cold jet in combination with the 1st cold jet will separate the first trapped fraction from the new forming fraction with components eluting from the first column. Also, the remaining co-eluting components in between the two cold jets are added to the

original fraction in a small band. This process prevents initial band broadening by the injection which has a devastating effect on the chromatography (peak tailing) in the second column.

After firing the last hot jet (Step 4), the small band containing the analytes will be injected (remobilized) finally into the second separating column.

The dimensions of the second column are such (for instance length 0.2-1 m, internal diameter 0.05- 0.1 mm and film thickness 0.1-0.2 μm) that the time for this column to complete the analysis, is in the order of seconds (2-12 sec). In standard GC, the analysis time is normally in the range of 1 to 1.5 h for jet fuel samples. The width of the comprehensive chromatographic peaks are in the order of 60-100 ms, compared to 5-15 sec for an analysis on a standard length column with standard dimensions for film thickness and internal diameter. Despite the fact that the components is sliced up in fractions, the (overall) intensity of the resulting peaks increases enormously.

The time from the first stage trapping of the components by switching on the 1st cold jet up to the end of the cycle when it is switched on again is called the modulation time. The components will (have to) elute from the 2nd column within this modulation time period. A phenomenon called ‘wrap around’ will occur if the elution time of the component on the 2nd column exceeds the modulation time. In that case, these components will appear within the subsequent analysis of the next modulation.

Figure 3 points out how GC*GC establishes resolution between two components that are not perfectly separated on the 1st column. After the first separation in the 1st column the eluted peak is sliced up in fractions by the modulator and directed towards the 2nd column for a second separation. In the first trapped fraction only the blue component is present. This will result in a single very narrow peak after the second analysis on the 2nd column. However, in the second trapped fraction not only a large portion of the blue component is present but also some of the red component. After separation on the 2nd column, two very sharp separated peaks representing the blue and the red component will elute. The intensity of these two peaks reflects the concentration of the two components in the analyzed fraction. In the last fraction only the red component is present, resulting in a single peak after the second separation on the 2nd column. Connecting the peak tops of the particular components in the individual analysis reflects the original eluting pattern from the 1st column. The summed peak area of all the individual peaks after the second separation from a component is comparable with the ‘original’ peak area, as if it was eluting only from the 1st column in a single stage separation. No mass is lost in this (GCxGC) process.

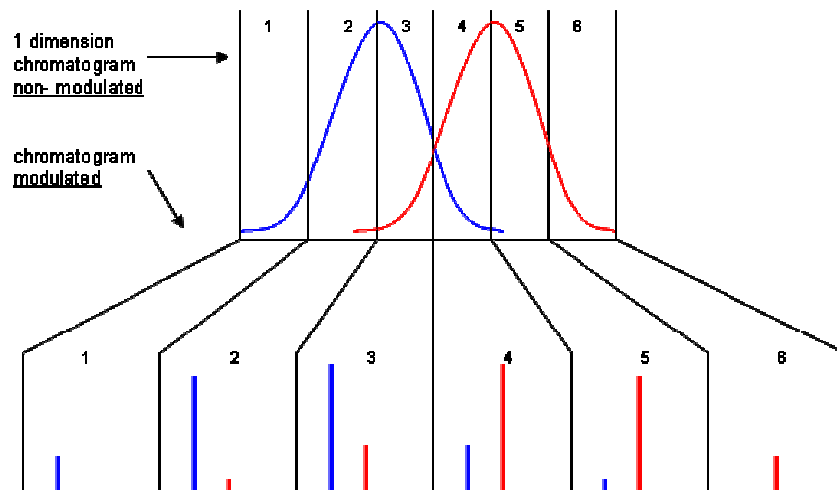


Figure 3. Schematic representation of a modulated chromatographic analysis (below) of two not perfectly separated peaks (top).

The second and important step in the comprehensive GC analysis is data processing. In a standard GC-analysis the data stream is continuous; in GCxGC the data stream is discontinuous due to the modulated process. Every modulation is a separate analysis on its own. Transposing every slice filled with data from a single modulation from a 1D array into a 2D array provides the user with a better view on and understanding of the process, see also Figure 4. In this schematic representation the individual analyses

from the second column are represented by the colors red, light blue, green and dark blue and lined up one after the other. This will also take place for actual GCxGC analysis where a constant data stream from the detector displays the result of the two combined columns. From this data array a fixed number of data points (acquisition frequency times modulation time) has to be taken to require the results from a single 2nd dimension analysis, scanning from the start. Next, this data fraction is used and transposed from a 1st dimension (e.g. horizontal) to a 2nd dimension (e.g. vertical) (row-to-column). In the described example the original horizontal colored bars are individually transposed to lined vertical bars. By doing this, the actual GCxGC process is better visualized as the separation of the two columns is actually based on two different separation principles, e.g. the first column based on boiling point separation versus the second column based on polarity separation.

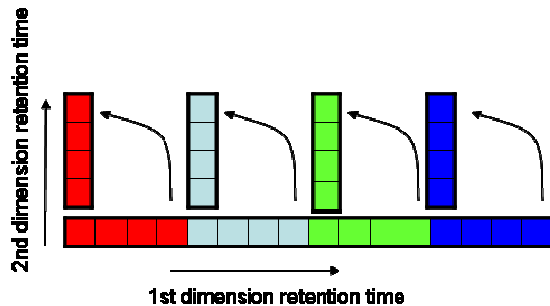


Figure 4. Schematic representation of the process of transposing separate modulated analysis to a 2nd dimension data array.

There are a number of viewing options for 2D chromatographic data, see also Figure 5. In this example three (blue(1), red(2) and green(3)) components were not completely separated which shows as a single peak after the first separation in the 1st column (black signal). After the modulation process and the 2nd dimension column these components were separated from each other. Next the 2D-data is transformed and the 2nd dimension chromatograms are stacked side by side which results in a 2D contour plot by colorization of the signal intensity or even a 3D plot. Also, in this example the elution order in the first dimension is different (blue, red, green) than for the second dimension (red, blue, green). Using different column phases for the two columns could result in this changed elution pattern.

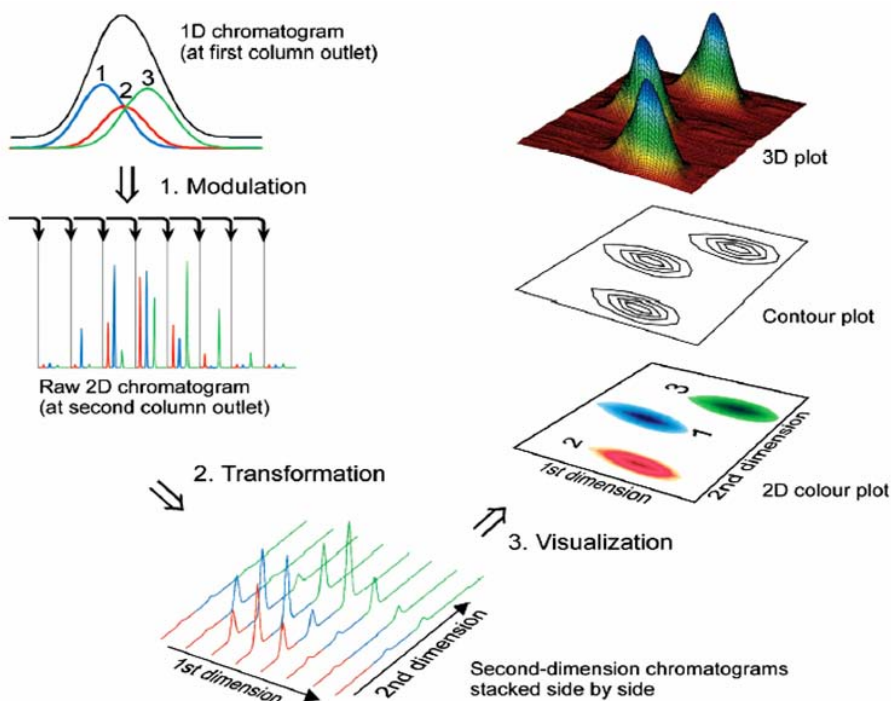


Figure 5. Schematic representation of the 2D and 3D viewing options of modulated chromatograms.

Adding a mass spectrometer (e.g. a Time-of-Flight Mass Spectrometer (ToF-MS)) to such a complex system not only multiplies the capabilities in terms of an increased flexibility and the possibility to identify the individual peaks/components, but makes it also very difficult to represent this additional dimension in the same graph or picture (4D!).

ToF-MS is more suitable for use in combination with GCxGC separation than for instance an Ion Trap or an Quadruple Mass Spectrometer, due to the much higher data acquisition speed of the ToF-MS in comparison with the other MS configurations. Other high speed detectors which can be used in combination with GCxGC are the Flame Ionization Detector (FID), Electron Capture Detector (ECD), Hot Wire Detector (HWD) and Flame Photometric Detector (FPD). A Nitrogen Phosphorus Detector (NPD) seems to be less suitable, due to its intrinsic slower data acquisition.

Apparently, a large number of presumed and suspected neurotoxic components are present in jet fuels such as JP-8. Extracting and analyzing these components from such a complex matrix is demanding due to the large number of interfering components, some present at relatively much higher concentrations, which could jeopardize the analysis. Therefore, multi-dimensional techniques such as GCxGC-ToF-MS seem to be most promising for discriminating small amounts of toxicologically interesting components in the presence of high abundant components in such a heavy matrix [Gregg 2006].

This report describes the study on the capabilities of GCxGC for profiling JP-8 from various sources and with various ages and application of GCxGC-ToF-MS to establishing the evaporation profiles of 20 potentially neurotoxic components in JP-8 at -10 and 20 °C. These evaporation profiles were used in rough toxicological evaluations of these 20 components. The Statement of Work for the study is presented in Annex A.

II. EXPERIMENTAL PROCEDURES

II.1. Materials

Four jet fuel (JP-8) samples were obtained from different sources. Dr. Sue Proctor (USARIEM) and Dr Kristen Weida Smith (Boston University) were helpful in acquiring the two US originating samples:

- I) Offloaded from a reserve tank in the actual wing area from a KC135 Stratotanker airplane,
- II) Drawn from a large storage tank holding JP-8 from the same wing area,
- III) Dutch originating, offloaded from a F16 jetfighter (Woensdrecht, The Netherlands), and
- IV) Dutch (Woensdrecht, The Netherlands) *aged* jet fuel JP-8 stored for more than 3 years in a metal container.

These four samples were used for the profiling and quantification experiments as well as for the screening of the neurotoxic components (see below) during low temperature evaporation. For the short term evaporation experiments at higher temperature only the US originated fuel samples were investigated. Twenty suspected neurotoxic components presumably present in JP-8 were chosen by conferring with USARIEM (Dr. Sue Proctor), see Table 1. These components were obtained commercially, or mixtures of standards were used without further purification. Since four of these compounds could not be detected in the jet fuels that we investigated, we decided to add 1 component to the selection that Dr. Proctor made, i.e. isopropylcyclopentane.

Table 1. Suspected neurotoxic components, selected for this study

Name	CAS Registry	Name	CAS Registry
Benzene	71-43-2	Heptane	142-82-5
Toluene	108-88-3	Octane	111-65-9
Ethylbenzene	100-41-4	Acenaphthene	83-32-9
m-Xylene	108-38-3	Methanol	67-56-1
p-Xylene	106-42-3	1-Butanol	71-36-3
o-Xylene	95-47-6	1,2-propanediol	57-55-6
Isopropylbenzene	98-82-8	Styrene	100-42-5
2-Ethyltoluene	611-14-3	Cyclohexane	110-82-7
1,2,3-trimethylBenzene	526-73-8	Cycloheptane	291-64-5
1,2-diethyl-Benzene	135-01-3	Isopropylcyclopentane [§]	3875-51-2
Naphthalene	91-20-3		

[§] ‘Bonus’ compound: not part of the selection of 20 as made by Dr. Sue Proctor (see above)

From Accustandard (New Haven, CT, USA) several standards were obtained: an ASTM/EPA Gasoline refinery standard which contains 24 different components, with fact sheets and calibration report. This standard contains the mono aromatics. The naphtene mixture (ASTM-P-0034) from Accustandard contains 30 components which covers the cyclopentanes and cyclohexanes, see Annex B. Separate individual standards from Accustandard were used for naphthalene (purity > 99 %) and acenaphthalene (purity > 99 %). Methanol (‘zur Rückstandsanalyse’) and 1-Butanol (purity > 98 %) were procured from Merck (Darmstadt, Germany). 1,2-propanediol (purity > 98 %) was procured from Sigma-Aldrich (Steinheim, Germany) Merck (Darmstadt, Germany). Styrene (purity > 98 %) was purchased from Fluka (Buchs, Switzerland). Dichloromethane (purity > 99.9 %) was procured from Acros Organics (Geel, Belgium). Dichloromethane was used as the solvent for the calibration mixtures.

II.2 Gas chromatographic configurations

Configuration 1: GCxGC-FID

An Agilent (Agilent Technol. Inc., Wilmington, DE, USA) 6890N gas chromatograph was equipped with an FID (Flame Ionization detector) and an ATAS (Veldhoven, The Netherlands) OPTIC 3 injector. This dedicated injector has several injection modes: split, split-less, on-column and direct injection, but also has possibilities for using an expert mode for instance for thermal desorption of samples or loaded packed injector liners. Helium was used as the carrier gas. For the FID hydrogen and pressurized air were used, whereas helium was used as the make-up gas. CO₂ was used as coolant for the Optic injector. A CombiPAL auto sampler (CTC analytics, Zwingen Switzerland) was installed on top of the GC. A LECO (St. Joseph, Mi, USA) GCxGC system was installed inside the GC-oven and connected to the injector as well as the FID, see also Figure 6. A normal length capillary separation column is connected to the injector and connected to a very short and very narrow secondary capillary separation column via an all glass press-fit connector. Via this all glass press-fit connector the secondary column is installed through the modulator box (D, Figure 1) to the secondary column and finally connected to the detector. Two hot jets and two cold jets are mounted close together inside the modulator. These jets are alternating switched on and off to focus the components eluting from the first separating column in a small band and re-inject (mobilize) this injection band onto the second separating column. Both columns are chosen in such a way that the separation principles of the columns are not overlapping. Liquid nitrogen gas was used for the cooling of the cooling jets. An additional flow controller was used to regulate the liquid nitrogen cooling flow used for the cooling jets. Hot air is used for the hot jets.

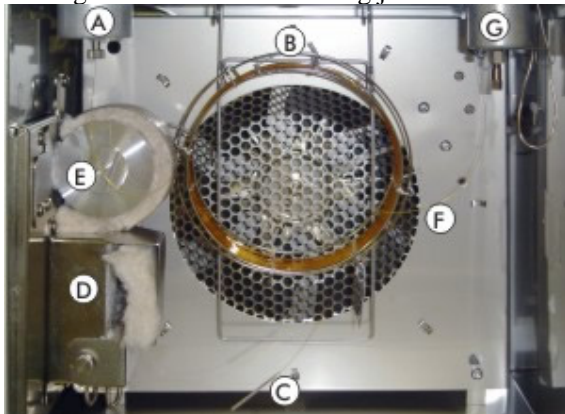


Figure 6. Photograph of the inside of the GC oven, showing GCxGC components and connections: (A) GC inlet, (B) Primary GC column, (C) Press fit connection between primary and secondary GC columns, (D) Quad-jet modulator, (E) Secondary oven, (F) Transfer line, (G) Detector.

Four sets of column combinations were used to optimize the separation of jet fuel samples. See for additional settings such as the oven temperature, injector conditions paragraph III.1.

Column set 1:

In the first dimension a Varian Chrompack (Middelburg, The Netherlands) non polar CP-Sil 8CB column was used (length, 30 m, i.d. 0.25 mm, film thickness, 0.25 µm) and in the second dimension a Varian Chrompack medium polar Vf 17-ms column (length, 2 m, i.d., 0.1 mm, film thickness, 0.2 µm).

Column set 2:

In the first dimension a Varian Chrompack non polar CP-Sil 8CB column (length, 30 m, i.d. 0.25 mm, film thickness, 0.25 µm) was used and in the second dimension an SGE (Victoria, Australia) medium polar BPX-50 column (length, 2 m, i.d., 0.1 mm, film thickness, 0.1 µm).

Column set 3:

In the first dimension a Varian Chrompack (Middelburg, The Netherlands) polar Vf 23-ms column (length, 30 m, i.d. 0.25 mm, film thickness, 0.25 µm) was used and in the second dimension a non polar Varian Chrompack Vf 1-ms column (length, 1.5 m, i.d., 0.1 mm, film thickness, 0.1 µm).

Column set 4:

In the first dimension a Varian Chrompack non polar CP-Sil 8CB column (length, 30 m, i.d. 0.25 mm, film thickness, 0.25 µm) was used and in the second dimension a polar Varian Chrompack CP-Wax 52 CB column (length, 2 m, i.d., 0.1 mm, film thickness, 0.2 µm).

ChromaTOF™ (version 3.22) software from LECO was used for data acquisition and processing the chromatographic data.

Configuration 2: GCxGC-ToF-MS

Using the above described system a LECO Pegasus® 4D HT Time of Flight Mass spectrometer was connected to the system. A short piece of deactivated uncoated fused silica (length *ca* 0.6 m, i.d. 0.1 mm) was connected via all glass press-fit connectors in between the first separating column and the secondary separating column. A second piece of deactivated uncoated fused silica (length *ca* 0.8 m, i.d. 0.1 mm) was connected via an all glass press-fit connector to the end of the secondary separating column and installed via the heated interface directly into the ion source of the mass spectrometer.

The ToF-MS was used in electron impact mode at 70 eV with a scan rate of 100 full spectra/sec (max 500 Hz). This allows accurate scanning of very narrow chromatographic peaks as they elute from the second capillary column. The scan range used was 30-500 amu (later on 40-500 amu)¹ and the detector voltage was set at 1700 V. An acquisition delay of 500 sec (*ca.* 8.3 min) was used for the weight percentage experiments with the different jet fuels to discriminate between high impact of the used solvent (dichloromethane) and the analytes in the fuels.

With the use of the ChromaTOF software it was possible to qualify not perfectly separated peaks by means of deconvolution techniques, see also Figure 7. Each mass trace of the selected scan range is followed and marked when peak maxima of this specific mass are occurring. This in combination with the mass intensity rise and decline of baseline signals could mean that there is a separate component in the mix of signals.

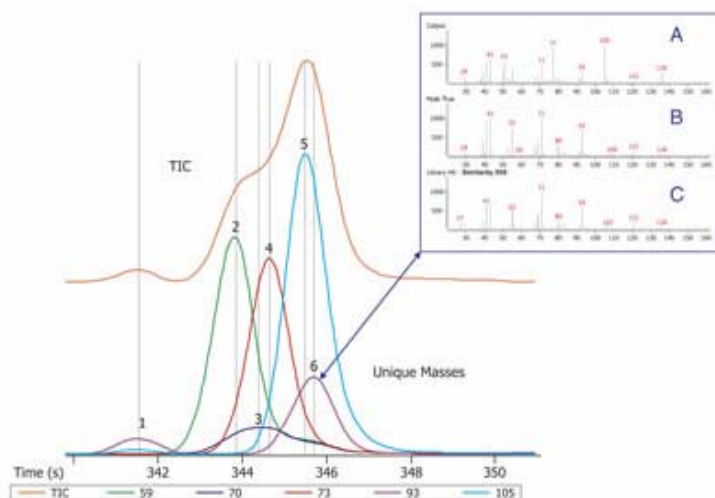


Figure 7. An example of the possibilities of the deconvolution software is shown with the TIC spectrum of Linalool which is automatically deconvoluted from five other coeluting peaks. The deconvoluted spectrum (B) is then matched against the NIST library (C) for improved spectral match and accurate compound identification.

¹ The scan range of the mass spectrometer was reduced from 30-500 to 40-500 later on during the vapor analysis experiments due to the presence of oxygen (mass 32) which causes a very high background signal. Reducing the scanned mass range from 40 to 500 does not influence the quality of the spectra and the reversed library searches as we observed.

Configuration 3: GCxGC-ToF-MS used for JP-8 vapor analysis

The system was expanded for the on-line analysis of vapor samples with a six-port port valve (Valco Instrument, Houston, TX, USA) which was installed initially in a heated oven connected to the side of the GC oven and controlled by the GC and the ChromaTOF software². This allows specific time settings for on- and off switching. Several configuration were tested before the final version could be implemented. Firstly, a fixed sample volume of 100 μl appeared to be insufficient to analyze the very low concentrations of some specific components of interest. Also, trapping the vapor sample onto the cryogenically cooled injector liner packed with Tenax TA™ (Varian Chrompack, Middelburg, Netherlands) resulted in inadequate chromatographic performance.

The final version of this configuration used a cryogenic cold trap (see also C in Figure 9) inside the GC oven. Also, the sample volume- which is directly correlated to the detection limit of the configuration - could be adjusted by varying the combination of sample flow and sampling time.

The vapor was sampled from the exit of the evaporation tube by using a piece of stainless steel tubing (SGE, Victoria, Australia), length *ca* 1 m and an i.d. of 1/16 inch which was also connected to this 6-port valve. From the valve a piece of uncoated deactivated fused silica (Varian Chrompack, Middelburg, Netherlands) with a length of *ca* 1 m and an i.d. of 0.32 mm is lead though a cryogenic trap which is installed inside the GC oven and directed back towards the 6-port valve. By using a second piece of stainless steel tubing (SGE, Victoria, Australia), length *ca* 1 m and an i.d. of 1/16 inch connected to a carbon filter and a mass flow controller and finally a small vacuum pump this sample flow is controlled. The combination of sampling time with sample flow allows accurate sampling of a fixed sample volume. The OPTIC injector is connected to the 6-port valve by means of a small piece of uncoated deactivated fused silica (Varian Chrompack, Middelburg, The Netherlands) with a length of *ca* 0.5 m and an i.d. of 0.32 mm. In this way the injector could still be used for calibration purposes. The GCxGC column combination is connected to the last port of the 6-port valve for the final analysis, see also Figure 8 for a schematic representation of the configuration.

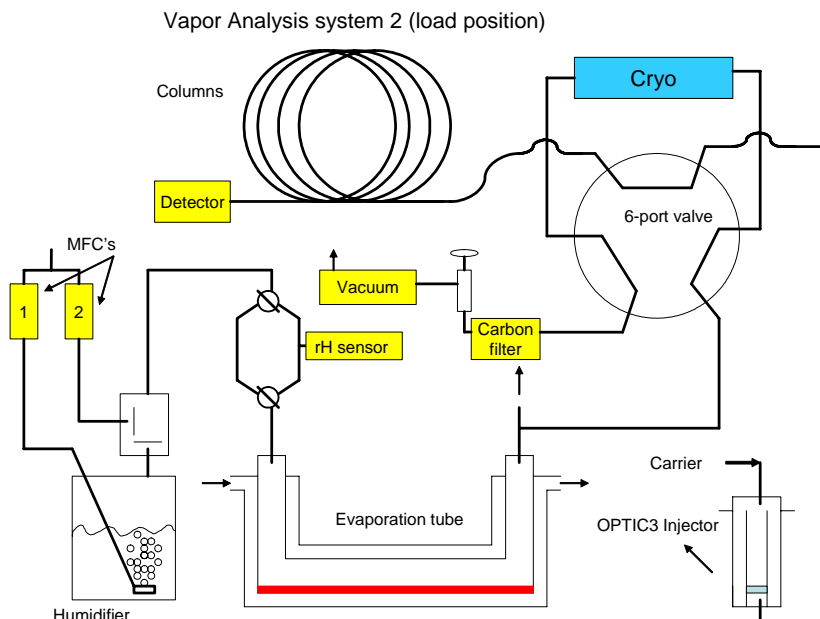


Figure 8. Schematic representation of the configuration used for the vapor analysis of JP-8.

² In the final configuration the 6-port valve was installed inside the GC oven, see also Figure 9.

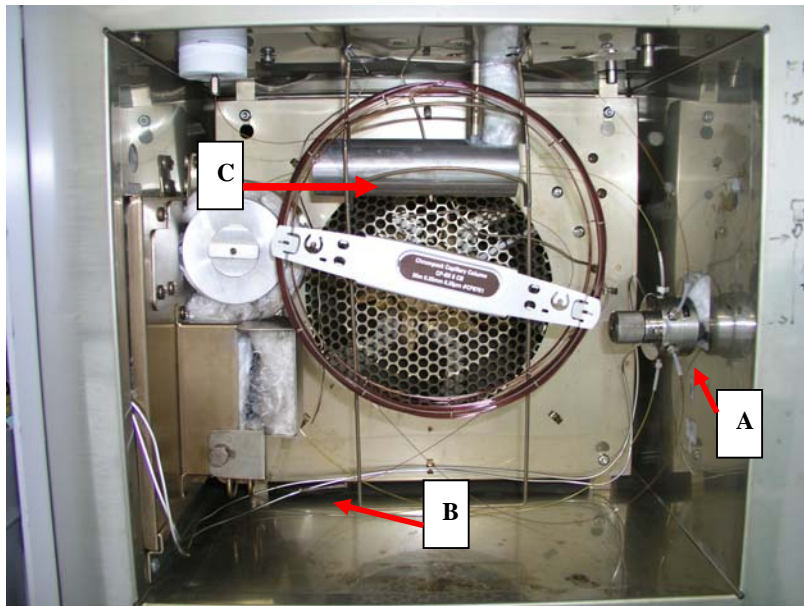


Figure 9. Photograph of the inside of the GC with on the right the 6-port valve(A). On the bottom (B) the connecting tubing from the evaporation unit to the 6-port valve and on the left top side the cryogenic cold trap (C).

The configuration described above is ideal for fully automated analysis at a fixed time interval, which is determined by the cycle time (analysis time + time to get ready) of the GCxGC-ToF-MS. To sample at shorter time intervals an alternative approach has to be used, as outlined below (see ‘Off-line sampling of JP-8 vapor).

Off-line sampling of JP-8 vapor.

The evaporation experiments at +20 °C were carried out using the off-line sampling method. This alternative but very laborious method was chosen in view of the anticipated high evaporation speed of the low boiling components. OPTIC injector liners were filled with *ca* 70 mg Tenax TA™ (60-80 mesh), placed in an oven at 250 ° and purged for 5 h with purified nitrogen gas to remove possible contaminants that might interfere in the GCxGC-ToF-MS analysis.

The generated JP-8 vapor was lead through the injector liner for a predetermined time span at a controlled flow rate. Next, the liners were capped and stored below -20 °C in a box filled with CO₂(s). These liners were subsequently placed in the OPTIC injector for further analysis with the GCxGC-ToF-MS system. A schematic representation of the off-line sampling configuration is seen in Figure 10. A piece of stainless steel with i.d. 1/16" connects the sample point to an electrical 8-port valve. Before sampling a combination of a carbon filter, a needle valve and a vacuum pump are used to establish a constant flow from the sample point. The already installed packed OPTIC liner is constantly purged with clean nitrogen to prevent contamination. At a certain moment in time the 8-port valve switches and the sample stream is loaded onto the liner, for a predetermined time period and a fixed flow.

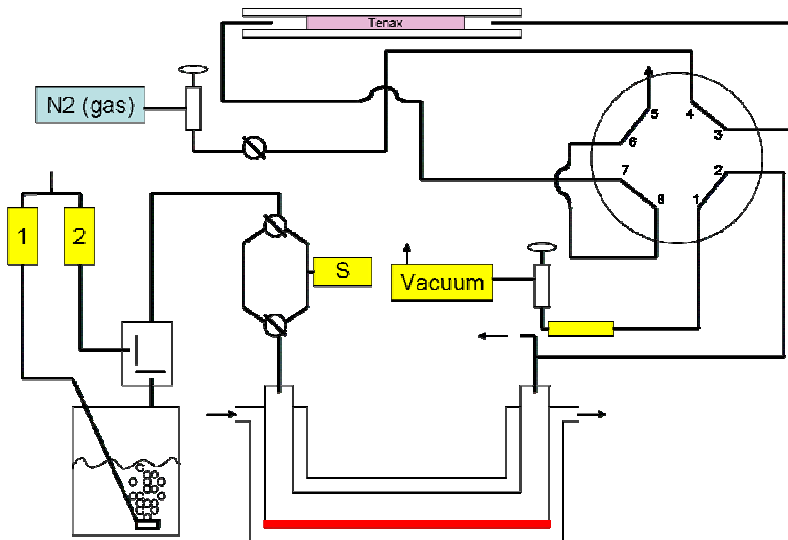


Figure 10. Schematic representation of the off-line sampling configuration. From the right of the evaporation tube (central below) a stainless steel tube is led to a 8-port valve. On top the OPTIC liner filled with Tenax TA which is used for sampling it is also connected to this the valve. Nitrogen gas is used to purge the packed liner.

II.3 JP-8 vapor generation experiments

Apparatus for controlled evaporation of jet fuel

A small scale configuration was constructed for controlled evaporation of JP-8 samples, see also Figure 10. This configuration consists of a glass thermostatted evaporation tube with an internal diameter of 10 mm and length 15 cm. The temperature is controlled by means of a Brinkman Lauda RE106 Refrigerated Bath Circulator (Westbury, NY, USA). A glass humidifier and a glass mixing chamber were used to generate the appropriate relative humidity during the experiment. The relative humidity was checked continuously with a HM31 Vaisala sensor (Helsinki, Finland). Bronkhorst mass-flow controllers (Veenendaal, The Netherlands) were used to generate in a controlled way the acquired air flow through the humidifier and mixing chamber, which was subsequently lead through the evaporation tube.

With Dr. Susan Proctor (USARIEM) is was agreed to study 2 evaporation scenarios:

- (1) A wind speed of 5 m/s, temperature -10 °C and a humidity of <10 %.
- (2) A wind speed of 5 m/s, temperature +20 °C and a humidity of *ca* 60 %.

To establish the appropriate wind speed through the evaporation tube the air flow was set to 24 l.min⁻¹ during the experiments. Just prior to the experiments a small volume of jet fuel (1 ml) was inserted into the thermostatted evaporation tube and was allowed to evaporate under influence of the humidified air flow. A T-connection was positioned at the end of the evaporation tube for on-line sampling, see also Figure 10, or off-line sampling onto an injector liner. The remaining vaporized jet fuel was finally vented via an exhaust exit.

II.4 Calibration and Quantification

Several calibration standards were prepared by using diluted stock solutions, see also Annex B, ranging from 0 to 100 µg/ml. There are three options for quantifying the ToF-MS signal:

- i) The total summed masses from a full spectrum of a chromatographic peak, which in a way is comparable to a FID signal,

- ii) The total of specific masses from the full spectrum of a chromatographic peak, and
- iii) The total of a single mass of a chromatographic peak.

Small intensity masses were used for quantifying at high concentration in order to prevent misinterpretation by signal overloading. High intensity masses were taken for quantifying at lower concentrations. The linear dynamic range for the components of interest was determined to be four to five orders of magnitude.

III. RESULTS (AND DISCUSSION)

III.I Chromatographic optimization (T.O. 1)

Various column combinations were tested to establish the best combination as well as the optimum separation conditions for the jet fuel samples, see also II.2. In view of the boiling point range of the jet fuel fraction and the differences in classes of the components combinations of non-polar (boiling point) and polar separation columns were tested. The objectives of this task were to achieve a relatively fast analysis and *an adequate* separation of the analytes.

The most suitable column combination was determined with a mild non-polar column for the 1st dimension (phase CP-Sil 8CB, length, 30 m, i.d. 0.25 mm, film thickness, 0.25 μm) and in the 2nd dimension a medium polar column (phase Vf 17-ms, length, 2 m, i.d., 0.1 mm, film thickness, 0.2 μm), see also Figure 11.

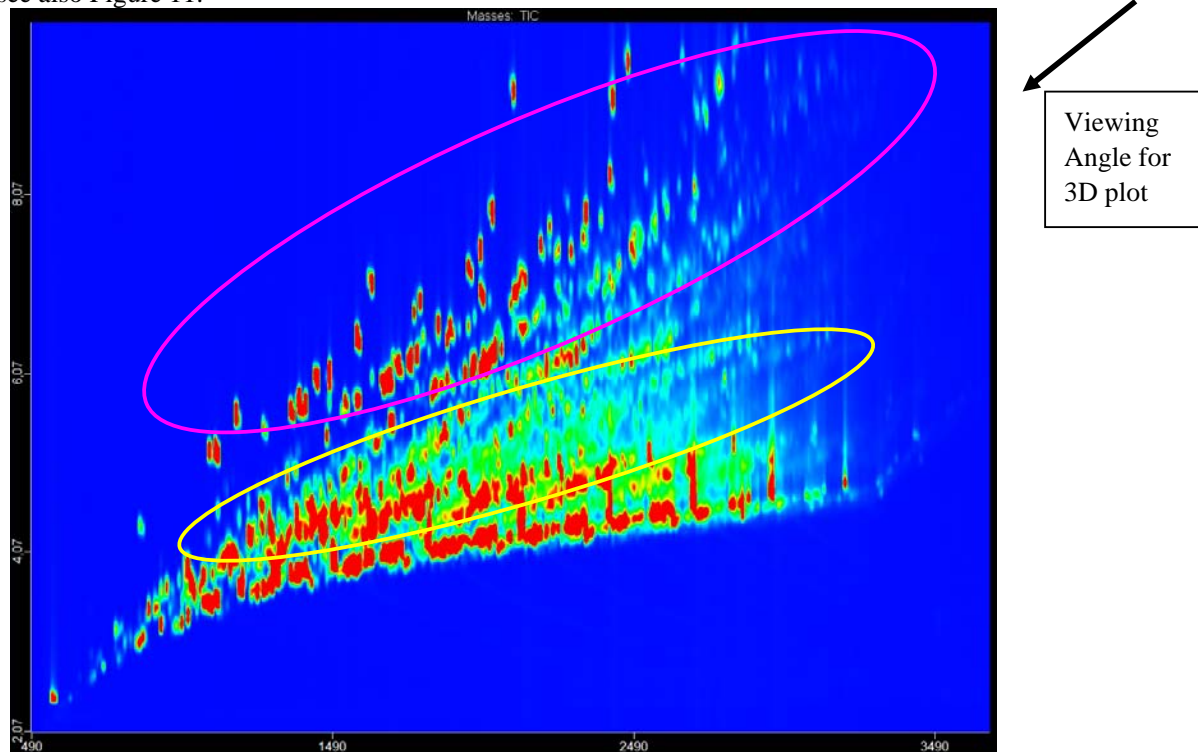


Figure 11. 2D Plot of an optimized 2D gas chromatographic separation of jet fuel using a medium non-polar first dimension column and a polar second dimension column. The yellow region below contains the alkanes and cyclo-alkenes, the upper pink regions contains the mono- and diaromatics and other more polar components. The arrow next to the graph indicates the angle that was used for the 3D-view.

The OPTIC injector was used in the split mode under a constant pressure of 300 kPa with a split flow of 250 ml/min. A jet fuel sample of 1 μl was injected into the fritted liner. During injection the injector was cooled and kept constant at 40 °C for 0 sec and then ramped at 5°C/sec to 230 ° where it was held constant until the end of the run. The GC oven was kept constant for 3 min at 40 °C and then ramped at 2°C/min to 250° where it was held constant for 10 min. The 2nd GC oven containing the 2nd dimension column was also temperature programmed. This 2nd oven was kept constant for 3 min at 50 °C and then ramped at 2°C/min to 250° where it was held constant for 10 min. The temperature of the hot jets was programmed at a temperature offset of 50 °C above the temperature of the 2nd oven. The hot jet pulse time was 0.6 sec; the modulation time was 10 sec. In Figure 12 the result of the optimized 2D separation is shown as a 3D plot. The viewing angle for this 3D plot is from the upper right corner towards the lower

left corner. By viewing the results along this angle the high boiling and polar components appear on the front side of the 3D-graph, whereas the low boiling non-polar components elute appear in the back.

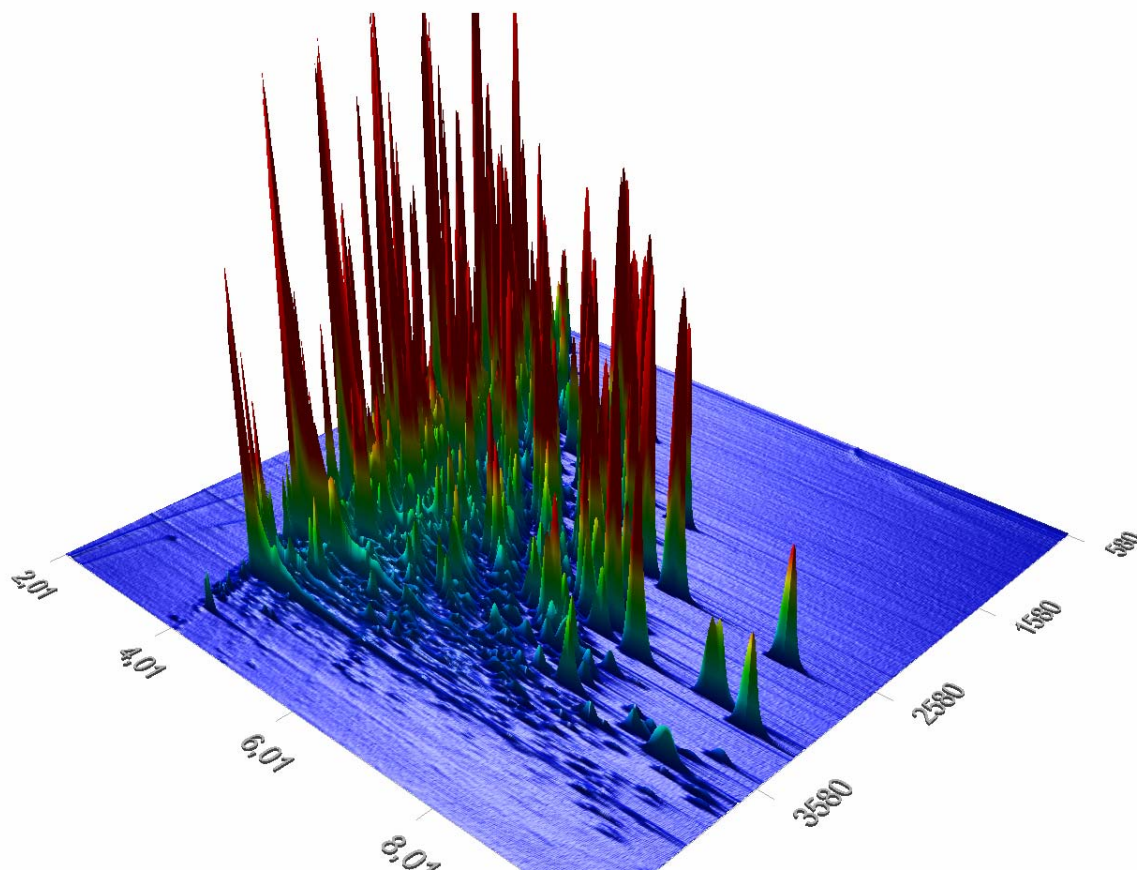


Figure 12. 3D plot of the TIC of an optimized 2D gas chromatographic separation of jet fuel using a medium non-polar first dimension column and a polar second dimension column.

Reversing this separation principle by replacing the 1st dimension column for a polar version and the 2nd dimension column for a non-polar version complicated the picture. Due to the ‘Wrap around³’ of non polar components such as the alkanes and cyclo alkanes in the 2nd dimension column, combined with the relatively high concentrations of some of those components (overloading), the separation achieved in the 1st column was completely neutralized. The more polar components, however, were more retained in the 1st column and were also present in lower concentrations. This results in a clean separation from the background, see also Figure 13. In this picture the non polar components are seen mostly on the left hand side of the 2D-plot and the more polar components on the right hand side. In Annex C the 3D plot of this analysis is shown in Figure 24.

The list of presumed neurotoxic components covers a wide range of polarity (e.g. Methanol versus Alkanes), but also from relatively low boiling to high boiling (e.g. Methanol and Cyclohexane versus Acenaphthalene), therefore the column combination which proves to be most adequate is based on a pre-separation (first dimension) on a non-polar column. In this way the majority of the components, which are present in fuels and which have similar polarity, are separated by their boiling point. The next step is to separate the fraction which have a similar boiling point. This means that a polar stationary phase has to be used for chromatographic separation in the second dimension.

³ ‘Wrap around’ will occur if the elution time of the component is longer than the modulation time. These peaks will appear in the subsequent analysis of the next modulation.

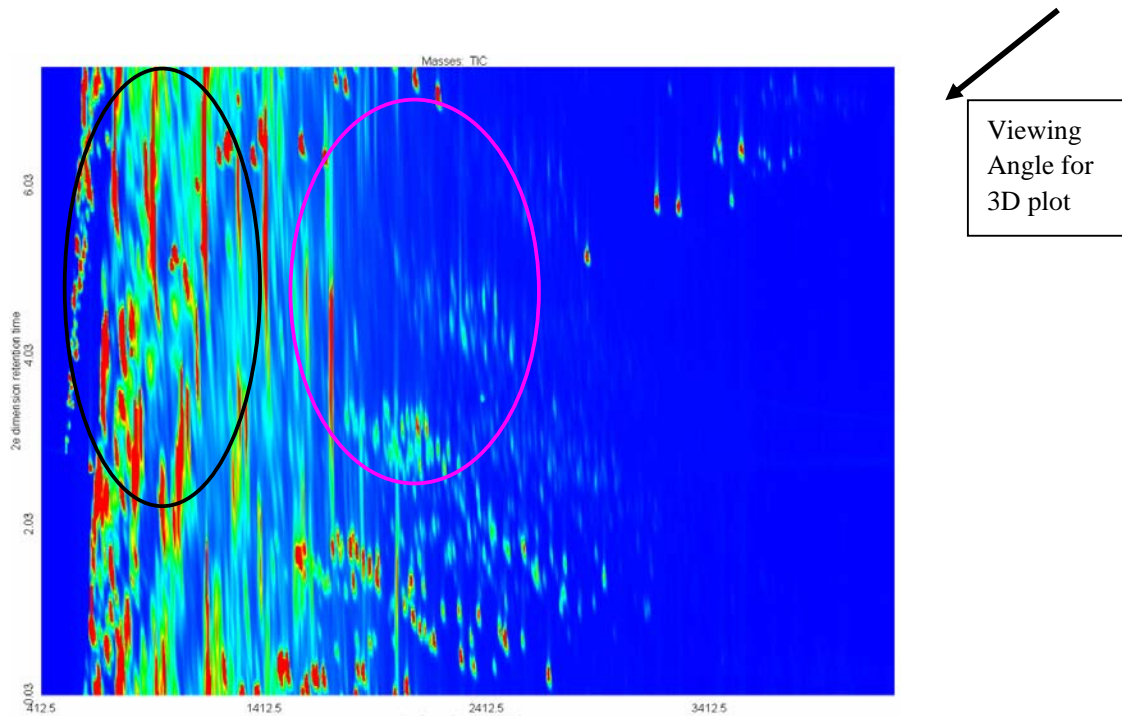


Figure 13. 2D gas chromatographic separation of jet fuel using a reversed column combination consist of a polar first dimension column and a non-polar second dimension column. The black region on the left contains the alkanes and cyclo-alkenes, the right pink regions contains the mono- and diaromatics and other more polar components.

III.2 Categorization/classification of components in the 2D chromatograms (T.O. 3 and 4)

After connecting the ToF-MS to the GCxGC system the analytical possibilities grew instantly. Combined with the ChromaTOF™ software the peaks in the chromatogram could be identified. The NIST-library, which contains over 60,000 components, is fully integrated into the software. Based on the structural resemblance of individual compounds belonging to a certain class of chemicals, specific mass traces in the 2D-chromatogram can be highlighted. This provides an opportunity to categorize peaks observed in the 2D-chromatogram into various classes of chemicals. An example of such a categorization is shown in Figure 14, for a Dutch Jet Fuel sample, offloaded from an F16 Jet Fighter (see also II.I sample III). In this figure the alkanes, sulfur containing components, napthenes, polycyclic aromatic hydrocarbons and monoaromatics are presented using different colors for each chemical class. This approach allows a rapid visual comparison of the composition of jet fuels from various sources. For example, the US KC135 jet fuel sample (see also II.I sample I) contains a series of sulfur containing compounds that are not present in the Dutch jet fuel, see Figure 15. Despite the sometimes high reversed fit factor of the mass spectrum of a chromatographic peak compared to the library spectrum, the identity of the peak could not always be established for the full 100%. For a rough screening of the jet fuel samples relatively high filters for the library fit ($> 80\%$) and signal-to-noise level ($> 50:1$) were used. An indication of the presence of sulfur containing components in the two jet fuel samples presented above is given in Table 2. No further data processing on the peak spectra was performed to obtain the true identity. This was beyond the scope of the proposed work.

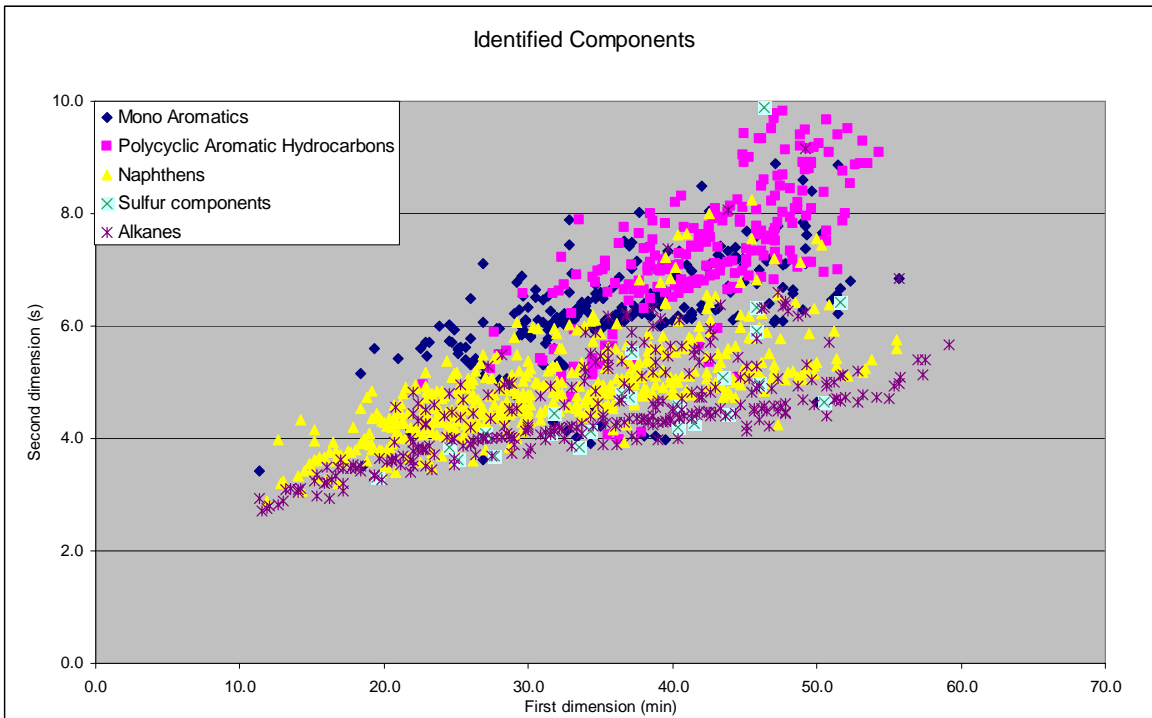


Figure 14. Schematic representation of the various classes of components in the Dutch Jet Fuel sample no III.

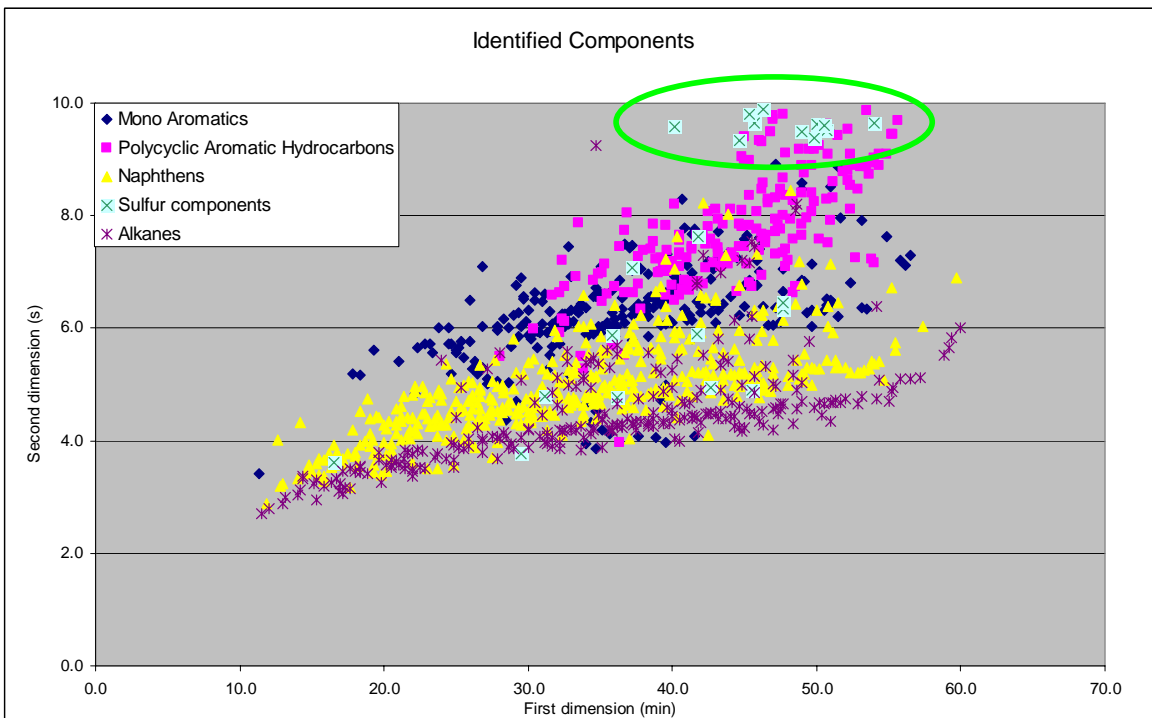


Figure 15. Schematic representation of the various classes of components in the US KC135 Jet Fuel sample no I. In green the area where a number of sulfur components emerge which are not present in the Dutch jet Fuel sample no III.

Table 2. Indication of the presence of sulfur containing components in two jet fuel samples.

Dutch JP-8, sample III	US KC135 JP-8, sample I
Sulfone, 2-hydroxybutyl t-butyl	2-Methyl-4-phenylthiolane, 1,1-dioxide
Sulfurous acid, butyl cyclohexylmethyl ester	2-Thiopheneacetic acid, 2-ethylcyclohexyl ester
Sulfurous acid, butyl hexadecyl ester	2-Thiopheneacetic acid, 2-ethylcyclohexyl ester
Sulfurous acid, cyclohexylmethyl hexyl ester	2-Thiopheneacetic acid, oct-3-en-2-yl ester
Sulfurous acid, di(cyclohexylmethyl) ester	2-Thiophenecarboxylic acid, 3,4-dichlorophenyl ester
Sulfurous acid, hexyl 2-pentyl ester	2-Undecanethiol, 2-methyl-
Sulfurous acid, hexyl heptyl ester	3-Cyclohexylthiolane,S,S-dioxide
Sulfurous acid, hexyl pentyl ester	3-Phenylthiolane,S,S-dioxide
Sulfurous acid, isobutyl pentyl ester	Benzo[b]thiophene, 2,7-dimethyl-
Sulfurous acid, octadecyl 2-pentyl ester	Benzo[b]thiophene, 2,7-dimethyl-
Sulfurous acid, octyl 2-propyl ester	Benzo[b]thiophene, 2-ethyl-5,7-dimethyl-
Sulfurous acid, pentyl tridecyl ester	Benzo[b]thiophene, 2-ethyl-5-methyl-
2-n-Propylthiolane, S,S-dioxide	Benzo[b]thiophene, 2-ethyl-7-methyl-
2-Undecanethiol, 2-methyl-	Benzo[b]thiophene, 3,6-dimethyl-
3,4-Dimethylbenzyl isothiocyanate	Benzo[b]thiophene, 5-methyl-
3-Cyclohexylthiolane,S,S-dioxide	Benzo[b]thiophene, 7-ethyl-
Benzo[b]thiophene, 7-ethyl-	Pyridine, 2-[(1,1-dimethylethyl)thio]-3,5-dimethyl-
	Thiophene, 2-(4-methylbenzylsulfonyl)-
	1H-1,2,4-Triazole, 1-benzyl-3-benzylthio-

The identified components that are shaded in this table were present in both jet fuel samples.

The list of investigated components is roughly divided into 5 groups. Each group has representative masses which can be used for the classification; the alkanes (71, 85 and 99), the mono aromatics (78 and 91), the di-aromatics naphtalene (128) and acenaphthene (153), the cyclopentanes (69) and the cyclohexanes (83). By selecting these masses, not only the target compounds, such as octane emerge from the background but also many other structural similar components, see also Figure 16. In this example masses 71+85+99 were selected to show the alkanes.

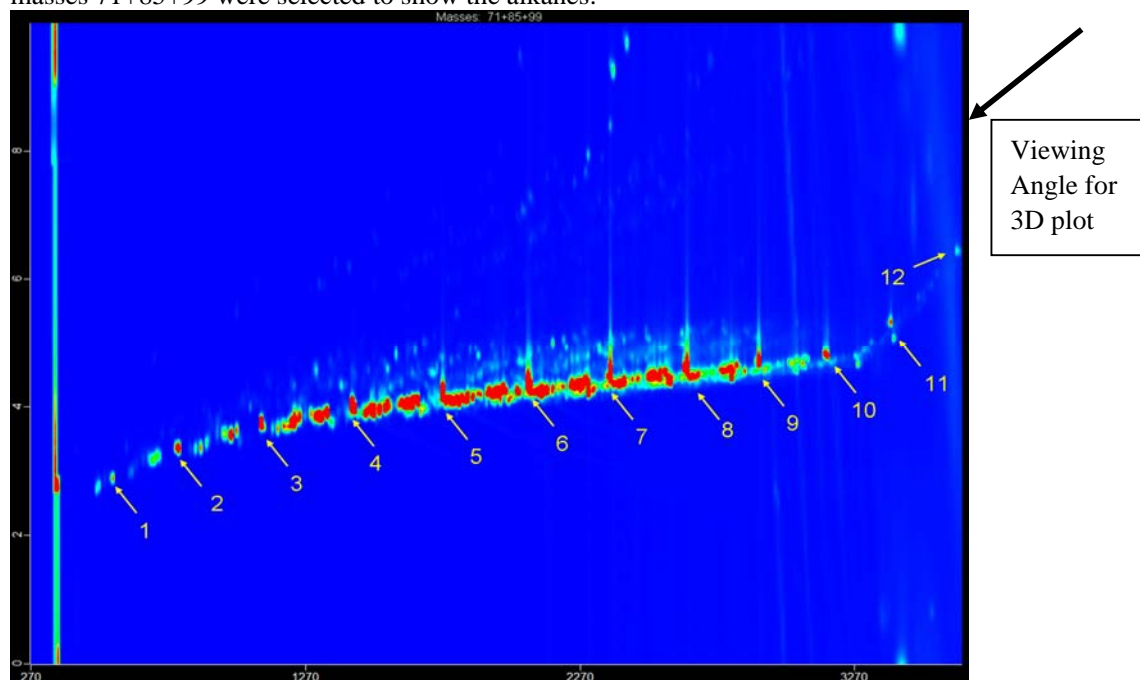


Figure 16. A 2D gas chromatographic separation of JP-8 sample I (KC135) where the masses 71, 85 and 99 are selected which are representative for the alkanes. The number 1 to 12 indicates the spots in the 2D chromatogram were the n-alkanes emerge starting 1 for n-Heptane (C_7H_{16}) to

12 for n-Octadecane ($C_{18}H_{38}$). The arrow next to the graph indicates the angle that was used for the 3D-view.

Annex C Figure 25 shows the 3D plot of the summed masses of 71, 85 and 99 which are representative for the alkanes.

Standards were used to pin-point the spot where the target neurotoxic components emerge in the chromatogram. Selecting masses 78 and 91 highlights the aromatics from the background, see also Figure 17. In this figure the categorization of the aromatics can be seen as they are lined up from left to upper right. The numbers 1 to 9 represent the spots where the ‘target’ aromatics emerge, 1 stands for benzene, 2 for toluene, 3 for ethylbenzene, 4 for m- and p-xylene, 5 for o-xylene, 6 stands for isopropylbenzene, 7 for 2-ethylbenzene, 8 for 1,2,3-trimethylbenzene and 9 for 1,2-diethylbenzene.

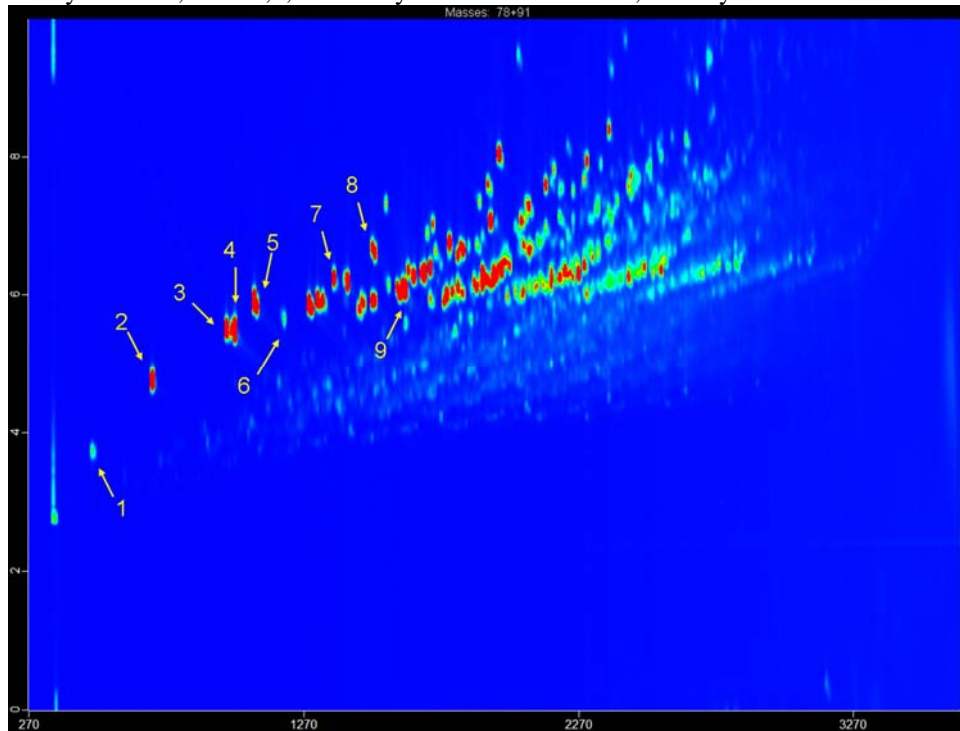


Figure 17. A 2D gas chromatographic separation of JP-8 sample I (KC135) where the masses 78 and 91 are selected which are representative for the aromatics. The numbers 1 to 9 indicate the spots in the 2D chromatogram where the ‘target’ mono aromatics emerge, see text for details.

Mass 83 was selected for the cyclohexanes to extract this subgroup from the background, see also Figure 18. In this figure a modulated chromatogram of sample I is shown next to the 2D plot of the same analysis. The very high intensity peaks represent the homologue series of the class starting with cyclohexane (1), methylcyclohexane (2), ethylcyclohexane (3), propylcyclohexane (4), butylcyclohexane (5) and pentylcyclohexane (6). No attempt was made to identify branched cycloalkanes or other high intensity peaks as this was beyond the scope of the proposed work. Similar classification could be made by selecting the representative masses for the di-aromatics naphthalene and acenaphthene.

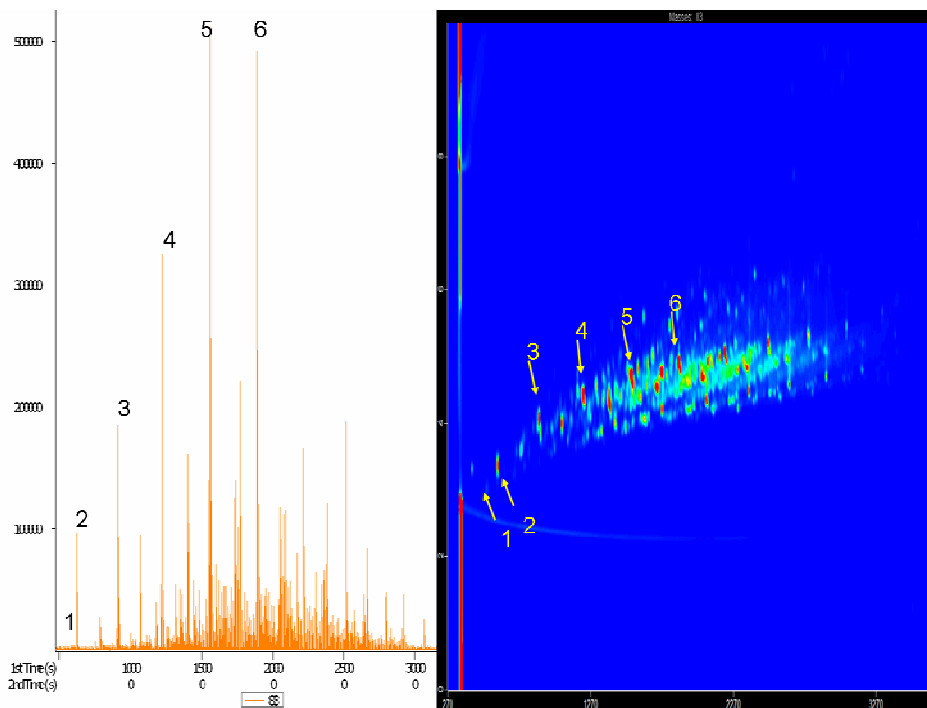


Figure 18. On the left a modulated chromatogram of sample I using mass 83 and on the right the 2D plot of the same analysis. The numbers 1 to 6 refer to the cyclohexanes, see text for details.

Specific integration regions were used to narrow the search in the list of emerging peaks. Also the amount of data for a single analysis is overwhelming as these data contain all aspects of an analysis such as the analytical conditions, the calibration data, all the spectra of every single peak and lots more. The time needed for data analysis was reduced by using integration regions. These integration regions are indicated by red circles in Annex D Figure 28 of an actual vapor analysis at the end (80 hr) of the evaporation experiment.

III.3 Concentration of neurotoxic components in Jet Fuel (JP-8) samples. (T.O. 5)

Samples of standards were used to screen the four jet fuel samples for the presence of the 20 neurotoxic components (cf. Table 1). Some changes were made for these analyses in comparison with the chromatographic optimization as described in paragraph III.I. The OPTIC injector was used in the split mode under a constant pressure of 175 kPa with a split flow of 250 ml/min. From the jet fuel samples 1 μ l was injected into the fritted liner. During injection the injector was cooled to 20 °C for 0 sec and then ramped at 5°C/sec to 230 °C where it was held constant until the end of the run. The GC oven was kept constant for 3 min at 40 °C and then ramped at 2°C/min to 200°C, where it was held constant for 5 min. The 2nd GC oven containing the 2nd dimension column was also temperature programmed. This oven was kept constant for 3 min at 45 °C and then ramped at 2°C/min to 200°C where it was held constant for 5 min. The temperature of the hot jets was programmed with a temperature offset of 50 °C above the 2nd oven. The hot jet pulse time was 0.6 sec. The modulation time was 10 sec.

To compare the results of the different sorts of analyses (liquid analysis, vapor analysis) the cold trap inside the GC oven is used to normalize the retention time. Due to the composition of the matrices, e.g. solvent or vapor, the retention time of the analytes differ from one another mostly as a result of the injection technique. To compare the results, which means that analytes elute at exactly the same time for both matrices a piece of uncoated deactivated fused silica column, length 0.5 m and internal diameter of 0.53 mm is placed in between the injector and the first separation column. This retention gap is directed through the cold trap housing. During injection this cold trap is cooled to -100 °C to prevent the analytes

from migrating through the first separation column, in this way the start of the different types of analysis is normalized.

The efficiency of this trapping was tested by comparing the results for a short cooling period as used in the experiments and cooling for more than 5 min. The analytes were retained for this exact period, whereas the peak areas and heights as well as the differences in retention time between the individual peaks were the same as before.

Table 3. Jet Fuel composition with respect to selected neurotoxic components.

Component	KC 135 JP-8 (I)	Storage Tank JP-8 (II)	F-16 Dutch JP-8 (III)	'Aged' Dutch JP-8 (IV)	Unit
Benzene	67.2	40.1	76.7	45.3	µg/ml
Toluene	0.78	0.66	0.78	0.74	mg/ml
Ethylbenzene	1.04	1.04	1.50	2.10	mg/ml
m,p-Xylene	3.11	3.22	4.82	7.01	mg/ml
o-Xylene	0.46	0.42	2.91	0.98	mg/ml
Isopropylbenzene	0.56	0.62	0.90	1.24	mg/ml
2-Ethyltoluene	3.02	3.47	2.68	3.95	mg/ml
Benzene, 1,2,3-trimethyl	3.48	3.88	3.71	2.47	mg/ml
Benzene, 1,2-diethyl-	0.87	1.08	0.68	0.74	mg/ml
Naphthalene	1.68	1.77	0.92	2.07	mg/ml
Heptane	0.58	0.42	0.59	0.66	mg/ml
Octane	0.52	2.25	2.58	3.98	mg/ml
Acenaphthene	8.4	9.9	7.8	15.2	µg/ml
Methanol	N. F.	N. F.	N. F.	N. F.	
1-Butanol	N. F.	N. F.	N. F.	N. F.	
1,2-propanediol	N. F.	N. F.	N. F.	N. F.	
Styrene	N. F.	N. F.	N. F.	N. F.	
Cyclohexane	76.2	164.4	374.3	247.7	µg/ml
Cycloheptane	507.2	38.5	59.2	59.4	µg/ml
Isopropylcyclopentane	96.0	287.3	301.8	357.7	µg/ml
Isopropylcyclohexane	0.53	1.78	2.40	2.88	mg/ml

N.F.; Not Found.

Methanol, 1-butanol, 1,2-propanediol and styrene were not measurable in any of the four jet fuel samples studied. For most of the investigated components the concentrations were quite comparable in the US originated samples, but not for the cycloalkanes and octane. The amount of cycloheptane, for instance, was about 10 times higher in the KC135 sample than in the US Storage Tank sample and in the Dutch fuel samples. The amount of cyclohexane however, was lower for the KC135 sample than for the other samples.

There was also a difference in concentration observed for octane which was for the KC135 sample about 4 times lower than for the US Storage Tank sample, and about 5 times lower than for the Dutch samples. Smaller differences were observed for the concentrations of the xylenes which were in lower quantities present in the US originated fuel samples than in the Dutch jet fuel samples.

III.4 On-Line and Off-line JP-8 vapor analysis (T.O. 2)

On-line vapor analysis.

For the evaporation experiments of the jet fuel samples two vapor sampling configurations were used. A discontinuous on-line system was tested for its suitability to analyze the low temperature evaporation of JP-8 for at least 48 h to 96 h.

At the start of the experiment 1 ml of JP-8 was introduced into the thermostatted evaporation tube. Air was led through this tube at a flow-rate of 24 l/min. A small portion of this vapor coming from the end of the cooled evaporation tube was directed towards the 6-port sampling valve with a flow-rate of 13 ml/min by using the carbon filter and mass flow controller combination and a small vacuum pump. During switching of the valve the sample flow through the cooled trap fused silica tubing fluctuates to some extent. Using these settings 2 ml of vapor sample were analyzed every hour until the end of the experiment. For the duration of the sampling period the cold trap inside the GC was cryogenically cooled at -100 °C to prevent breakthrough of the analytes. At 0.02 min after the start of the chromatographic run, the 6-port valve switched and the vapor sample was directed through this cold trap for 0.17 min, end switch time 0.19 min. The cold trap was kept constant at -100 °C for 0.5 min and then ramped at 15 °C/s to 230 °C and kept constant until the end of the run. Carrier flow for the GC columns was provided by the OPTIC injector at a constant pressure of 175 kPa. The injector was used in the split mode with a split flow of 50 ml/min to prevent contamination and held at a constant temperature of 200 °C. The GC oven was kept constant for 3 min at 40 °C and then ramped at 3 °C/min to 180° where it was held constant for 5 min. The oven for the 2nd column was kept constant for 3 min at 45 °C and then ramped at 3°C/min to 180° where it was held constant for 5 min. The temperature of the hot jets was programmed with a temperature offset of 20 °C above the temperature of the 2nd oven. The hot jet pulse time was 0.6 sec. The modulation time was 10 sec.

The modulated chromatogram of the first analysis at 5 min after start of the evaporation experiments of the KC134 JP-8 sample (I) at -10 °C is presented in Figure 19, and for 80 hr in Figure 20.

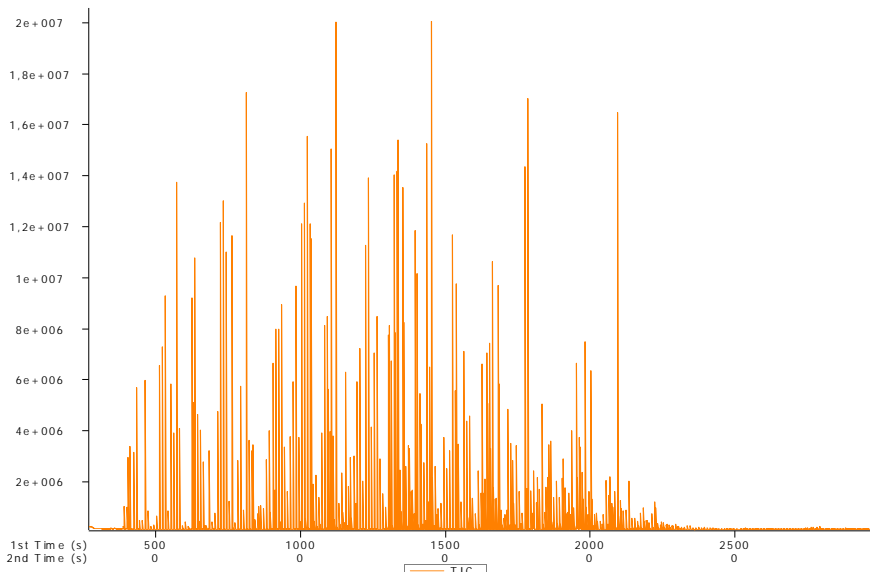


Figure 19. The modulated chromatogram (TIC) of the first vapor sample taken at 5 min after start of the evaporation of jet fuel sample I, the KC135 JP-8, at -10 °C.

The signal of the total ion current (TIC) is shown in both chromatograms which gives an indication of the concentration of the components in the vapor. The use of specific mass traces in combination with the

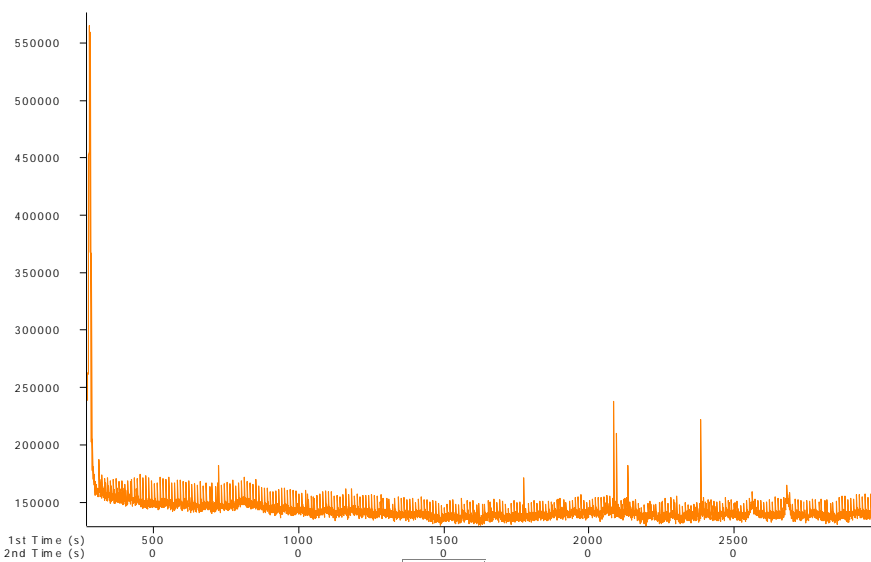


Figure 20. The modulated chromatogram (TIC) of the vapor at 80 hr after start of the evaporation of the jet fuel sample I, the KC135 JP-8, at -10 °C.

deconvolution capabilities of the software improves the spectrum quality and decreases the detection limits (increases the sensitivity). This approach appeared to be ideal for the identification and quantification of the components of interest. Figure 21 shows the 3D plot of the mass traces 78 and 91 which are representative for the aromatics. Small traces of benzene and toluene could be detected in the sample taken at 80 h ($t = 79.92$ h) after the start of the evaporation experiment, see also Table 8 Annex F.

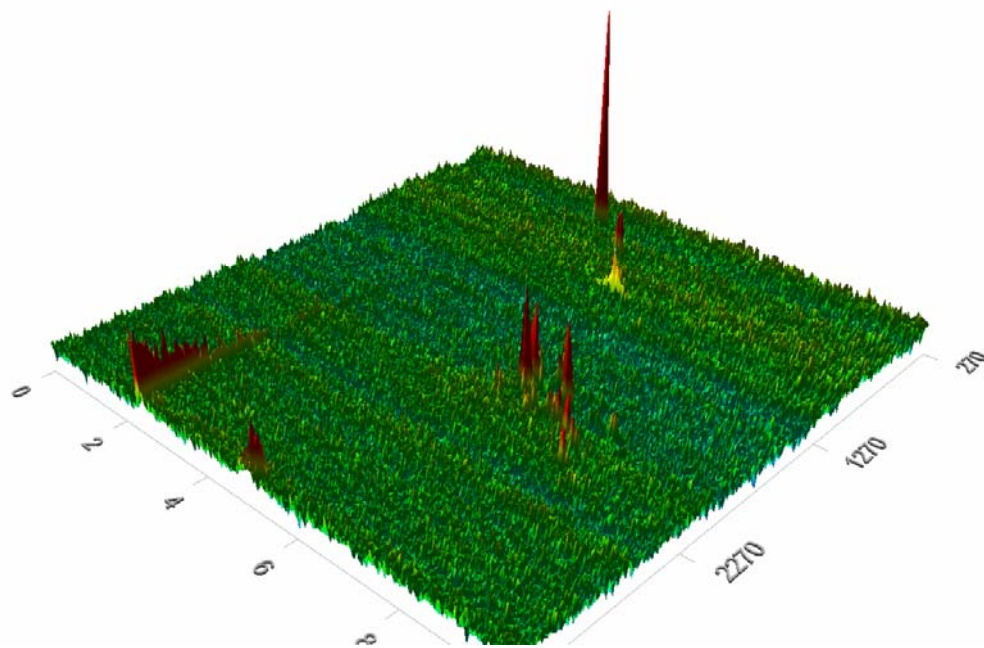


Figure 21. 3D plot of the modulated chromatogram (masses 78 + 91, which represents the aromatics) of the vapor at 80 hr after start of the evaporation of the jet fuel sample I, the KC135 JP-8, at -10 °C. The retention time for the X- (on the right hand side) and Y-axis (on the left hand side) is given in seconds.

Off-line vapor analysis.

By switching the electric actuator of the 8-port valve for 30 seconds a small part of the sample flows through the packed injector liner with a flow-rate of 6 ml/min. In this way 3 ml of vapor is trapped onto the packed injector liner. After sampling, the injector liners were capped and stored in a cooled container. Prior to the analysis the OPTIC injector was cooled to -80 °C. Next, the 'head' of the injector was removed and the liner was introduced into the injector body, which was followed by replacing the injector head. After reaching pressure equilibrium (175 kPa) the program of the analytical configuration was started by ramping the temperature of the injector to 200 °C at 12 °C/s and held constant to the end of the run. The sample was injected splitless: after 1 min the split line opened with a flow-rate of 50 ml/min. The program for the oven, the cryogenic trap and for the 2nd oven were as described above.

The suitability of this method was tested by storing loaded and capped liners in a box filled with solid CO₂ to analyze if the amount of adsorbed components decreased with time and also to screen if contaminating components were diffusing into the liners, thereby disturbing the analysis. The capacity of the liner 'trap' was tested by introducing a known amount of the standard mixture followed by purging with an excess (> 5 l) of clean air. This was compared to a non-purged sample.

Using this sampling methodology more samples at a shorter or different time interval could be taken. The obvious disadvantage of this method is the laborious way of taking samples.

III.5 Evaporating profile of the JP-8 samples (T.O. 6 and 7)

Evaporation experiments at -10 °C.

For each experiment 1 ml of the JP-8 samples was taken and introduced into the cooled evaporation tube. The tubing for the air supply was connected to the evaporation chamber and the flow was switched on. This time point was marked as time 0 min. The analytical configuration was started for the first time at about 5 min after this point. Each experiment was considered to be ended when more than 4 consecutive analyses resulted in no measurable levels of the target components. The results of the evaporation experiments at -10 °C are presented in Annexes F and G.

We observed a very rapid decline in vapor concentration from the initial (at t = 5 min) concentration for cyclohexane, benzene, heptane, toluene, octane, cycloheptane, and isopropylcyclopentane. Of these compounds only benzene and toluene were detectable after that time point.

An example of the evaporation profile of benzene in a single experiment is given in Figure 22. The combined result from the 4 evaporation experiments with the samples I to IV for benzene is presented in Figure 23. As can be seen in this example the evaporation rate is far from constant and tends to fluctuate with time. It could very well be possible that the evaporation rate of benzene is influenced by the actual composition of the mixture, which is obviously constantly changing with time due to evaporation of various components at various rates.

The detection limit for these relatively low boiling components, benzene and toluene (Figure 31) was rather low, i.e., in the range of 0.2 and 0.6 µg/m³. Obviously, as the detection limit is lower, the chances of measuring a meaningful vapor concentration-time curve increase.

The detection limit for the low and medium boiling alkanes and cycloalkanes of this subgroup varies from 0.5 µg/m³ (octane), 0.7 µg/m³ (cycloheptane), 1.6 µg/m³ (heptane) to 2.5 µg/m³ (isopropylcyclopentane). After the initial vapor analysis of cyclohexane at t = ca 5 min, this component was not detectable in subsequent JP-8 vapor samples. Therefore, the detection limit for actual vapor samples of this component was not established but was estimated at ca 1 µg/m³.

Despite the relatively low detection limits and the anticipated lower volatility in comparison with benzene and toluene, the detection of the vapor ends already at 4 h for isopropylcyclopentane (see also Figure 34); at 7 h for cycloheptane (see also Figure 33); and at 8 h for octane (see also Figure 32). Heptane however, could be detected in the vapor of the JP-8 samples up to 35 to 70 h, see also Figure 30. The results of two

consecutive analyses at 70 h of the vapor of one particular sample (sample II, US storage tank) however, follows a period of more than 30 to 40 hr of absence of this component. We have double checked the results and found no indication that these results were faulty and therefore should be eliminated. As stated

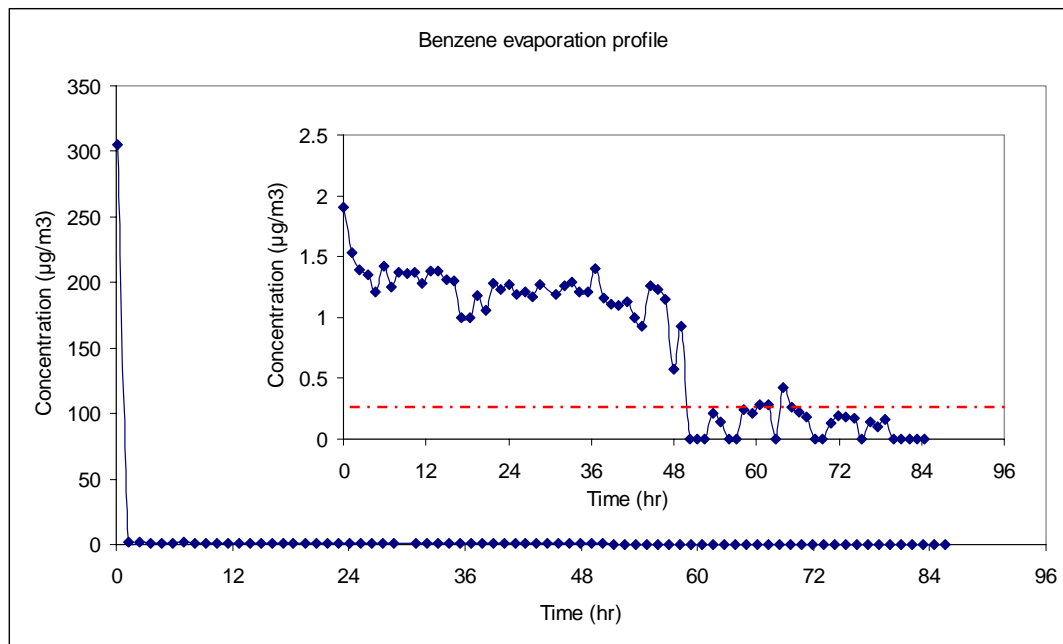


Figure 22. Concentration time course of benzene in the vapor phase during evaporation of JP-8 sample I (KC135) at -10 °C. The red line indicates the limit of detection of *ca* 0.2 $\mu\text{g}/\text{m}^3$ for this particular component.

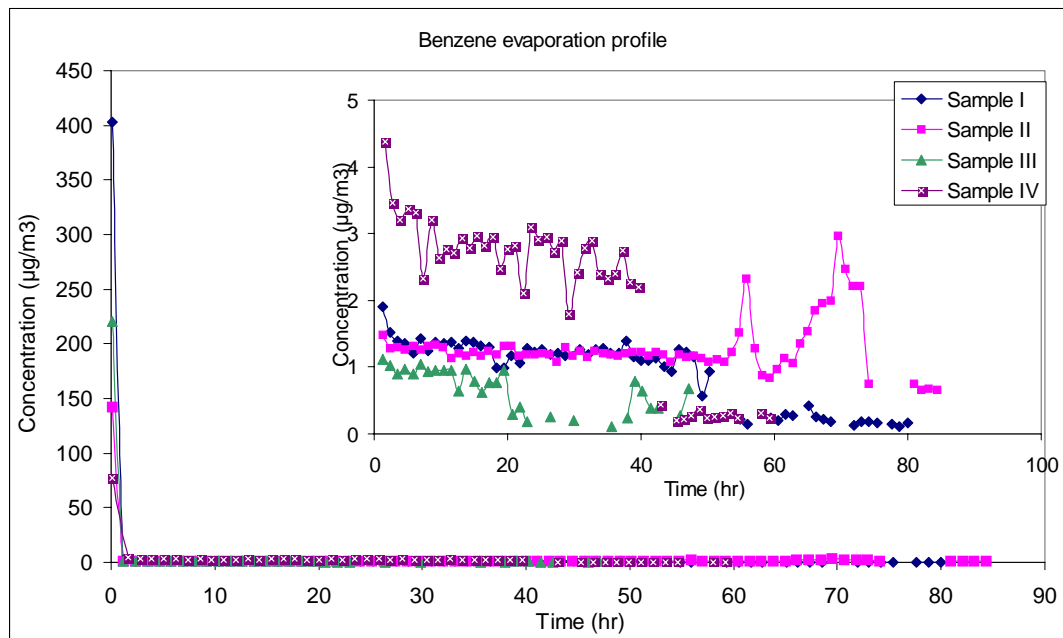


Figure 23. Concentration time courses of benzene in the vapor phase during evaporation of JP-8 samples I to IV at -10 °C. The discontinuities in the measurements are due to the detection limit of the analytical configuration of *ca.* 0.2 $\mu\text{g}/\text{m}^3$.

before, it is likely that the evaporation rate of each compound is influenced by the presence of other components and their volatility in the complex liquid fuel. Therefore, an evaporation profile such as observed for heptane may very well occur.

The other monoaromatics could be detected in the vapor for a longer time period, despite there somewhat higher detection limits of $9.7 \mu\text{g}/\text{m}^3$ for ethylbenzene (Figure 35), $8.3 \mu\text{g}/\text{m}^3$ for p- and m- xylene⁴ together (Figure 36), $18 \mu\text{g}/\text{m}^3$ for o-xylene (Figure 37), $3.4 \mu\text{g}/\text{m}^3$ for isopropylbenzene (Figure 39), $4.6 \mu\text{g}/\text{m}^3$ for 2-ethyltoluene (Figure 40), $5.6 \mu\text{g}/\text{m}^3$ for 1,2,3-trimethylbenzene (Figure 41) and $60 \mu\text{g}/\text{m}^3$ for 1,2-diethylbenzene (Figure 42). The evaporation profile could also be measured for a long time period isopropylcyclohexane (Figure 38) (detection limit of $3.3 \mu\text{g}/\text{m}^3$) and for naphtalene (Figure 43) (detection limit of $110 \mu\text{g}/\text{m}^3$). Acenaphtene was not measurable in the vapor throughout the entire evaporation experiment.

The evaporation rate of isopropylcyclohexane was far from constant in all samples from 5 to 20 h and seems to fade out with time. The evaporation rate of ethylbenzene from the fuel samples was after the initial high vapor concentration quite constant subsequent to the concentration drop at 8 to 10 h, up to the point where this component was no longer detectable. Other mono aromatics seem to follow this evaporation profile. For some components we observed a rise in the vapor concentration at about 10 to 15 h after a first decline in vapor concentration.

Evaporation experiments at +20 °C

As outlined in the experimental section, a different sampling technique was used for these evaporation experiments. Like in the -10 °C evaporation experiments 1 ml of the JP-8 samples was taken and introduced into the thermostatted evaporation chamber. After the tubing with the air supply was connected to the evaporation chamber the flow was switched on. This event was marked as time 0 min and considered as the starting point for the experiment. Only the two US originated JP-8 samples (Samples I and II) were tested under these conditions, due to restrictions in terms of time and budget.

At about 5 min after the start of the evaporation experiment the first liner was loaded with JP-8 vapor and transferred to the injector for further analysis. Subsequent samples were capped and stored in a cooled container. These samples were analyzed as soon as the analytical configuration was ready for the next analysis. The evaporation experiments ended at 5 h. Samples were taken at 5 min (0.08 h), 10 min (0.17 h), 20 min (0.33 h), 30 min (0.50 h), 40 min (0.67 h), 50 min (0.83 h), 1, 1.5, 2, 3, 4 and 5 h.

As expected, the vapor concentrations for all of the investigated components were much higher than those observed in the -10 °C evaporation experiments. Even so, acenaphtene was not measurable in the vapor during the entire evaporation experiment. We noticed large fluctuations for the vapor concentrations for a number of low boiling components such as cyclohexane (Figure 44), benzene (Figure 45), heptane (Figure 46) and octane (Figure 48). Other relatively higher boiling components such as the branched aromatics and the di-aromatics, seemed to evaporate in a more predictable way. The vapor concentration of isopropylcyclohexane (Figure 54), however, was low at the start of the experiment, reached a maximum of about $500 \mu\text{g}/\text{m}^3$ within 30 min, and fell below the detection limit of $3.3 \mu\text{g}/\text{m}^3$ within 90 min after the start of the experiment. Unfortunately, in none of the vapor samples of fuel sample II (Storage Tank), cycloheptane (Figure 49) could be detected. The samples from sample I however, indicate a decline of the evaporation for this component from an initial $2,100 \mu\text{g}/\text{m}^3$ to about 30 to $40 \mu\text{g}/\text{m}^3$ in 60-120 min.

After an initial high vapor concentration of more than $3,200 \mu\text{g}/\text{m}^3$ for toluene (Figure 47), the concentration decreased rapidly, varying between 10 and $200 \mu\text{g}/\text{m}^3$. The evaporation of benzene was far from constant and varied between nearly $4,000 \mu\text{g}/\text{m}^3$ and $20 \mu\text{g}/\text{m}^3$. Again, it seems that evaporation of this component is very much influenced by the remaining solvent mixture from which it evaporates. The evaporation profile for the alkane heptane was reasonably as expected and dropped after an initial high

⁴ The mono aromatics p-Xylene and m-Xylene could not be analysed individually, they were not separated in the 2D analysis.

vapor concentration of almost 4,000 $\mu\text{g}/\text{m}^3$ to about 300 $\mu\text{g}/\text{m}^3$. The concentration of octane in the vapor phase at the start of the evaporation experiment was one of the highest among the investigated components: up to 12,000 $\mu\text{g}/\text{m}^3$ after some 40 min it reached a very high concentration of almost 40,000 $\mu\text{g}/\text{m}^3$ for sample II, after which it declined to about 30 to 600 $\mu\text{g}/\text{m}^3$ at 2 h after the start of the experiment.

There is not enough meaningful data for isopropylcyclopentane (Figure 50) to interpret the evaporation profile of this component.

The summed vapor concentration for p- and m-xylene (Figure 52) follows a different profile for sample I compared to sample II. In the vapor originating from sample I starts at a relatively low concentration of about 14 $\mu\text{g}/\text{m}^3$ and increases to about 5,300 $\mu\text{g}/\text{m}^3$ at 30 min after which it drops to about 10 to 150 $\mu\text{g}/\text{m}^3$. The profile for sample II starts at a vapor concentration of about 3500 $\mu\text{g}/\text{m}^3$ until it deceases to 18 $\mu\text{g}/\text{m}^3$. So far we have no solid explanation for this marked discrepancy between these two fuel samples. The evaporation of o-xylene (Figure 53) starts at about 1,800 to 5,000 $\mu\text{g}/\text{m}^3$ and decreases within the hour to below 200 $\mu\text{g}/\text{m}^3$. The evaporation profiles for ethylbenzene (Figure 51) and isopropylbenzene (Figure 55) are quite comparable, the first starts at about 3,300 $\mu\text{g}/\text{m}^3$ and decreases to 6 $\mu\text{g}/\text{m}^3$, the second starts at about 1,600 $\mu\text{g}/\text{m}^3$ and decreases to about 6 $\mu\text{g}/\text{m}^3$, both within 1 h after the start of the experiment. Also the evaporation profiles for 2-ethyltoluene (Figure 56) and 1,2,3-trimethylbenzene (Figure 57) are reasonably comparable. Despite the fact that the concentration of these agents in the liquid fuel are comparable (see Table 3), the vapor concentrations at the start of the experiment differ considerably. In sample I the vapor concentration for 2-ethyltoluene starts at about 5,800 $\mu\text{g}/\text{m}^3$, whereas for sample II it starts at 1,400 $\mu\text{g}/\text{m}^3$. In sample I the vapor concentration for 1,2,3-trimethylbenzene starts at about 7,200 $\mu\text{g}/\text{m}^3$, whereas for sample II it starts at 1,500 $\mu\text{g}/\text{m}^3$. The decline in the vapor concentration seems to be comparable for both agents and levels off to about 40 to 75 $\mu\text{g}/\text{m}^3$.

The sudden decline in the vapor concentration in sample I for 1,2-diethylbenzene (Figure 58) at 10 min from about 9,500 $\mu\text{g}/\text{m}^3$ to 125 $\mu\text{g}/\text{m}^3$ and the increase to about 3,500 $\mu\text{g}/\text{m}^3$ is most remarkable. We have not observed this pattern in sample II where the vapor concentration starts at about 4,300 $\mu\text{g}/\text{m}^3$ and gradually declines down to 30 to 150 $\mu\text{g}/\text{m}^3$. The evaporation profile for naphtalene (Figure 59) is for sample I quite constant until it dropped from the initial value of 120 $\mu\text{g}/\text{m}^3$ to 65 $\mu\text{g}/\text{m}^3$. In sample II, the naphtalene vapor concentration peaks at 10 min to about 880 $\mu\text{g}/\text{m}^3$ after an initial vapor concentration of 130 $\mu\text{g}/\text{m}^3$ and then declined to about 8 $\mu\text{g}/\text{m}^3$. By using this sampling method (trapping on packed injector liners) the limit of detection is for naphtalene has improved spectacularly from about 110 $\mu\text{g}/\text{m}^3$ for the on-line direct injection of vapor to 7.5 $\mu\text{g}/\text{m}^3$.

III.6 Toxic load estimate of the JP-8 samples (T.O. 8)

In Table 4 the external exposures for the selected components are presented for the evaporation experiments at -10 and +20 °C. These exposures are expressed as concentration multiplied by time (C^*t) in $\text{mg} \cdot \text{min} \cdot \text{m}^{-3}$. For the experiments at -10 °C time was 96 h, for those at 20 °C 5 h.

In the following an attempt is made to perform a rough toxicological evaluation, by comparing the measured external exposure with existing military exposure guidelines (MEGs, USACHPPM 2004) and/or occupational exposure limits. Threshold limit values (TLV), permissible exposure limits (PEL), recommended exposure limits (REL) and/or short term exposure limits (STEL) were obtained from the websites of the Occupational Safety and Health Organization (OSHA) and the American Congress of Governmental Industrial Hygienists (ACGIH).

For four compounds, i.e. methanol, 1-butanol, 1,2-propanediol and styrene, this evaluation is very simple, as these compounds were not detected in the vapor originating from JP-8 at either -10 or +20 °C.

Therefore, no health effects are expected from these components.

For five other compounds, i.e. 2-ethyltoluene, 1,2-diethylbenzene, acenaphthene, cycloheptane and isopropylcyclopentane, neither MEG- nor TLV-values appear to exist. Consequently, it is not possible to perform a toxicological evaluation for these components based on the results of the evaporation experiments.

For benzene the highest exposure at 20 °C is 0.011 mg.m⁻³ for 5h (sample III). This value is well below the 8-h MEG (1.6 mg.m⁻³). At -10 °C the external exposure is 0.0006 mg.m⁻³, which is well below the 14-day MEG for this compound (0.16 mg.m⁻³). Both values are also well below the 1-year MEG of 0.039 mg.m⁻³. So, no health risks are anticipated as a result of exposure to benzene in the JP-8 vapor under these conditions.

For toluene,ethylbenzene, o-xylene and p,m-xylene the same conclusion can be drawn: the external exposures are well below the 8-h, 14-day and 1-year MEG-values as listed in the TG230 with January 2004 addendum.

For naphthalene only a 1-year MEG has been defined of 0.0071 mg.m⁻³. Both the exposure at -10 °C (0.015 mg.m⁻³) and at +20 °C (0.25 mg.m⁻³) are above this 1-year MEG. Obviously, a 1-year MEG is not the adequate standard for exposures of 96 and 5 h, respectively, but could be for personnel that is more or less continuously working with JP-8. Both the TLV- (TWA, ACGIH) and the PEL-values (OSHA) for naphthalene are listed as 10 ppm, which corresponds with 53 mg.m⁻³. The measured external exposures are well below these occupational safety and health values.

Table 4. Calculated external exposure⁵.

	Evaporation at -10 °C				Evaporation at +20 °C	
	Sample I Dose (mg.min.m ⁻³)	Sample II Dose (mg.min.m ⁻³)	Sample III Dose (mg.min.m ⁻³)	Sample IV Dose (mg.min.m ⁻³)	Sample I Dose (mg.min.m ⁻³)	Sample II Dose (mg.min.m ⁻³)
Methanol	0	0	0	0	0	0
1-butanol	0	0	0	0	0	0
1,2-propanediol	0	0	0	0	0	0
Styrene	0	0	0	0	0	0
Cyclohexane	3.18	6.85	15.60	10.32	3.18	6.85
Benzene	2.80	1.67	3.20	1.89	2.80	1.67
Heptane	24.17	17.50	24.58	27.50	24.17	17.50
Toluene	32.50	27.50	32.50	30.83	32.50	27.50
Octane	21.67	93.75	107.50	165.83	21.67	93.75
Cycloheptane	21.13	1.60	2.47	2.48	21.13	f.a.
Isopropylcyclopentane	4.00	11.97	12.58	14.90	4.00	11.97
Ethylbenzene	43.33	43.33	62.50	87.50	43.33	43.33
p,m-Xylene	129.58	134.17	200.83	292.08	129.58	134.17
o-Xylene	19.17	17.50	121.25	40.83	19.17	17.50
Isopropylcyclohexane	22.08	74.17	100.00	120.00	22.08	74.17
Isopropylbenzene	23.33	25.83	37.50	51.67	23.33	25.83
2-Ethyltoluene	125.83	144.58	111.67	164.58	125.83	144.58
1,2,3-Trimethylbenzene	145.00	161.67	154.58	102.92	145.00	161.67
1,2-Diethylbenzene	36.25	45.00	28.33	30.83	36.25	45.00
Naphthalene	70.00	73.75	38.33	86.25	70.00	73.75
Acenaphthene	n.d.	n.d.	n.d.	n.d.	n.d.	n.d.

⁵ Evaporation of 1 ml of jet fuel (JP-8) at -10 °C and +20 °C, relative humidity <15 % and 70%, respectively. The air flow was set at 5 m.s⁻¹.

For heptane and octane TLV values have been defined of 1,670 mg.m⁻³ (ACGIH) and 1,400 mg.m⁻³ (ACGIH), respectively. The OSHA PEL for octane for maritime workers is 1,900 mg.m⁻³, the OSHA PEL for heptane is 2,000 mg.m⁻³. In our evaporation experiments the calculated external exposures are at least three orders of magnitude lower than these TLV and PEL values. The same holds for cyclohexane, for which the TLV (ACGIH), PEL (OSHA), and REL (NIOSH) are 1,030, 1,050 and 1,050 mg.m⁻³, respectively.

The TLV (ACGIH) for 1,2,3-trimethylbenzene is set at 125 mg.m⁻³, that of isopropylbenzene at 250 mg.m⁻³. Also for these components the external exposures as calculated on the basis of the evaporation experiments is well below these TLV values.

In summary, for none of the individual components of interest for which a form of exposure guideline exist a health risk is anticipated under the chosen evaporation scenarios.

However, it needs to be stressed here that the toxicity of combinations and mixtures is very hard to predict, since both synergistic and antagonistic effects may occur. Although currently the topic gets more and more attention, there are still no adequate models available to predict the overall toxicity of highly complex mixtures such as JP-8 from measurements of the external exposures of individual components. Furthermore, it is argued that inhalation of JP-8 aerosols may be more toxic than inhalation of vapors (NRC, 2003). Recently, it was demonstrated that the chemical composition of aerosols and vapors differs (Gregg *et al.*, 2007), which may be a partial explanation of toxicity difference.

The most appropriate way to estimate toxic effects on humans of combinations and mixtures is via studies in an animal model that is relevant for man, which is in itself difficult enough. In addition, some *in vitro* systems may provide useful information. Recently, we have observed that human A549 lung cells in culture in a CULTEX® apparatus, when exposed to controlled mixtures of toxic substances, show different cellular responses to the combination of components than to each of the individual substances, and also with a high sensitivity (Van der Kleij, personal communication, 2007).

Obviously, evaluation of potential adverse health effects of respiratory exposure to vapors and/or aerosols of JP-8 and of dermal exposure to JP-8 vapors, aerosols and liquid requires more study, in which the GCxGC-technology would be a highly useful tool.

III.7 Suggestions for further research

A next step for future research on jet fuels could be made by investigating the effects of other temperature settings, especially low temperature, but also the effects of the amount of liquid used for the experiment on the evaporation profile. Another aspect is the influence of material the fuel is spread on, like concrete and asphalt.

Next to the risks of exposure of involved personnel to jet fuel vapor there is the risk of exposure to jet fuel aerosol particles. Aerosol particles tend to deposit more efficiently in the airways such as the bronchi and the larynx than vapor. This phenomenon is influenced by the tissue-air partition and wash-in and wash-out effects of the investigated agents in the upper-airways. Due to the physical characteristics, these particles tends to deposit mostly in the bronchi after which the chemicals which are presents in the particles, migrate into the lung cells followed by diffusion into the arterial blood stream.

The formation of aerosols depends among others on the presence of condensation particles such as smoke or water particles (mist) but also on environmental conditions, especially cold weather conditions.

Armendariz *et al* (2003) has pointed out some aspects concerning the formation of aerosols of jet propulsion fuel under cold weather conditions but also with respect to the analysis of these particles, such as:

- 1) The variability in particle size.

There seems to be a strong relationship between the particle size, its penetration depth and deposition efficiency into the lungs. The particle size is influenced by the combination of temperature and humidity and the presence of condensation particles such as smoke particles from combustion engines like used in jet planes.

2) The integrity of the aerosol samples from sampling to analysis

Aerosol particles formed under arctic conditions (for instance < -25 °C) are most likely not stable in terms of their chemical composition if transported and warmed up for analysis. Also, due to this warming up the distribution of the particles size may alter.

3) Chemical composition of jet fuel aerosol particles in relation to temperature.

From our evaporation experiments of the jet fuel samples at two different temperatures (-10 °C and +20 °C) it became clear that the composition of the vapor is very much influenced by the evaporation temperature. It is logical, due to the differences in boiling point and polarity of the chemicals present in the jet fuel that the condensation to aerosol particles is influenced by the temperature. Next, in the formation state of the particles the chemical composition is constantly altering in time and most probably in particle size.

4) Determine the total exposure to jet fuel aerosol particles.

This is probably one of the most difficult questions to answer. A common method is to determine the dose of a number of selected chemicals in the jet fuel aerosol in relation to the concentration of these chemicals in the jet fuel. Due to the limitation of analyzing techniques, this is a very rough estimation, while a number of toxic very potent components tend to be underestimated or ignored in this way.

Multidimensional techniques such as GCxGC could provide a capability to discriminate between the classes of toxicants and between individual components.

5) Neurological response.

There are a number of papers indicating the toxicological effect of aerosols compared to vapors of jet fuel. There are also indications that this effect is influenced by the smoking behavior of the exposed population. Also, exposure experiments with jet fuel vapor performed with mice and rats show for these animals a high neurological sensitivity. To estimate the toxicological risk or the neurological response for humans to JP-8 aerosols, these animals are well suited for human exposure studies. Small scale nose-only exposure studies with rats to JP-8 aerosols under arctic conditions could contribute to understand the relation of neurological response and the combined chemical exposure of JP-8 aerosol particles.

Clearly there is a need for gathering more information on the physical process during these cold weather conditions. Also, to understand the uptake of vapor/ aerosol combination in the lungs as well as the dermal uptake (the latter is probably of less toxicological importance for aerosols) toxicokinetic experiments for relevant exposition scenarios under controlled conditions in laboratory animals is an important step. By screening blood for 'intact' components and specific biomarkers (e.g. benzene oxide adducts to albumin for benzene exposure), valuable information could be obtained for the toxicokinetics of the investigated neurotoxic components and formed metabolites.

Exposing groups of rats to predetermined (= synthetically composed) aerosols at different temperatures to establish a neurotoxic response (e.g. EEG, MRI, behavioral test) would provide insight into the toxicological effects of the various aerosols with presumably different compositions. As it is very difficult to expose animals whole body under cold weather conditions it is necessary to make some adaptations to the aerosol composition due to the change by evaporation of the low boiling components in the jet fuel mixture. A possibility is to distill the fraction of interest and use this for the aerosol experiments.

Proteome analysis is also an option for a more generic approach to understand which proteins are up or down regulated as a result of an exposure to JP8 aerosol and vapor. Hopefully there are specific early responding proteins for instance in cerebrospinal fluid which are related to the expected neurological damage. Maybe this could lead to an early warning test for these syndromes, as suggested by Dr. Kristin Heaton (USARIEM).

V. CONCLUSIONS

1. Comprehensive Gas Chromatography (GCxGC) in combination with Time of Flight Mass Spectrometry (ToF-MS) is a highly suitable technology for analysis of complex fuel samples such as JP-8.
2. From the top 20 target list of suspected neurotoxic components, provided by Dr. Susan Proctor (USARIEM), styrene, methanol, 1-butanol and 1,2-propanediol could not be detected in any of the four investigated fuel samples from different sources.
3. Small and large differences within two US originated fuel samples and two Dutch originated fuel samples could be clarified by zooming into specific classes or individual components.
4. An off-line and an on-line vapor sampling system was configured and connected to the GCxGC-ToF-MS system, which was successfully applied for the analysis of jet fuel vapor samples.
5. A small scale evaporation unit was constructed to evaporate the fuel samples at predetermined environmental conditions. In this way, airflow, humidity and temperature can be controlled throughout the evaporation experiment.
6. The variations in the vapor concentration of the investigated components between the -10 °C and the +20 °C evaporation experiments is huge.
7. There is no apparent relationship between the measured evaporation profiles of the selected components in the various JP-8 samples and their composition as measured in the liquid fuel itself. The effects of all other constituents in JP-8 outweigh the subtle differences in concentration of the selected components.
8. A rough toxicological evaluation learns that for none of the individual components of interest for which military or civilian occupational exposure guidelines exist a health risk is anticipated under the chosen evaporation scenarios. It is stressed here that only vapor exposure has been considered here.
9. A more meaningful (neuro) toxicological evaluation requires more study on the effect of combinations and mixtures of components in JP-8 and is preferentially performed by exposing laboratory animals via the respiratory route to vapors and aerosols of JP-8 and dermal exposure to JP-8 vapors, aerosols, and/or liquid. As an alternative, it could be attempted to assess the toxicity of JP-8 vapors, aerosols and liquid in a relevant *in vitro* screening system.

REFERENCES

- Armendariz, Alfredo J. and David Leith, "A Personal Sampler for Aircraft Engine Cold Start Particles: Laboratory Development and Testing", American Industrial Hygiene Association Journal, **64**: 755-762 (2003).
- Armendariz, Alfredo J., David Leith, Maryanne Boundy, Randall Goodman, Les Smith and Gary Carlton, "Development and Field Demonstration of an Electrostatic Personal Particle Sampler", American Industrial Hygiene Association Journal, **64**: 777-784, (2003).
- ATSR, Toxicological profile for JP-5 and JP-8, U.S. Department of Health and Human Services, Public Health Service, Agency for Toxic Substances and Registry, (June 1998).
- Baldwin, C.M., Figueiredo, A.J., Wright, L.S., Wong, S.S., and Witten, M.L., Repeated aerosol-vapor JP-8 jet fuel exposure affects neurobehavior and neurotransmitter levels in a rat model. *J. Toxicol. Environ. Health A.*, (2007), **70**, 1203-1213.
- Baynes, R.E., Brooks, J.D., Budsaba, K., Smith, C.E., and Riviere J.E., Mixture effects of JP-8 additives on the dermal disposition of jet fuel components, *Toxicol. Appl. Pharmacol.*, (2001), **175**, 269-281.
- Beens J., Blomberg J., and Schoenmaker P.J., Proper tuning of Comprehensive two-dimensional gas chromatography to optimize the separation of complex oil fractions, *J. High Resol. Chromatogr.*, (2000), **23**, 182-188.
- Beens, J., Boelens, H., Tijssen, R., Blomberg, J., Quantitative aspects of comprehensive two-dimensional gas chromatography (GCxGC), *J. High Resol. Chromatogr.*, (1998), **21**, 47-54.
- Blomberg, J., Schoenmaker, P.J., Beens, J., and Tijssen, R., Comprehensive two-dimensional gas chromatography and its applicability to the characterization of complex (petrochemical) mixtures, *J. High Resol. Chromatogr.*, (1997), **20**, 539-544.
- Blomberg, J., and Brinkman, U.A.Th., Practical and theoretical aspects of designing a flame-ionization detector/ mass spectrometer Deans' switch Pressure- flow relations in gas chromatograph-detector interfaces using vacuum outlet conditions., *J. Chrom. A.*, (1999), **831**, 257-265.
- Bruckner, C. A., Prazen, B.J. and Synovec, R.E., Comprehensive Two-dimensional high-speed gas chromatography with chemometric analyses, *Anal. Chem.*, (1998), **70**, 2796-2804.
- Carlto, G.,N., Smith, L.,B., Exposures to jet fuels and benzene during aircraft fuel tank repair in the U.S. Air Force, *Appl. Occup. Environ. Hyg.*, (2000), **15**(6), 485-491.
- Chao, Y-C., E., Gibson, R.L., and Nylander-French, L.A., Dermal exposure to jet fuel (JP-8) in US Air Force personnel, *Ann. Occup. Hyg.*, (2005), **49**(7), 639-645.
- Cooper, J.R. and Mattie, D.R., Developmental toxicity of JP-8 jet fuel in the rat, *J. Appl. Toxicol.*, (1996), **16**(3), 197-200.
- Dick, F.D., Solvent Neurotoxicity, *Occup Environ Med*, (2006), **63**, 221-226.
- Deursen van, M., Beens, J., Reijenga, J., Lipman, P., and Cramers, C., Group type identification of oil samples using comprehensive two-dimensional gas chromatography coupled to a Time-of-Flight Mass spectrometer (GCxGC-TOF), *J. High Resol. Chromatogr.*, (2000), **23**, 507-510.

Edam, R., Blomberg, J., Janssen, H.G., Schoenmaker, P.J., Comprehensive Multi-dimensional chromatographic studies on the separation of saturated hydrocarbon ring structures in petrochemical samples, *J. Chrom. A*, (2005), **1086**, 12-20.

Fechter, L. D., Gearhart, C., Fulton, S., Campbell, J., Fisher, J., Na, K., Cocker, D., Nelson-Miller, A., Moon, P., Pouyatos, B., JP-8 Jet Fuel Can Promote Auditory Impairment Resulting From Subsequent Noise Exposure in Rats, *Toxicol. Sci.* (2007a), **98**, 510-525.

Fechter, L.D.D., Gearhart, C., Fulton, S., Campbell, J., Fisher, J., Na, K., Cocker, D., Nelson-Miller, A., Moon, P., and Pouyatos, B., Promotion of Noise-Induced Cochlear Injury by Toluene and Ethylbenzene in the Rat, *Toxicol. Sci.* (2007b), **98**, 542-551.

Federal Facilities Assessment Branch, Division of Health Assessment and Consultation, Agency for Toxic Substances and Disease Registry, ATSDR-PHA (Public Health Assessment) Naval air station Fallon (a/k/a Fallon Naval Air Station) Fallon, Churchill County, Nevada, USA, (2003),
http://www.atsdr.cdc.gov/HAC/PHA/fallon/nas_p0.html

Fraga, C.G., Prazen, B.J., and Synovec, R.E., Comprehensive two-dimensional gas chromatography and chemometrics for the high-speed quantitative analysis of aromatic isomers in a Jet Fuel using the standard addition method and a n objective retention time alignment algorithm, *Anal. Chem.*, (2000), **72**, 4154-4162.

Frysinger, G.S. and Gaines, R.B, Determination of oxygenates in gasoline by GC-GC, *J. High Resol. Chromatogr.* (2000), **23**, 197-201.

Frysinger, G.S., Gaines, R.B and Ledford, E.B., Quantitative determination of BTEX and Total aromatic compounds in gasoline by comprehensive Tow-dimensional gas chromatography (GCxGC), *J. High Resol. Chrom.*, (1999), **22**, (4), 195-200

Frysinger, G.S. and Gaines, R.B, Separation and identification of petroleum biomarkers by comprehensive two-dimensional gas chromatography, *J. Sep. Sci.*, (2001), **24**, 87-96.

Gregg, S.D., Fisher, J.W., and Bartlett, M.G., A Review of analytical methods for the identification and quantification of hydrocarbons found in jet propellant 8 and related petroleum based fuels, *Biochem. Chrom.*, (2006), **20**, 492-507.

Gregg, S.D., Campbell, J.L., Fisher, J.W., and Bartlett, M.G., Methods for the characterization of Jet Propellant-8: vapor and aerosol, *Biochem. Chrom.*, (2007), **21**, 463-472.

Harris, D.T., Sakiestewa, D., Robledo, R.F., and Witten, M., Short-term exposure to JP-8 jet fuel results in long-term immunotoxicity, *Toxicol. Indus. Health*, (1997), **13**(5), 559-570.

Johnson, K.J., Synovec, R.E., Pattern recognition of jet fuels: comprehensive GCxGC with ANOVA-based feature selection and principal components analysis, *Chemom. Intel. Labor. Sys.*, (2002), **60**, 225-237.

Kanikkannan, N., Patel, R., Jackson, T., Sudhan M., and Singh, M., Percutaneous absorption and skin irritation of JP-8 (jet fuel), *Toxicol.*, (2001), **161**, 1-11

Kim D., Anderssen, M.E. and Nylander-French, L.A., Dermal absorption and penetration of jet fuel components in humans, *Toxicol. Lett.*, (2006), **165**, 11-21

- Kim, D. Anderssen, M.E., and Nylander-French, L.A., A Dermal toxicokinetic model of human exposure to jet fuel, *Toxicol. Sci.*, (2006), **93**, 22-33.
- Lavine, B.K., Moores, A.J., Mayfield, H., and Faraque, A., Genetic algorithms applied to pattern recognition analysis of high-speed gas chromatograms of aviation turbine fuels using an integrated jet-A/JP-8 database, *J. Microchem.*, (1999), **61**, 69-78.
- Liu, Z.Y., Philips, J.B.J., Comprehensive two-dimensional gas chromatography using an on-column thermal modulator interface, *J. Chromatogr. Sci.*, (1991), **29**, 227-231.
- Mayfield, H.T., JP-8 Composition and variability, Final tech. rep., AL/EQ-TR-1996-0006, (1996)
- Muhammad, F., Monteiro-Riviere, N.A., Baynes, R.E., and Riviere, J.E., Effect of *in vivo* jet fuel exposure on subsequent *in vitro* dermal absorption of individual aromatic and aliphatic hydrocarbon fuel constituents. *J. Toxicol. Environ. Health., part A*, (2005), **68**, 719-737.
- Nessel, C.S., A comprehensive evaluation of the carcinogenic potential of middle distillate fuels, *Drug Chem. Toxicol.*, (1999), **22**(1), 165-180.
- NRC, Permissible Exposure Levels for Selected Military Fuel Vapors, National Academy Press, (1996).
- NRC, Toxicologic assessment of Jet-Propulsion Fuel 8, National Academies Press, (2003).
- Puhala II, E., Lemasters, G., Smith, L., Talaska, G., Simpson, S., Joyce, J., Trinh, K., and Lu, J., Jet fuel exposure in the United States Air Force. *Appl. Occup. Environ. Hyg.*, (1997), **12**(9), 606-610.
- Reichenbach, S.E., Ni, M., Kottapalli, V., Visvanathan, A., Ledford, E.B., Oostdijk, J. and Trap, H.C., Chemical warfare agents detection in complex environments with comprehensive two-dimensional gas chromatography, *Chemical and Biological Sensing*, (2003), 28-36.
- Riviere, J.E., Brooks, J.D., Monteiro-Riviere, N.A., Budsaba, K., and Smith, C.E., Dermal absorption and distribution of topical dosed jet fuels Jet-A, JP-8, and JP-8(100), *Toxicol. Appl. Pharmacol.*, (1999), **160**, 60-75.
- Schoenmaker, P.J., Oomen, J.L.M.M., Blomberg, J., Genuit, W., and Van Velzen, G., Comparison of comprehensive two-dimensional gas chromatography and gas chromatography – mass spectrometry for the characterization of complex hydrocarbon mixtures, *J. Chrom. A.*, (2000), **892**, 29-46.
- Serdar, B., Egeby, P.P., Waidyanatha S., Gibson, R., and Rappaportt, S.M., Urinary biomarkers of exposures to jet fuel (JP-8), *Environ. Health Persp.*, (2003), **111**(14), 1760-1764.
- Spila, E., Secgi, E., and Bernabei, M., Determination of organophosphate contaminants in jet fuel, *J. Chrom. A.*, (1999), **847**, 331-337.
- Tu, R.H., Mitchell, C.S., Kay, G.G., and Risby, T.H., Human exposure to the jet fuel, JP-8, *Aviat Space Environ. Med.*, (2004), **75**(1), 49-59.
- USACHPPM, Chemical Exposure Guidelines for Deployed Military Personnel, USACHPPM Technical Guide 230, Version 1.3 – With January 2004 Addendum (2004).
- Van der Kleij, D., TNO Defense, Security and Safety, Rijswijk, October 2007, personal communication.

Van Mispelaar, V.G., Smilde, A.K., De Noord, O.E., Blomberg, J., and Schoenmaker, P.J., Classification of highly similar crude oils using data sets from comprehensive two-dimensional gas chromatography and multivariate techniques, *J. Chrom. A*, (2005), **1096**, 156-164.

Wang, G., Karnes, J., Bunker, C.E., and Geng, M.L., Two-dimensional correlation coefficient mapping in gas chromatography: Jet Fuel classification for environmental analysis, *J. Mol. Structure*, (2006), **799**, 247-252.

Yang, J-H, Lee, C-H., Monteiro-Riviere, N.A., Riviere, J.E., Tsang, C-L., and Chou, C-C., Toxicity of jet fuel aliphatic and aromatic hydrocarbon mixtures on human epidermal keratinocytes: evaluation based on *in vitro* cytotoxicity and interleukin-8 release, *Arch. Toxicol.*, (2006), **80**, 508-523.

Zimmer, H., Uhlich, H., Knecht, U., and Triebig, G., Biological monitoring of experimental human exposure to hydrocarbon solvent mixtures, *Toxicol. Lett.*, (2006), **162**, 263-269.

**ANNEX A. Statement of Work/Technical Objectives FOR COOPERATIVE AGREEMENT
W81XWH-07-1-0002 (May 10, 2006)**

The goal that is set for the proposed research is:

To screen Jet Fuel JP-8 samples on neurotoxic compounds. The presence of these compounds in fuels could have an impact on the toxic load of the vapors of these fuels during the evaporation. An attempt will be made by means of pattern recognition to discriminate between several brands of JP-8 with respect to the presence of these compounds, which may have implications for their toxicity.

First quarter

1. Several GC-column combinations will be tested for optimal separation of the fuel samples.
2. It will be investigated whether the chromatographic system is optimal for the proposed fuel vapor analysis: trapping on an injection liner filled with a solid adsorbent (e.g. Tenax) or direct injection with a large volume syringe followed by cryofocusing and flash heating.

Second quarter

3. A ToF-MS connected to the GCxGC system will be used to screen and identify a large number of neurotoxic components in the fuel samples.
4. The ChromaTOF software will be used for pattern recognition and to differentiate between several brands of fuel samples.

Third quarter

5. Up to twenty compounds of interest with respect to neurotoxicity, or groups/classes thereof, will be quantified in several fuel brands and aged jet fuel. The compounds of interest and the scenarios will be chosen after conferring with USARIEM (Dr. Sue Proctor).

Fourth quarter

6. A device will be constructed to simulate some evaporation scenarios of fuel spills in direct relation with the residual amount of liquid fuel, temperature and humidity.
7. With the device constructed in t.o. 6 and the analytical method developed in t.o. 2 the concentration time course will be measured for a specific number (up to 20) of components for two relevant scenarios.
8. Based on the concentration profile of the neurotoxic agents in the vapor it will be attempted to estimate for the toxic load for this multi-component mixture under the scenarios mentioned in t.o. 7.

ANNEX B Analytical reference standards

Materials

Table 5. Content of the Gasoline refinery standard ASTM/EPA

Benzene	1,2,4-Trimethylbenzene
Toluene	1,2,3-Trimethylbenzene
Ethylbenzene	Indan
m-Xylene	p-Diethylbenzene
p-Xylene	n-Butylbenzene
o-Xylene	o-Diethylbenzene
Isopropylbenzene	1,2,4,5-Tetramethylbenzene
n-Propylbenzene	1,2,3,5-Tetramethylbenzene
m-Ethyltoluene	Naphthalene
p-Ethyltoluene	1-Methylnaphthalene
1,3,5-Trimethylbenzene	2-Methylnaphthalene
2-Ethyltoluene	Isooctane

Table 6. Content of the naphtene mixture ASTM-P-0034

Cyclopentane	1-Ethyl-1-methylcyclopentane
Methylcyclopentane	cis-1,2-Dimethylcyclohexane
Cyclohexane	trans-1,2-Dimethylcyclohexane
EthylCyclopentane	trans-1,4-Dimethylcyclohexane
1,1-Dimethylcyclopentane	Isobutylcyclopentane
trans-1,2-Dimethylcyclopentane	n-Butylcyclopentane
cis-1,3-Dimethylcyclopentane	ctc-1,2,4-Trimethylcyclohexane
trans-1,3-Dimethylcyclopentane	ctt-1,2,4-Trimethylcyclohexane
Methylcyclohexane	ccc-1,2,4-Trimethylcyclohexane
Isopropylcyclopentane	Isopropylcyclohexane
n-Propylcyclopentane	1,1,2-trimethylcyclohexane
ccc-1,2,3-Trimethylcyclopentane	1,1,4-trimethylcyclohexane
ctc-1,2,3-Trimethylcyclopentane	Isobutylcyclohexane
ccc-1,2,4-Trimethylcyclopentane	t-1-Methyl-2-propylcyclohexane
ctc-1,2,4-Trimethylcyclopentane	t-1-Methyl-2-(4MP)cyclopentane

ANNEX C 3D PLOTS OF JET FUEL ANALYSIS

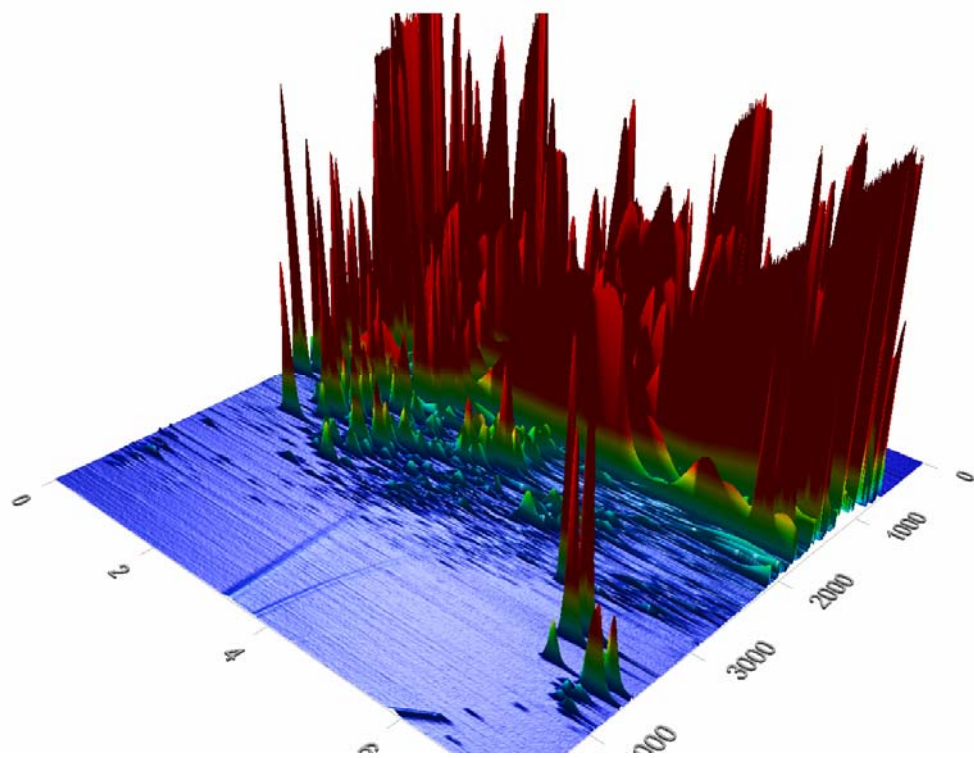


Figure 24. 3D plot of the TIC signal of an 2D gas chromatographic separation of JP-8 using a reversed column combination consisting of a polar first dimension column and a non-polar second dimension column.

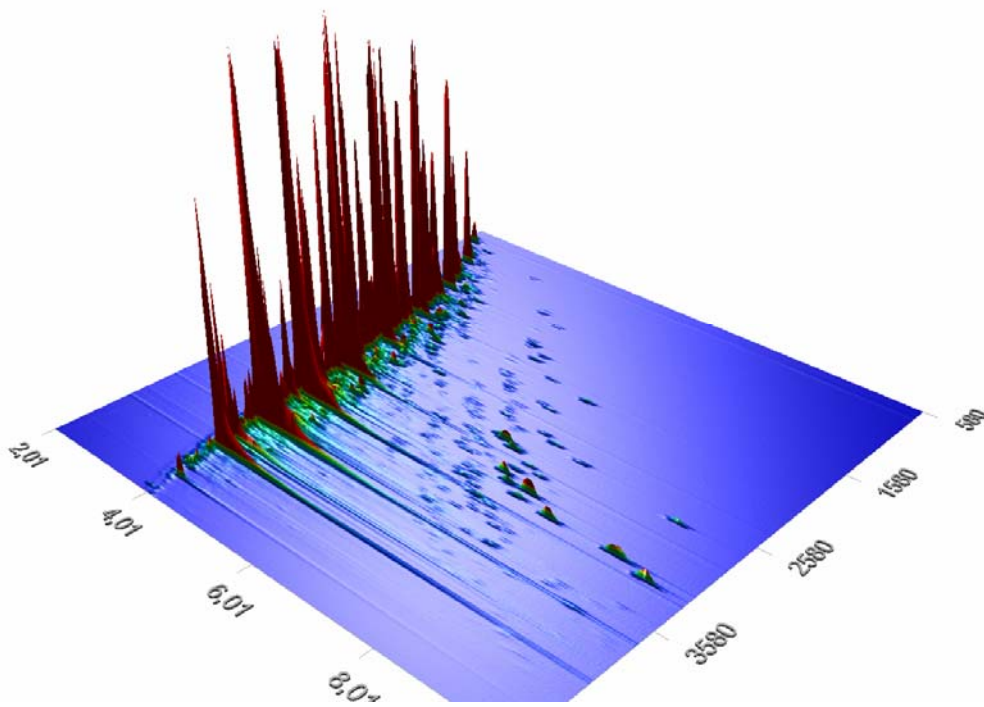


Figure 25. 3D plot of the summed masses of 71, 85 and 99 of the 2D gas chromatographic separation of JP-8 using a medium non-polar first dimension column and a polar second dimension column .

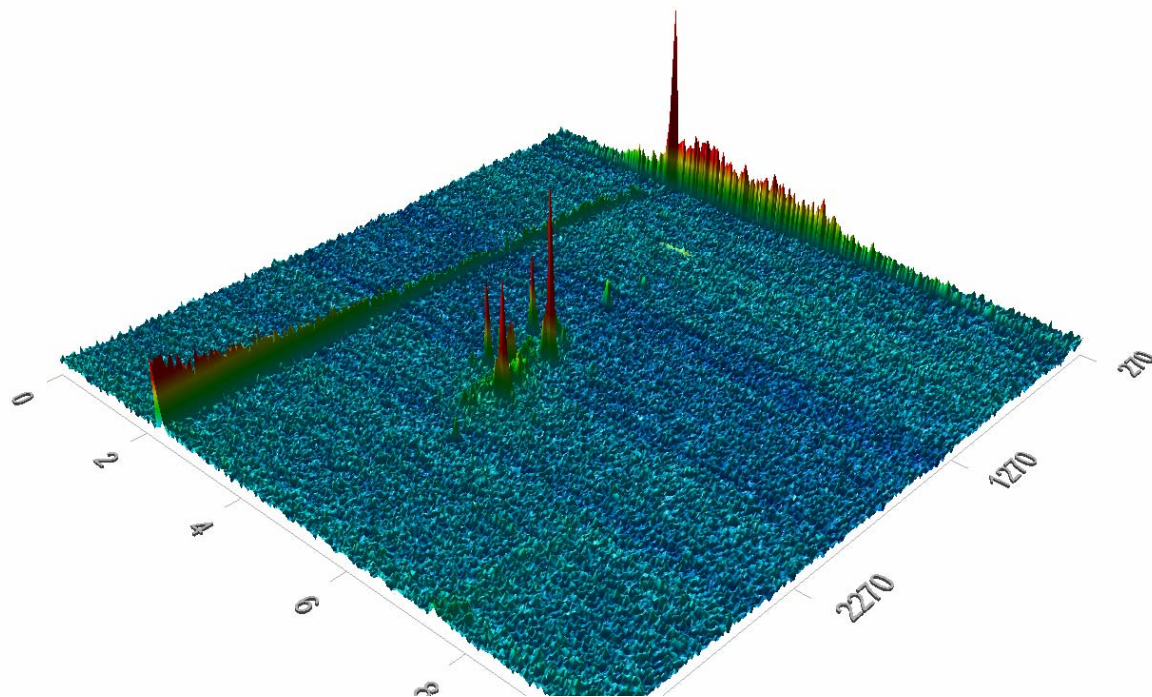


Figure 26. 3D plot of the modulated chromatogram (mass 83, which represents the cyclohexanes) of the vapor at 80 h after start of the evaporation of JP-8 sample I (KC135), at -10 °C.

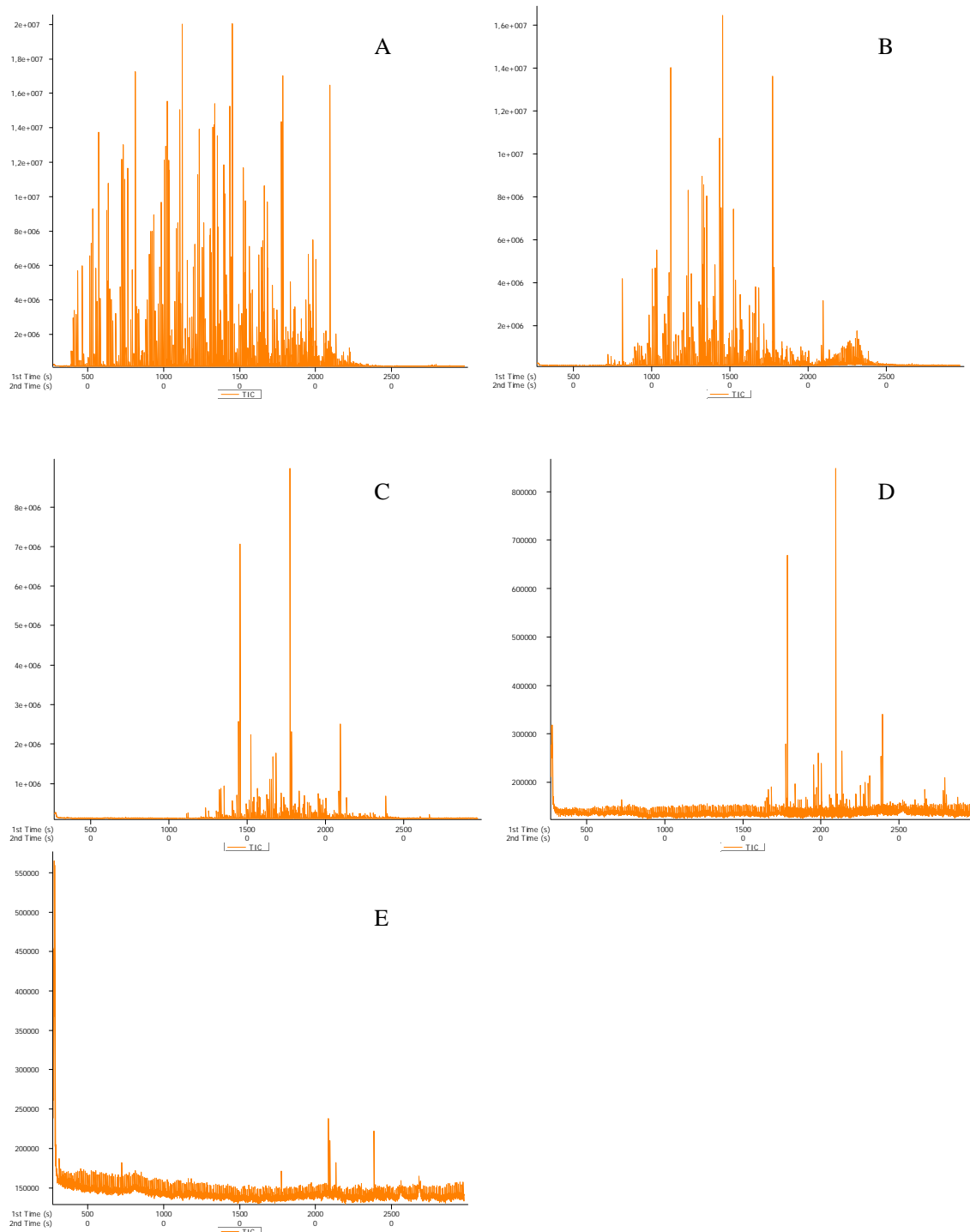
ANNEX D EVAPORATION PROFILE OF THE KC135 JP-8 SAMPLE


Figure 27. The modulated chromatograms of the vapor of the KC135 JP-8 sample (I) evaporated at -10 °C. After 5 min (A), after 1 hr (B), after 10 hr (C), after 24 hr (D) and after 80 hr (E) from the start of the experiment.

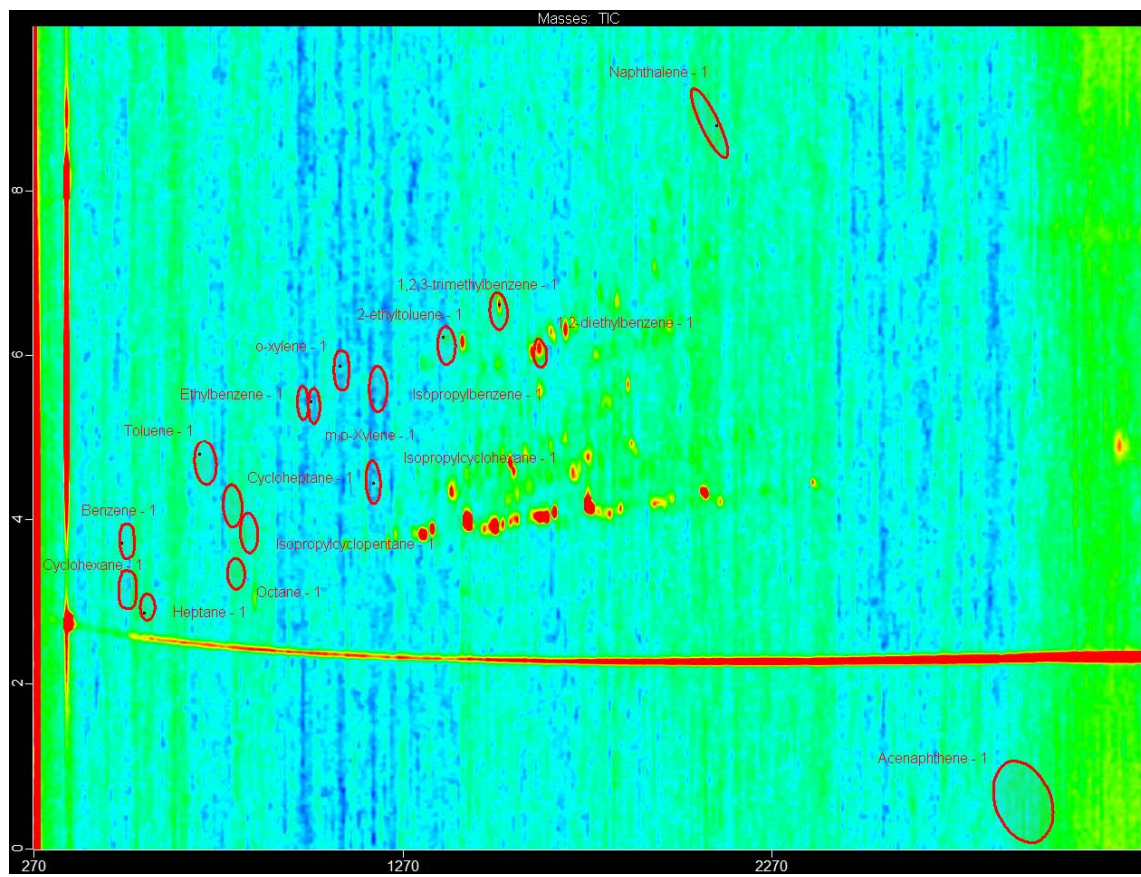
ANNEX E 2D PLOT OF THE KC135 JP-8 SAMPLE


Figure 28. A 2D plot of the vapor analysis, sample taken at 80 h after start of the evaporation of the JP-8 sample I (KC135) at -10 °C. The red circles indicated the regions where the neurotoxic components from the target list (see Table 1) emerge in the 2D plot.

ANNEX F VAPOR CONCENTRATION TIME COURSES OF THE NEUROTOXIC COMPONENTS IN JP-8 VAPOR AT -10 °C.

Table 7. Concentration time course of 9 neurotoxic components in JP-8 vapor at -10 °C, sample I (KC135). Concentrations in $\mu\text{g.m}^{-3}$. b.d. = below detection limit

Time (h)	Cyclo- hexane	Benzene	Heptane	Toluene	Octane	Cyclo- heptane	Isopropyl- cyclopentane	Ethyl- benzene	p,m- Xylene
0.08	776	403	3,252	2,327	4,526	583	135	1,427	8,178
1.23	b.d.	1.91	26.6	53.0	831	74.4	18.6	311	2,090
2.38		1.53	2.00	2.34	132	6.74	2.94	195	456
3.52		1.39	b.d.	2.13	b.d.	28.5	b.d.	69.5	153.
4.67		1.35	1.75	1.78	5.41	b.d.		29.2	55.4
5.81		1.21	b.d.	1.71	b.d.	2.14		20.8	35.1
6.95		1.42	b.d.	0.39		0.76		14.9	20.9
8.09		1.25	b.d.	1.26		b.d.		12.1	14.2
9.23		1.37	b.d.	0.49				11.0	11.5
10.37		1.36	b.d.	0.68				10.6	10.5
11.51		1.37	b.d.	1.49				10.4	9.99
12.64		1.28	b.d.	0.61				10.3	9.75
13.78		1.39	b.d.	0.44				9.90	9.81
14.92		1.38	b.d.	0.54				9.85	9.37
16.05		1.31	1.90	0.81				10.2	9.56
17.18		1.30	b.d.	0.76				10.2	9.56
18.32		0.99	b.d.	0.98				10.2	9.46
19.47		1.00	b.d.	0.00				10.3	9.67
20.61		1.17	b.d.	0.91				10.1	9.27
21.76		1.06	b.d.	0.93				10.1	9.36
22.90		1.28	1.62	0.28				10.1	9.33
24.05		1.23	b.d.	0.75				10.1	9.21
25.19		1.27		0.73				10.1	9.17
26.34		1.19		0.87				10.0	9.05
27.48		1.21		0.74				9.99	9.02
28.63		1.16		0.78				9.95	8.93
30.91		1.27		0.36				9.98	8.98
32.05		1.19		0.00				9.92	8.85
33.19		1.26		0.53				9.77	9.37
34.33		1.29		0.51				9.97	b.d.
35.47		1.21		0.51				9.94	8.89
36.61		1.21		0.40				b.d.	b.d.
37.75		1.40		0.85				9.90	8.79
38.88		1.16		0.45				9.88	8.74
40.02		1.10		0.36				9.99	9.01
41.15		1.10		0.83				9.88	8.76
42.28		1.13		0.43				9.96	8.94
43.41		1.00		0.61				b.d.	b.d.
44.54		0.93		0.65				9.82	8.60
45.67		1.26		0.71				b.d.	b.d.
46.80		1.23		0.54				9.83	8.62
47.94		1.15		0.64				9.93	8.88

Table 8. Concentration time course of 9 neurotoxic components in JP-8 vapor at -10 °C, sample I (KC135) - Continued. Concentrations in $\mu\text{g.m}^{-3}$. b.d. = below detection limit

Time (h)	Cyclohexane	Benzene	Heptane	Toluene	Octane	Cycloheptane	Isopropylcyclopentane	Ethylbenzene	p,m-Xylene
49.09	b.d.	0.58	b.d.	0.49	b.d.	b.d.	b.d.	9.73	8.88
50.23		0.93		0.50				9.87	8.73
51.38		b.d.		0.52				9.89	8.76
52.52		b.d.		0.60				9.93	8.86
53.67		b.d.		0.63				b.d.	b.d.
54.81		0.22		0.55				b.d.	b.d.
55.95		0.14		0.61				b.d.	b.d.
57.09		b.d.		0.50				b.d.	b.d.
58.23		b.d.		0.65				9.82	8.59
59.37		0.24		0.59				9.87	8.72
60.51		0.21		0.63				b.d.	b.d.
61.65		0.29		0.56				b.d.	8.58
62.79		0.28		0.57				9.80	8.54
63.93		b.d.		0.62				9.86	8.70
65.07		0.42		0.44				b.d.	b.d.
66.21		0.26		0.50				b.d.	b.d.
67.35		0.23		0.57				9.82	8.59
68.49		0.18		0.50				b.d.	b.d.
69.63		b.d.		0.52				b.d.	b.d.
70.77		b.d.		0.55				9.79	8.52
71.92		0.13		b.d.				b.d.	8.51
73.06		0.19		0.51				b.d.	b.d.
74.20		0.19		0.46				b.d.	b.d.
75.35		0.17		0.46				b.d.	b.d.
76.49		b.d.		0.49				b.d.	b.d.
77.64		0.14		0.53				b.d.	b.d.
78.78		0.10		0.53				b.d.	b.d.
79.92		0.16		0.50				9.87	8.72
81.06		b.d.		0.47				9.75	8.43
82.19		b.d.		b.d.				b.d.	b.d.
83.33		b.d.		b.d.				b.d.	b.d.
84.47		b.d.		b.d.				b.d.	b.d.
85.62		b.d.		b.d.				b.d.	b.d.

Table 9. Concentration time course of 8 neurotoxic components in JP-8 vapor at -10 °C, sample I (KC135). Concentrations in $\mu\text{g} \cdot \text{m}^{-3}$. b.d. = below detection limit.

Time (h)	o-Xylene	Isopropyl-cyclohexane	Isopropyl-benzene	2-Ethyl-toluene	1,2,3-Trimethylbenzene	1,2-Diethyl-benzene	Naphthalene	Acenaphthene
0.08	2,068	287	604	2,456	3,517	b.d.	217	b.d.
1.23	593	104	195	802	1,004	b.d.	130	
2.38	173	44.1	69.6	346	462	259	111	
3.52	75.6	25.0	35.0	218	319	205	110	
4.67	40.3	15.6	18.2	145	231	b.d.	110	
5.81	33.6	16.1	17.5	178	325	224	114	
6.95	26.9	13.3	13.8	167	336	248	114	
8.09	21.2	8.96	9.82	133	299	116	114	
9.23	19.8	34.0	7.73	110	274	b.d.	117	
10.37	19.2	5.67	5.96	85.6	246	b.d.	113	
11.51	18.8	5.74	5.06	70.0	220	b.d.	110	
12.64	18.7	14.4	4.34	55.9	196	b.d.	124	
13.78	18.6	10.9	4.18	46.0	175	b.d.	112	
14.92	18.4	7.86	3.61	30.9	127	b.d.	114	
16.05	18.5	4.10	b.d.	25.5	114	b.d.	110	
17.18	b.d.	4.71	3.61	18.5	83.6	b.d.	113	
18.32	b.d.	3.77	b.d.	11.0	51.3	111	110	
19.47	b.d.	3.56	3.66	8.73	40.9	105	111	
20.61	b.d.	3.39	3.47	7.26	31.6	95.6	110	
21.76	18.4	b.d.	3.49	6.07	21.6	88.2	b.d.	
22.90	b.d.	b.d.	b.d.	5.08	17.7	b.d.	112	
24.05	b.d.	3.65		5.06	14.6	b.d.	b.d.	
25.19	b.d.	3.61		b.d.	11.9	60.4	b.d.	
26.34	b.d.	3.56		4.70	11.4	b.d.	110	
27.48	b.d.	3.36		4.69	11.5	b.d.	b.d.	
28.63	b.d.	3.41		4.79	10.4	60.5	110	
30.91	b.d.	3.45		4.84	11.2	b.d.	112	
32.05	b.d.	3.60		b.d.	11.3	b.d.	111	
33.19	b.d.	3.52			11.0	b.d.	110	
34.33	b.d.	3.72			10.7	67.1	110	
35.47	b.d.	3.66			9.75	b.d.	112	
36.61	18.3	3.61			8.88	66.9	111	
37.75	b.d.	3.76			8.50	b.d.	111	
38.88	b.d.	3.74			7.64	66.0	110	
40.02	18.4	3.52			7.43	b.d.	114	
41.15	b.d.	3.61			6.52	59.7	111	
42.28		3.52			6.20	b.d.	110	
43.41		3.53			7.69	68.7	110	
44.54		b.d.			6.92	b.d.	114	
45.67		3.59			6.50	b.d.	112	
46.80		3.48			5.80	b.d.	111	
47.94		3.71			5.65	b.d.	113	
49.09		3.53			b.d.	b.d.	b.d.	
50.23		3.25			b.d.	b.d.	b.d.	

Table 10. Concentration time course of 8 neurotoxic components in JP-8 vapor at -10 °C, sample I (KC135) - Continued. Concentrations in $\mu\text{g} \cdot \text{m}^{-3}$. b.d. = below detection limit.

Table 11. Concentration time course of 9 neurotoxic components in JP-8 vapor at -10 °C, sample II (storage tank). Concentrations in $\mu\text{g.m}^{-3}$. b.d. = below detection limit.

Time (h)	Cyclo-hexane	Benzene	Heptane	Toluene	Octane	Cyclo-heptane	Isopropyl-cyclopentane	Ethyl-benzene	p,m-Xylene
0.08	417	142	2,535	1,698	3,288	409	101	900	4,962
1.22	b.d.	1.48	27.7	43.9	791	68.5	20.4	268	1,771
2.36		1.29	1.96	1.97	216	12.0	5.45	92.1	677
3.50		1.29	b.d.	b.d.	b.d.	66.8	2.50	38.4	287
4.64		1.26		b.d.	19.9	b.d.	b.d.	19.2	131
5.78		1.33		0.35	6.48			12.7	64.2
6.92		1.26		b.d.	1.68			10.7	33.3
8.06		1.31		b.d.	0.51			13.4	17.4
9.20		1.34		0.34	b.d.			11.2	11.8
10.33		1.30		0.40				10.4	8.63
11.47		1.14		b.d.				9.98	8.98
12.61		1.20		b.d.				b.d.	8.66
13.74		1.17		b.d.				b.d.	b.d.
14.88		1.23		b.d.				9.80	8.55
16.01		1.17		b.d.				b.d.	b.d.
17.15		1.24		b.d.				b.d.	b.d.
18.28		1.20		b.d.				b.d.	b.d.
19.42		1.31		b.d.				b.d.	b.d.
20.56		1.31		0.29				b.d.	b.d.
21.70		1.17		0.32				9.81	8.58
22.83		1.18		0.30				b.d.	b.d.
23.97		1.20		0.26				b.d.	b.d.
25.12		1.21		0.42				9.81	8.59
26.26		1.19		0.28				b.d.	b.d.
27.40		1.08		b.d.				9.74	8.42
28.54		1.29		0.35				b.d.	b.d.
29.68		1.18		b.d.				9.84	8.64
30.82		1.24		b.d.				b.d.	b.d.
31.96		1.16		b.d.				b.d.	b.d.
33.10		1.24		b.d.				b.d.	b.d.
34.24		1.21		b.d.				b.d.	b.d.
35.38		1.18		b.d.				9.73	8.38
36.52		1.17		b.d.				b.d.	b.d.
37.65		1.21		b.d.				9.76	b.d.
38.79		1.23		b.d.				b.d.	b.d.
39.93		1.22		0.22				b.d.	b.d.
41.07		1.18		b.d.				b.d.	b.d.
42.20		1.23		b.d.				b.d.	b.d.
43.34		1.20		b.d.				b.d.	b.d.
44.48		1.09		0.37				b.d.	b.d.
45.63		1.18		b.d.				b.d.	b.d.
46.77		1.15		b.d.				b.d.	b.d.
47.91		1.17		b.d.				b.d.	b.d.
49.04		1.14		b.d.				b.d.	b.d.

Table 12. Concentration time course of 9 neurotoxic components in JP-8 vapor at -10 °C, sample II (storage tank).- Continued. Concentrations in $\mu\text{g.m}^{-3}$. b.d. = below detection limit.

Time (h)	Cyclohexane	Benzene	Heptane	Toluene	Octane	Cycloheptane	Isopropylcyclopentane	Ethylbenzene	p,m-Xylene
50.17	b.d.	1.09	b.d.	b.d.	b.d.	b.d.	b.d.	b.d.	b.d.
51.30		1.12		0.28				b.d.	b.d.
52.44		1.08		b.d.				b.d.	b.d.
53.58		1.22		0.30				b.d.	b.d.
54.72		1.53		0.46				b.d.	b.d.
55.85		2.32		0.62				b.d.	8.67
56.99		1.28		0.43				b.d.	b.d.
58.13		0.88		b.d.				b.d.	b.d.
59.27		0.84		0.38				b.d.	b.d.
60.41		0.97		0.37				b.d.	b.d.
61.55		1.14		b.d.				b.d.	b.d.
62.68		1.06		b.d.				b.d.	b.d.
63.82		1.36		0.38				b.d.	b.d.
64.96		1.53		b.d.				b.d.	b.d.
66.10		1.84		0.27				b.d.	b.d.
67.24		1.96		0.41				b.d.	8.59
68.38		2.00		0.58				b.d.	8.64
69.51		2.98		b.d.				9.90	8.79
70.65		2.47		0.67				9.93	8.87
71.79		b.d.		0.78				b.d.	b.d.
72.94		2.22		0.75				9.84	8.64
74.08		0.75		0.51				9.85	8.67
75.22		b.d.		0.62				b.d.	b.d.
76.36		b.d.		b.d.				b.d.	b.d.
77.50		b.d.		0.72				b.d.	b.d.
78.64		b.d.		b.d.				b.d.	8.59
79.78		b.d.						9.81	8.57
80.92		0.74						b.d.	b.d.
82.05		0.66							
83.19		0.67							
84.33		0.65							

Table 13. Concentration time course of 8 neurotoxic components in JP-8 vapor at -10 °C, sample II (storage tank). Concentrations in $\mu\text{g} \cdot \text{m}^{-3}$. b.d. = below detection limit.

Time (h)	o-Xylene	Isopropyl-cyclohexane	Isopropyl-benzene	2-Ethyl-toluene	1,2,3-Trimethylbenzene	1,2-Diethyl-benzene	Naphthalene	Acenaphthene
0.08	1,206	147	307	1,080	1,373	386	136	b.d.
1.22	517	90.0	171	694	768	b.d.	120	
2.36	242	61.9	100	513	620	b.d.	113	
3.50	131	207	66.8	420	563	b.d.	111	
4.64	71.0	162	45.9	362	535	255	114	
5.78	49.8	129	32.3	319	521	b.d.	111	
6.92	32.1	18.3	20.0	258	472	b.d.	111	
8.06	25.4	15.9	14.4	212	420	b.d.	113	
9.20	21.7	10.6	9.80	170	366	b.d.	110	
10.33	20.0	8.65	8.00	144	337	b.d.	114	
11.47	19.1	32.5	6.12	115	301	b.d.	127	
12.61	18.8	6.02	5.48	95.9	275	b.d.	110	
13.74	b.d.	19.0	4.56	74.0	233	b.d.	114	
14.88		14.6	4.01	58.3	202	b.d.	111	
16.01		11.8	3.94	45.4	181	b.d.	112	
17.15		8.64	3.55	34.4	145	b.d.	111	
18.28		7.10	b.d.	29.3	128	b.d.	111	
19.42		3.31	b.d.	18.1	83.1	b.d.	114	
20.56		4.16	b.d.	14.4	65.6	b.d.	111	
21.70		3.90	b.d.	12.1	54.8	b.d.	111	
22.83		3.34	b.d.	9.85	39.2	80.4	113	
23.97		3.26	b.d.	8.14	31.1	b.d.	110	
25.12		b.d.	b.d.	5.42	25.0	74.2	110	
26.26		b.d.	b.d.	5.11	20.4	b.d.	b.d.	
27.40		3.32	b.d.	6.18	20.6	b.d.	112	
28.54		b.d.	b.d.	4.94	18.6	63.0	110	
29.68		b.d.	b.d.	b.d.	18.7	73.1	116	
30.82		b.d.	b.d.	4.93	17.6	b.d.	113	
31.96		b.d.	b.d.	b.d.	15.6	b.d.	110	
33.10		3.51	b.d.	4.76	14.9	b.d.	111	
34.24		b.d.	b.d.	4.68	13.2	62.8	111	
35.38		b.d.	b.d.	b.d.	11.7	b.d.	110	
36.52		b.d.	b.d.	b.d.	11.1	b.d.	115	
37.65		b.d.	b.d.	b.d.	10.0	70.0	111	
38.79		b.d.	b.d.	b.d.	9.29	b.d.	114	
39.93		b.d.	b.d.	b.d.	8.38	b.d.	110	
41.07		b.d.	b.d.	b.d.	8.00	b.d.	111	
42.20		b.d.	b.d.	b.d.	7.13	b.d.	113	
43.34		b.d.	b.d.	b.d.	6.80	b.d.	113	
44.48		b.d.	b.d.	b.d.	6.17	60.2	110	
45.63		b.d.	b.d.	b.d.	5.73	60.1	110	
46.77		b.d.	b.d.	b.d.	5.47	59.9	b.d.	
47.91		b.d.	b.d.	b.d.	6.48	b.d.	110	

Table 14. Concentration time course of 8 neurotoxic components in JP-8 vapor at -10 °C, sample II (storage tank) - Continued. Concentrations in $\mu\text{g} \cdot \text{m}^{-3}$. b.d. = below detection limit.

Table 15. Concentration time course of 9 neurotoxic components in JP-8 vapor at -10 °C, sample III (Dutch F16). Concentrations in $\mu\text{g.m}^{-3}$. b.d. = below detection limit.

Time (h)	Cyclo- hexane	Benzene	Heptane	Toluene	Octane	Cyclo- heptane	Isopropyl- cyclopentane	Ethyl- benzene	p,m- Xylene
0.09	1,555	220	4,225	1,362	5,178	50.1	31.5	1,909	6,858
1.24	b.d.	1.12	59.0	54.9	2,203	376	85.5	1,046	4,678
2.38		1.03	b.d.	1.70	615	85.2	b.d.	335	1,928
3.52		0.90		0.57	147	b.d.	4.44	108	677
4.67		0.96		0.61	32.2		b.d.	42.8	245
5.81		0.90		0.59	6.13			24.5	88.3
6.96		1.04		0.46	b.d.			b.d.	33.5
8.10		0.94		0.61					29.0
9.24		0.95		0.44					b.d.
10.39		0.96		0.40					
11.53		0.96		0.50					
12.67		0.64			b.d.				
13.81		0.97		0.43					
14.95		0.80			b.d.				
16.10		0.62			b.d.				
17.24		0.77			b.d.				
18.38		0.77			b.d.				
19.52		0.95		0.33					
20.66		0.29		0.55					
21.81		0.41			b.d.				
22.97		0.19			b.d.				
24.12		b.d.			b.d.				
25.26		b.d.			b.d.				
26.42		0.26			b.d.				
27.57		b.d.			b.d.				
28.72		b.d.		0.33					
29.87		0.19			b.d.				
31.03		b.d.			b.d.				
32.18		b.d.			b.d.				
33.33		b.d.			b.d.				
34.48		b.d.			b.d.				
35.63		0.11			b.d.				
36.78		b.d.			b.d.				
37.93		0.24			b.d.				
39.08		0.78			b.d.				
40.23		0.64			b.d.				
41.38		0.38			b.d.				
42.52		0.39			b.d.				
43.67		b.d.		0.54					
44.82		b.d.		0.59					
45.96		0.28		0.51					
47.11		0.68		0.85					
48.26		b.d.		0.42					
49.41				0.52					

Table 16. Concentration time course of 8 neurotoxic components in JP-8 vapor at -10 °C, sample III (Dutch F16). Concentrations in $\mu\text{g}\cdot\text{m}^{-3}$. b.d. = below detection limit.

Table 17. Concentration time course of 9 neurotoxic components in JP-8 vapor at -10 °C, sample IV (Dutch, aged). Concentrations in $\mu\text{g}\cdot\text{m}^{-3}$. b.d. = below detection limit.

Time (h)	Cyclohexane	Benzene	Heptane	Toluene	Octane	Cycloheptane	Isopropylcyclopentane	Ethylbenzene	p,m-Xylene
0.10	368	76.8	1,388	1,009	2,760	455	92.9	1,064	4,687
1.64	b.d.	4.38	2.90	4.95	292	31.3	b.d.	157	847
2.79		3.46	b.d.	0.44	39.8	b.d.		33.1	176
3.94		3.20	b.d.	0.45	1.15	b.d.		b.d.	25.0
5.10		3.37	b.d.	1.59	b.d.				14.0
6.26		3.32	b.d.	1.43	b.d.				13.0
7.41		2.32	b.d.	1.38					12.3
8.57		3.21	b.d.	1.26					b.d.
9.72		2.64	b.d.	0.46					
10.87		2.76	b.d.	1.18					
12.01		2.71	b.d.	0.48					
13.16		2.94	b.d.	0.48					
14.31		2.79	b.d.	0.54					
15.45		2.97	b.d.	1.04					
16.60		2.81	b.d.	0.60					
17.74		2.94	b.d.	0.95					
18.89		2.47	b.d.	1.04					
20.04		2.76	b.d.	0.36					
21.19		2.81	b.d.	0.60					
22.33		2.11	b.d.	1.05					
23.48		3.09	b.d.	1.09					
24.64		2.91	b.d.	0.98					
25.79		2.95	b.d.	0.90					
26.94		2.72	2.05	0.87					
28.09		2.89	b.d.	0.82					
29.24		1.80		0.84					
30.39		2.42		0.90					
31.54		2.79		0.70					
32.69		2.89		0.86					
33.84		2.41		0.80					
34.99		2.32		0.58					
36.14		2.39		0.68					
37.29		2.75		0.66					
38.43		2.27		0.33					
39.58		2.20		0.67					
40.72		b.d.		0.79					
41.87		b.d.		0.77					
43.01		0.44		0.65					
44.14		b.d.		0.64					
45.29		0.20		0.53					
46.45		0.22		0.67					
47.60		0.28		0.70					
48.76		0.36		0.95					
49.92		0.23		0.76					

Table 18 Concentration time course of 9 neurotoxic components in JP-8 vapor at -10 °C, sample IV (Dutch, aged) - Continued. Concentrations in $\mu\text{g.m}^{-3}$. b.d. = below detection limit.

Time (h)	Cyclohexane	Benzene	Heptane	Toluene	Octane	Cycloheptane	Isopropylcyclopentane	Ethylbenzene	p,m-Xylene
51.08	b.d.	0.26	b.d.	0.88	b.d.	b.d.	b.d.	b.d.	b.d.
52.24		0.28		0.75					
53.41		0.31		0.73					
54.57		0.25		0.59					
55.74		b.d.		0.74					
56.91		b.d.		0.80					
58.07		0.30		0.86					
59.24		0.24		0.70					
60.40		b.d.		0.71					

Table 19. Concentration time course of 8 neurotoxic components in JP-8 vapor at -10 °C, sample IV (Dutch, aged). Concentrations in $\mu\text{g} \cdot \text{m}^{-3}$. b.d. = below detection limit.

ANNEX G VAPOR CONCENTRATION TIME COURSES OF THE NEUROTOXIC COMPONENTS IN JP-8 VAPOR AT +20 °C.

Table 20. Concentration time course of 9 neurotoxic components in JP-8 vapor at +20 °C, sample I (KC135). Concentrations in $\mu\text{g} \cdot \text{m}^{-3}$. b.d. = below detection limit.

Time (h)	Cyclohexane	Benzene	Heptane	Toluene	Octane	Cycloheptane	Isopropylcyclopentane	Ethylbenzene	p,m-Xylene
0.08	200	3,628	3,866	3,203	9,438	2,102	283	3,313	14.0
0.17	24.5	2,778	914	983	6,089	607	14.4	1,773	661
0.33	5.46	3,702	166	165	2,473	166	40.7	713	5,077
0.50	35.7	3,855	0.00	94.6	2,729	147	5.99	631	5,288
0.67	122	2,462	1,547	97.7	4,327	b.d.	b.d.	158	1,989
0.83	80.1	402	568	67.4	719	34.4		47.8	574
1.00	27.4	381	1,148	276	4,050	b.d.		71.0	1,183
1.50	b.d.	b.d.	b.d.	b.d.	b.d.	b.d.		b.d.	b.d.
2.00	b.d.	b.d.	b.d.	b.d.	2,264	64.7		b.d.	b.d.
3.00	1.56	0.86	107	186	b.d.	b.d.		1.99	144
4.00	b.d.	7.10	b.d.	9.05	3.20			b.d.	8.70
5.00	17.2	22.8	903	30.5	660			11.8	151

Table 21. Concentration time course of 8 neurotoxic components in JP-8 vapor at +20 °C, sample I (KC135). Concentrations in $\mu\text{g} \cdot \text{m}^{-3}$. b.d. = below detection limit.

Time (h)	o-Xylene	Isopropylcyclohexane	Isopropylbenzene	2-Ethyltoluene	1,2,3-Trimethylbenzene	1,2-Diethylbenzene	Naphthalene	Acenaphthene
0.08	4,899	164	1,623	5,835	7,201	9,478	120	b.d.
0.17	2,976	416	516	3,809	4,773	128	100	
0.33	1,451	269	563	2,524	3,076	3,489	132	
0.50	1,372	491	1.47	2,821	3,409	3,283	54.5	
0.67	354	28.0	192	1,223	2,109	b.d.	225	
0.83	153	67.0	98.0	625	939	1,361	109	
1.00	62.2	b.d.	6.72	13.8	14.2	b.d.	28.6	
1.50	b.d.		b.d.	b.d.	b.d.	b.d.	b.d.	
2.00	b.d.		b.d.	b.d.	b.d.	b.d.	b.d.	
3.00	5.19		29.4	8.87	16.4	34.6	47.1	
4.00	b.d.		b.d.	b.d.	b.d.	b.d.	b.d.	
5.00	9.56		8.56	2.51	5.09		65.3	

Table 22. Concentration-time course of 9 neurotoxic components in JP-8 vapor at +20 °C, sample II (storage tank). Concentrations in $\mu\text{g} \cdot \text{m}^{-3}$. b.d. = below detection limit.

Time (h)	Cyclo- hexane	Benzene	Heptane	Toluene	Octane	Cyclo- heptane	Isopropyl- cyclopentane	Ethyl- benzene	p,m- Xylene
0.08	200	3,408	982	1,018	11,699	f.a.	131	1,358	3,507
0.17	196	f.a.	826	2,021	10,735		114	1,301	3,172
0.33	26.4	969	50.1	95.9	3,886		b.d.	340	1,652
0.50	15.8	317	32.3	101	5,850			67.7	988
0.67	99.6	568	579	192	39,756			190	889
0.83	654	1,900	315	201	10,280			150	477
1.00	144	2,260	246	140	3,172			97.2	286
1.50	350	2,448	313	213	11,034			91.7	310
2.00	322	1,873	356	203	5,008			82.7	221
3.00	b.d.	147	13.3	14.2	31.5			6.85	24.3
4.00		221	b.d.	15.9	83.0			6.80	31.2
5.00		1,588		21.2	774			5.06	17.6

Table 23. Concentration time course of 8 neurotoxic components in JP-8 vapor at +20 °C, sample II (storage tank). Concentrations in $\mu\text{g} \cdot \text{m}^{-3}$. b.d. = below detection limit.

Time (h)	o- Xylene	Isopropyl- cyclohexane	Isopropyl- benzene	2- Ethyl- toluene	1,2,3- Trimethyl benzene	1,2-Diethyl- benzene	Naphthalene	Acenaphthene
0.08	1,711	47.8	386	1,359	1,503	4,250	133	b.d.
0.17	1,611	293	399	1,780	2,069	5,180	884	
0.33	1,002	168	305	1,420	1,801	3,441	309	
0.50	586	137	216	1,185	1,500	4,255	121	
0.67	189	75.8	19.4	1,083	621	4,039	123	
0.83	236	75.0	102	674	870	856	64.3	
1.00	112	19.0	51.5	332	456	1,245	53.0	
1.50	45.4	16.2	18.1	245	438	107	156.7	
2.00	32.9	b.d.	18.8	72.0	192	32.3	40.7	
3.00	3.22		b.d.	b.d.	22.9	144	13.7	
4.00	3.96		12.6		45.4	b.d.	73.4	
5.00	4.28		6.81		b.d.		5.78	

ANNEX H VAPOR CONCENTRATION-TIME COURSES AT -10 °C, GRAPHICAL REPRESENTATIONS.

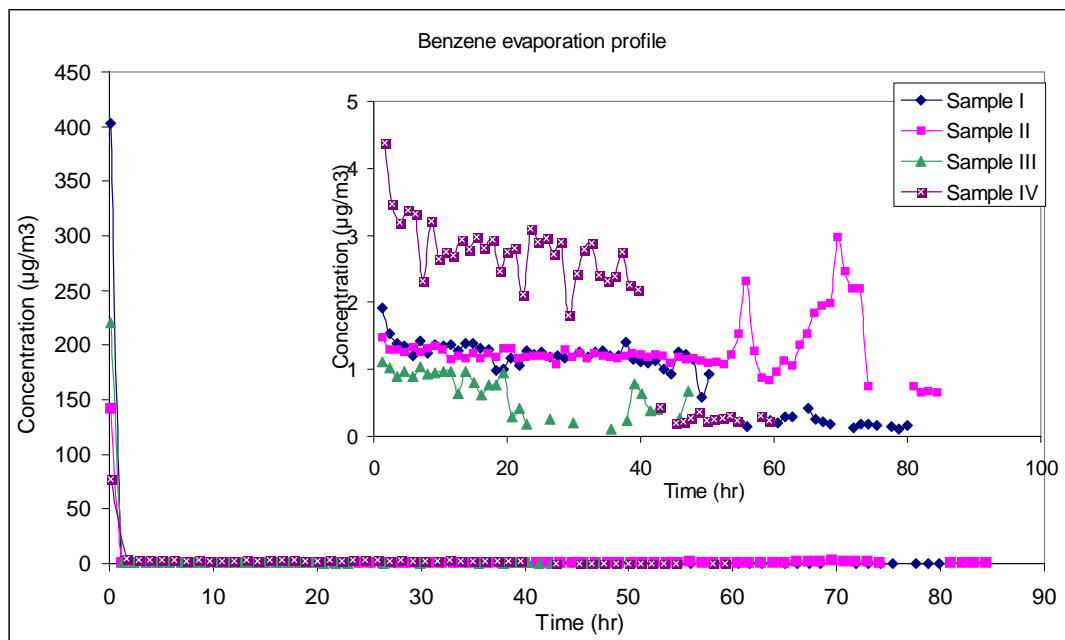


Figure 29. Concentration-time courses of benzene in the vapor phase during evaporation of JP-8 samples I to IV at -10 °C. The discontinuities in the measurements are due to the detection limit of the analytical configuration of *ca* 0.2 $\mu\text{g}/\text{m}^3$.

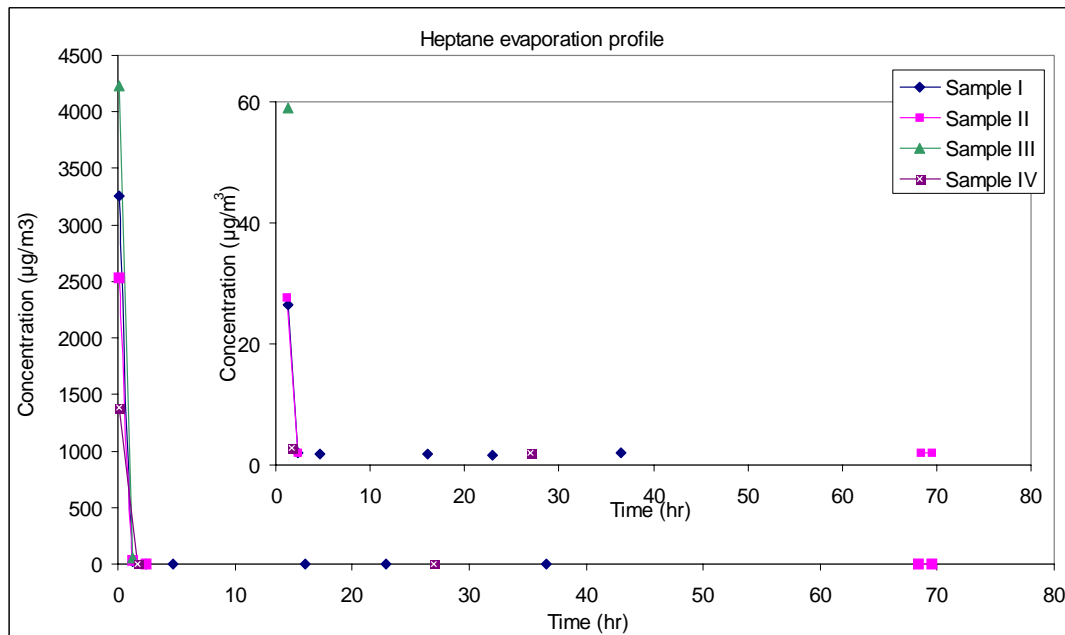


Figure 30. Concentration-time courses of heptane in the vapor phase during evaporation of JP-8 samples I to IV at -10 °C. The discontinuities in the measurements are due to the detection limit of the analytical configuration of *ca* 1.5 $\mu\text{g}/\text{m}^3$.

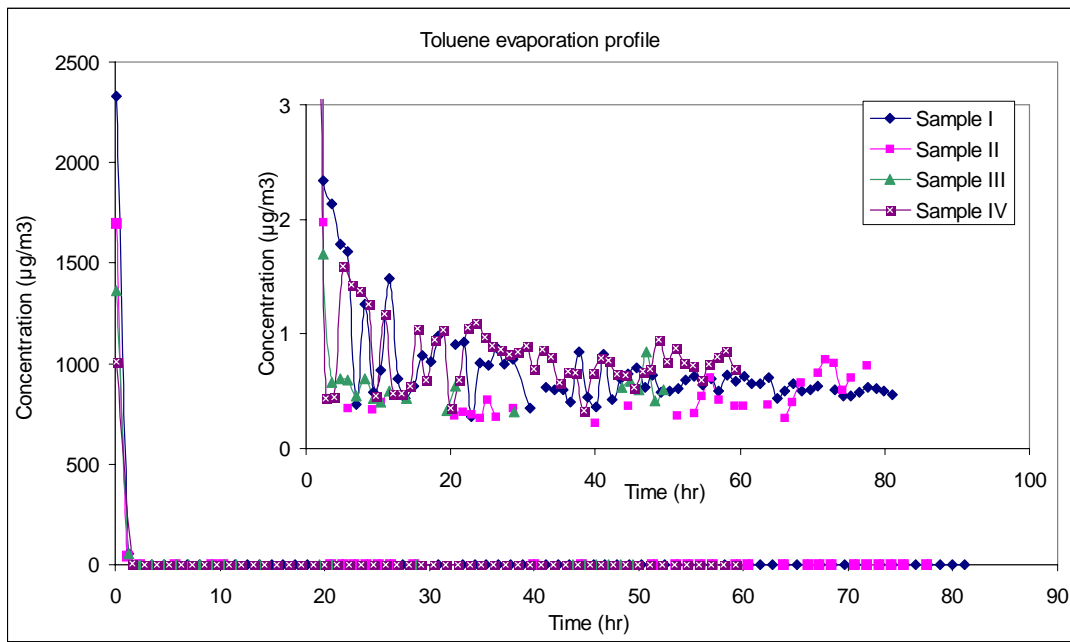


Figure 31. Concentration-time courses of toluene in the vapor phase during evaporation of JP-8 samples I to IV at -10°C . The discontinuities in the measurements are due to the detection limit of the analytical configuration of $ca\ 0.5\ \mu\text{g}/\text{m}^3$.

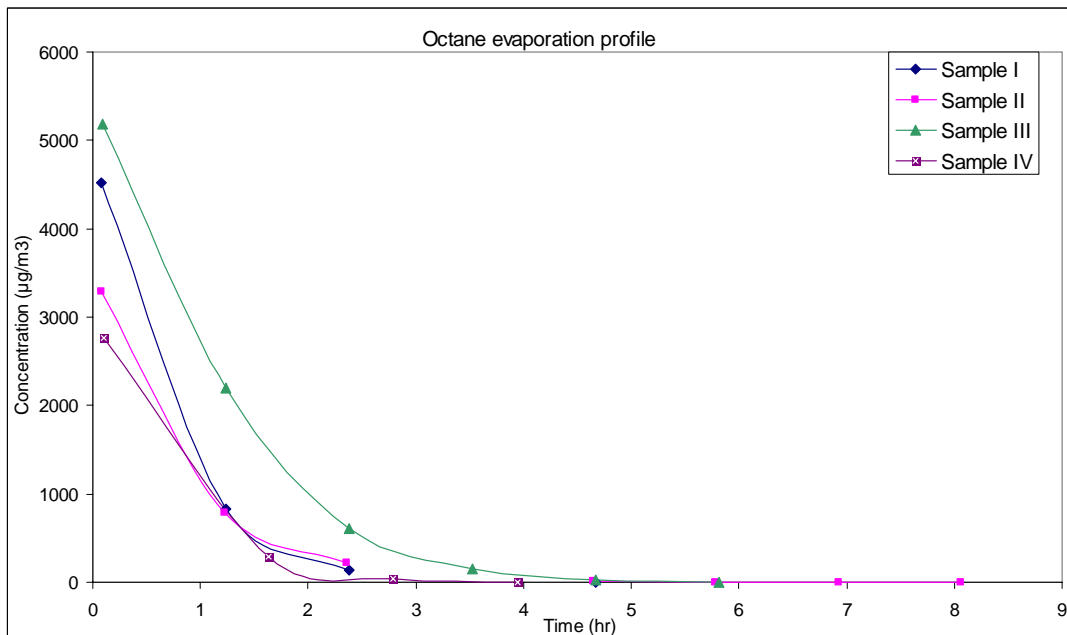


Figure 32. Concentration-time courses of octane in the vapor phase during evaporation of JP-8 samples I to IV at -10°C . Within 8-9 h the vapor concentration has dropped below the detection limit of the analytical configuration of $ca\ 0.5-2\ \mu\text{g}/\text{m}^3$.

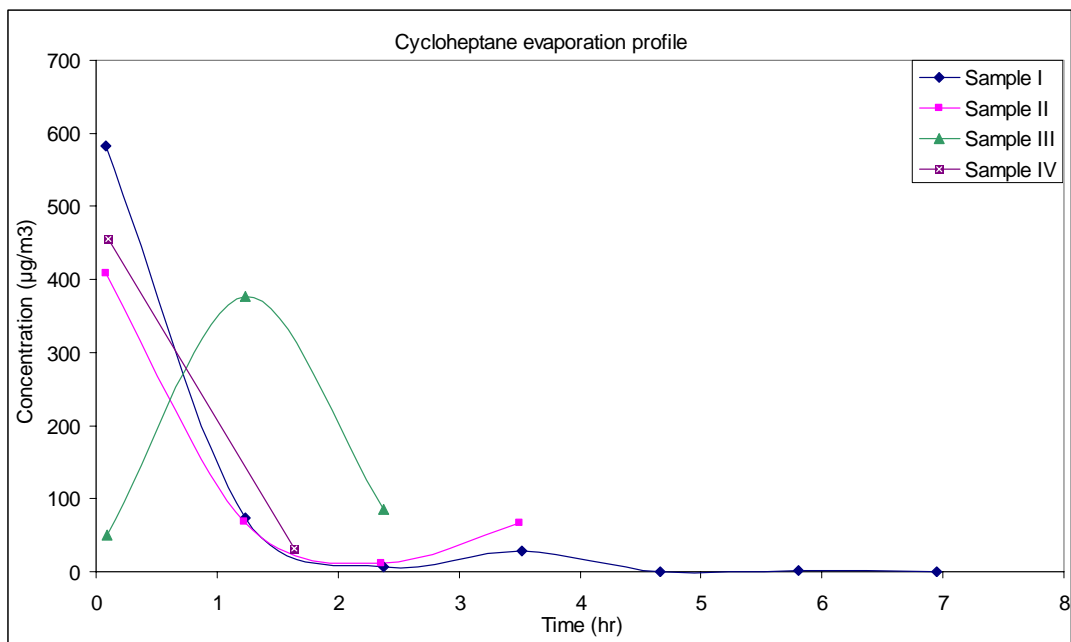


Figure 33. Concentration-time courses of cycloheptane in the vapor phase during evaporation of JP-8 samples I to IV at -10 °C. Within 7 h the vapor concentration has dropped below the detection limit of the analytical configuration of *ca* 2 $\mu\text{g}/\text{m}^3$.

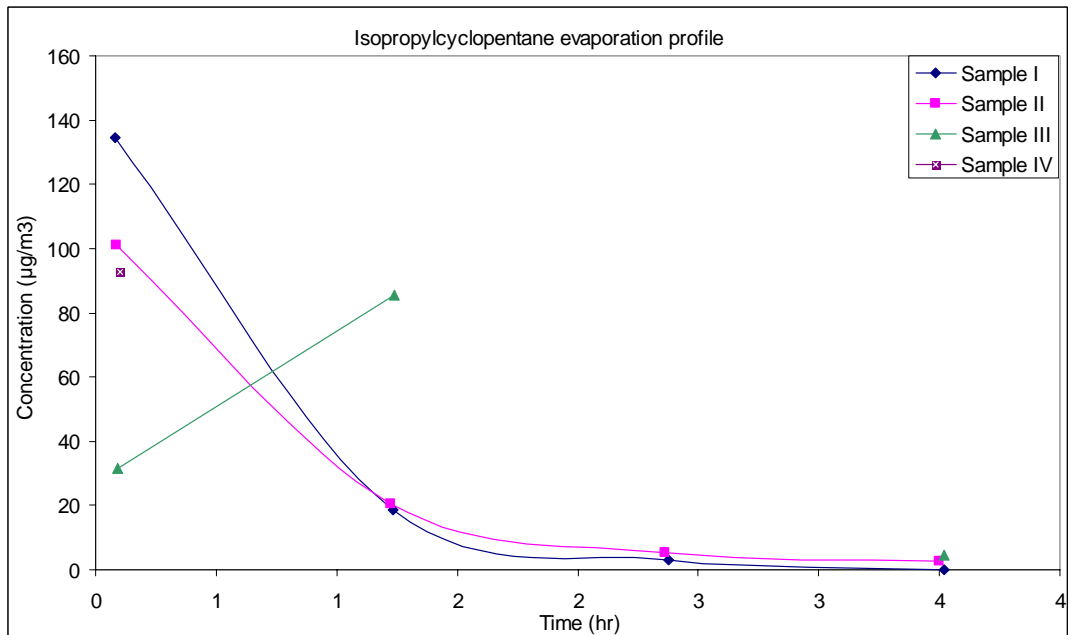


Figure 34. Concentration-time courses of isopropylcyclopentane in the vapor phase during evaporation of JP-8 samples I to IV at -10 °C. In about 4 h the vapor concentration has dropped below the detection limit of the analytical configuration of *ca* 2 $\mu\text{g}/\text{m}^3$.

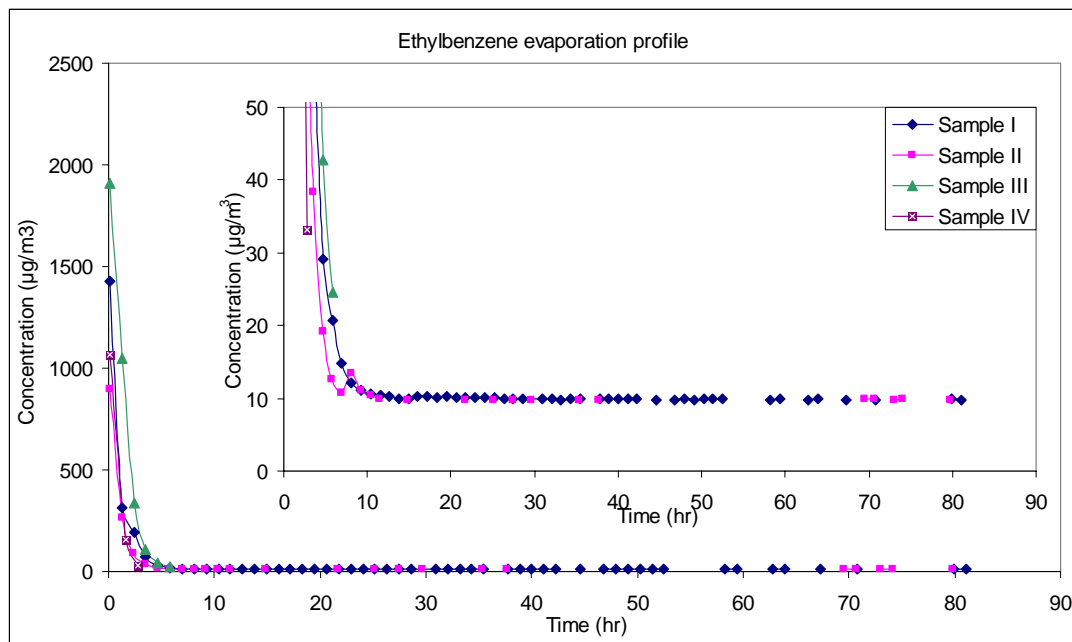


Figure 35. Concentration-time courses of ethylbenzene in the vapor phase during evaporation of JP-8 samples I to IV at -10 °C. The discontinuities in the measurements are due to the detection limit of the analytical configuration of *ca* 10 $\mu\text{g}/\text{m}^3$.

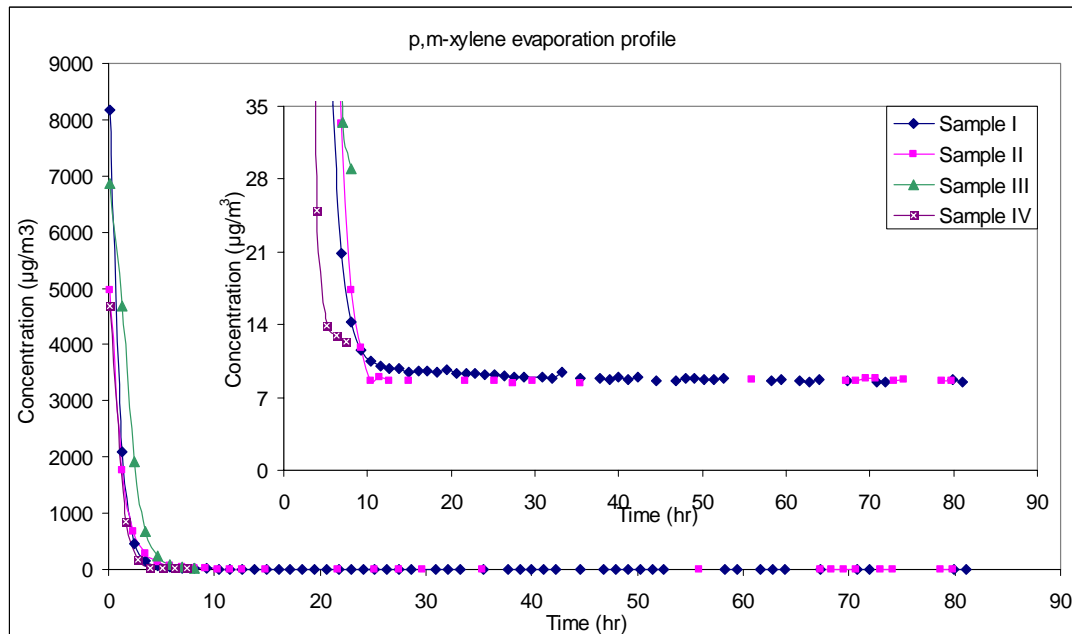


Figure 36. The summed concentration-time courses of p- and m-xylene in the vapor phase during evaporation of JP-8 samples I to IV at -10 °C. The discontinuities in the measurements are due to the detection limit of the analytical configuration of *ca* 8 $\mu\text{g}/\text{m}^3$.

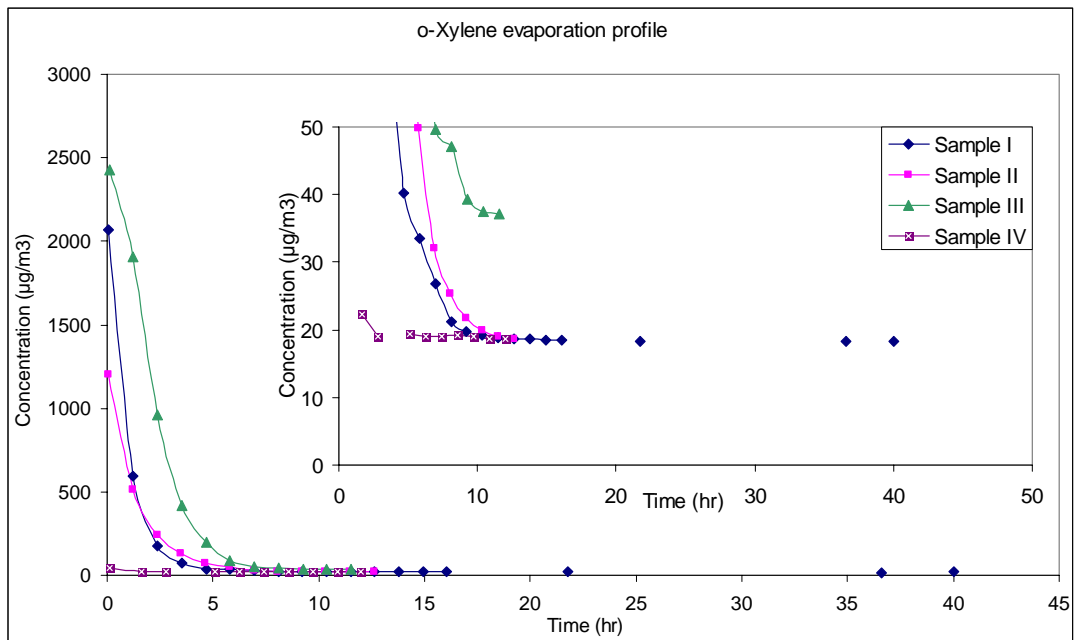


Figure 37. Concentration-time courses of o-xylene in the vapor phase during evaporation of JP-8 samples I to IV at -10°C . The discontinuities in the measurements are due to the detection limit of the analytical configuration of $\text{ca } 18 \mu\text{g}/\text{m}^3$.

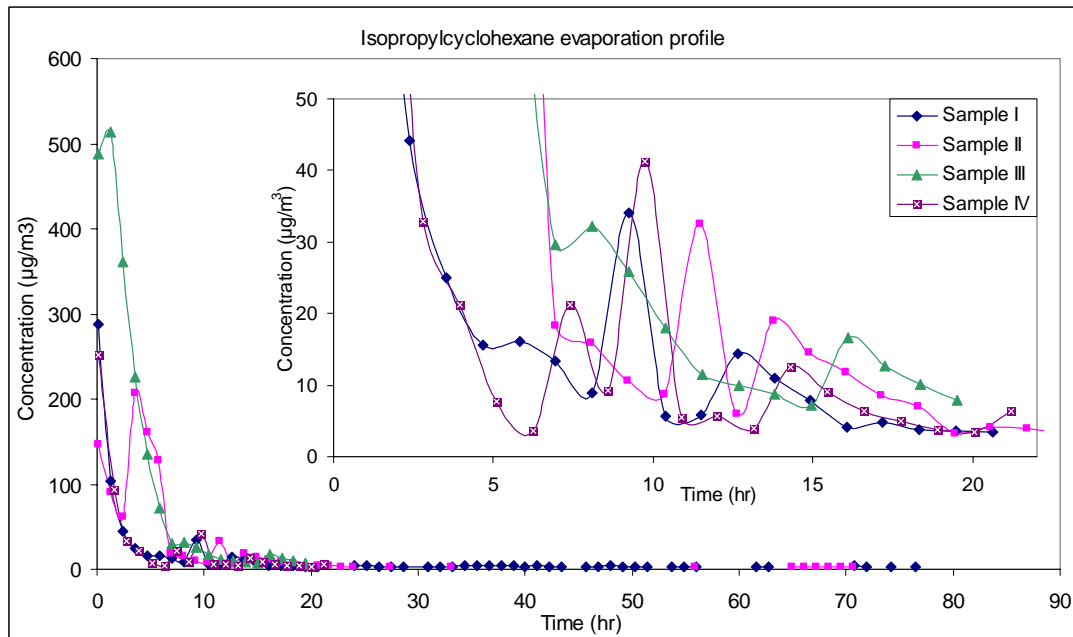


Figure 38. Concentration-time courses of isopropylcyclohexane in the vapor phase during evaporation of JP-8 samples I to IV at -10°C . The detection limit for this compound is $\text{ca } 3 \mu\text{g}/\text{m}^3$.

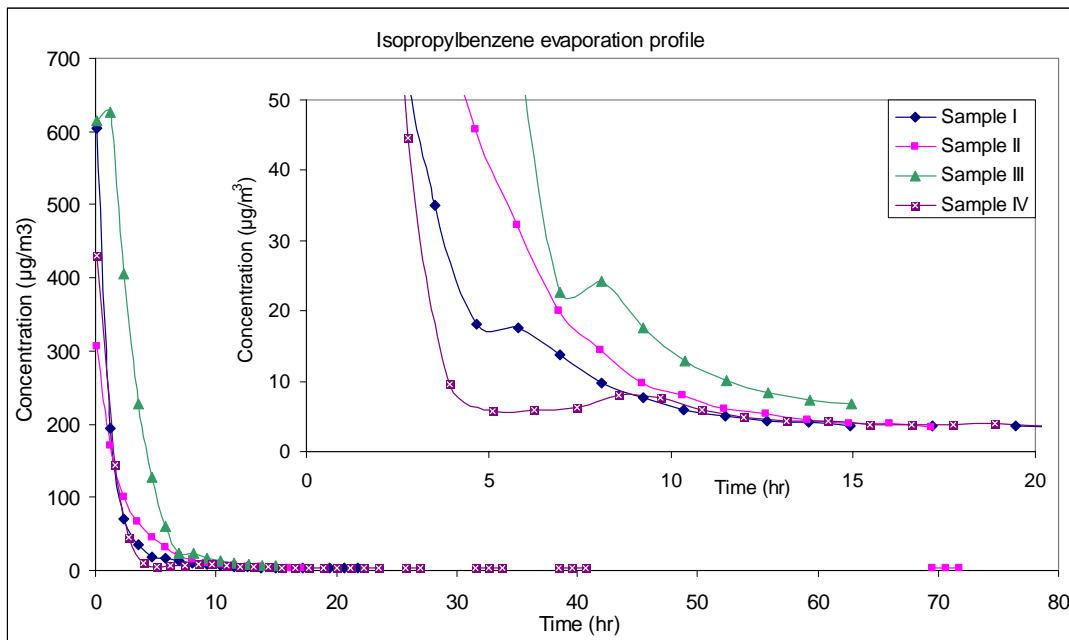


Figure 39. Concentration-time courses of isopropylbenzene in the vapor phase during evaporation of JP-8 samples I to IV at -10 °C. The discontinuities in the measurements are due to the detection limit of the analytical configuration of *ca* 3.4 $\mu\text{g}/\text{m}^3$.

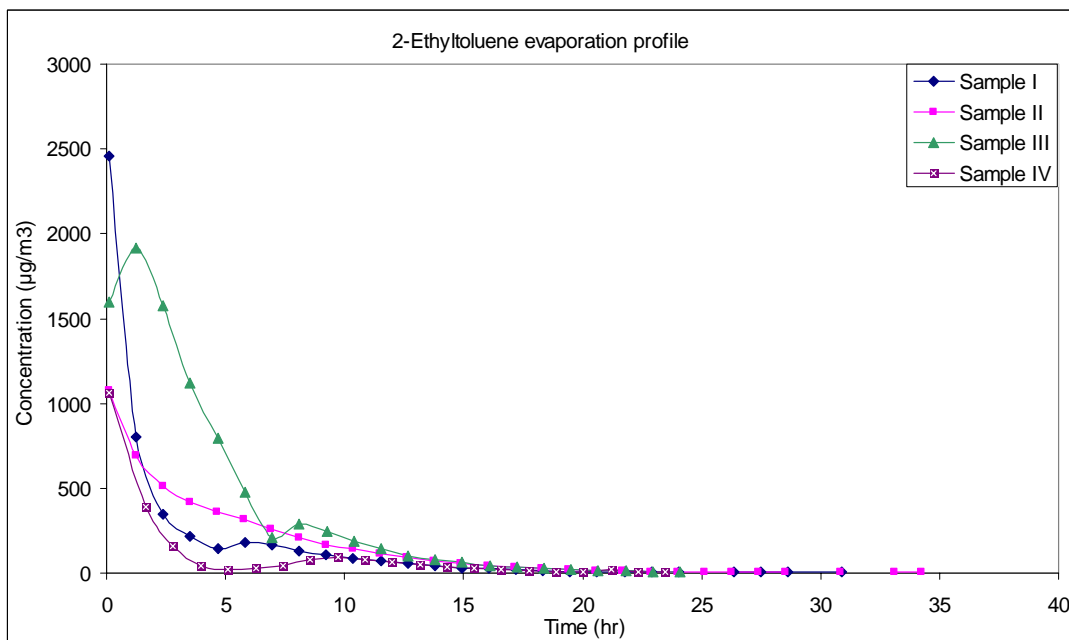


Figure 40 Concentration time-courses of 2-ethyltoluene in the vapor phase during evaporation of JP-8 samples I to IV at -10 °C. The detection limit for this compound is *ca* 5 $\mu\text{g}/\text{m}^3$.

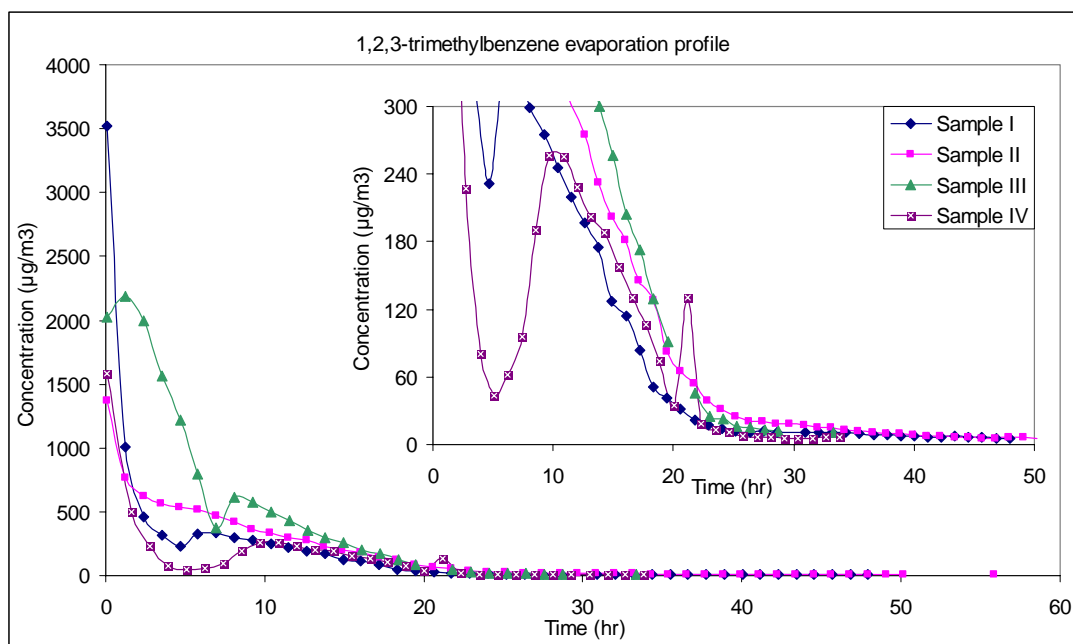


Figure 41. Concentration-time courses of 1,2,3-trimethylbenzene in the vapor phase during evaporation of JP-8 samples I to IV at -10°C . The detection limit for this compound is *ca* $6 \mu\text{g}/\text{m}^3$.

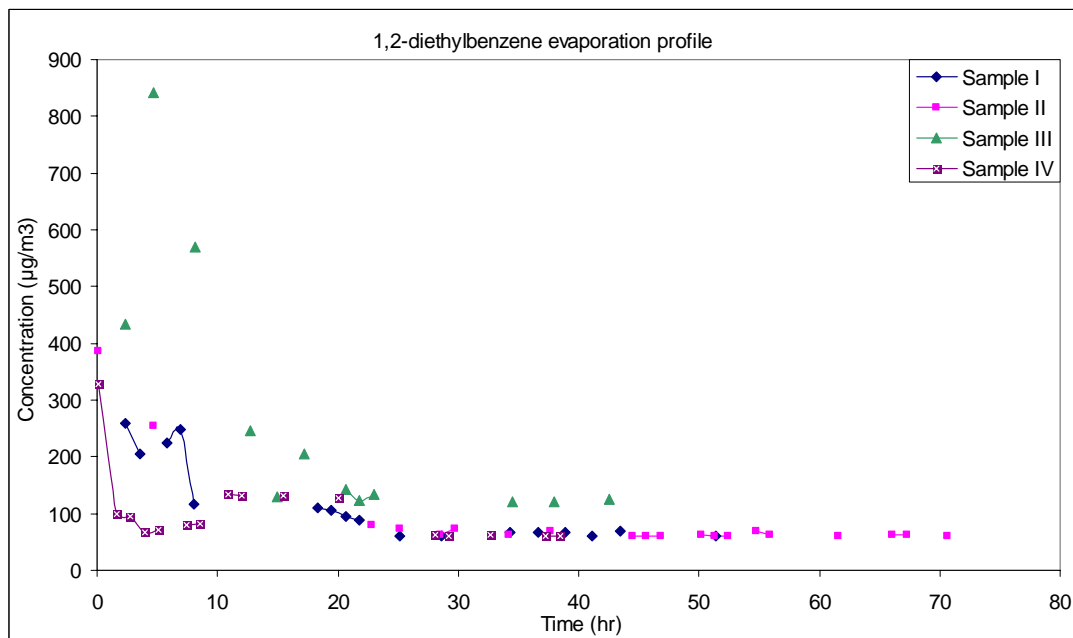


Figure 42. Concentration-time courses of 1,2-diethylbenzene in the vapor phase during evaporation of JP-8 samples I to IV at -10°C . The discontinuities in the measurements are due to the detection limit of the analytical configuration of *ca* $60 \mu\text{g}/\text{m}^3$.

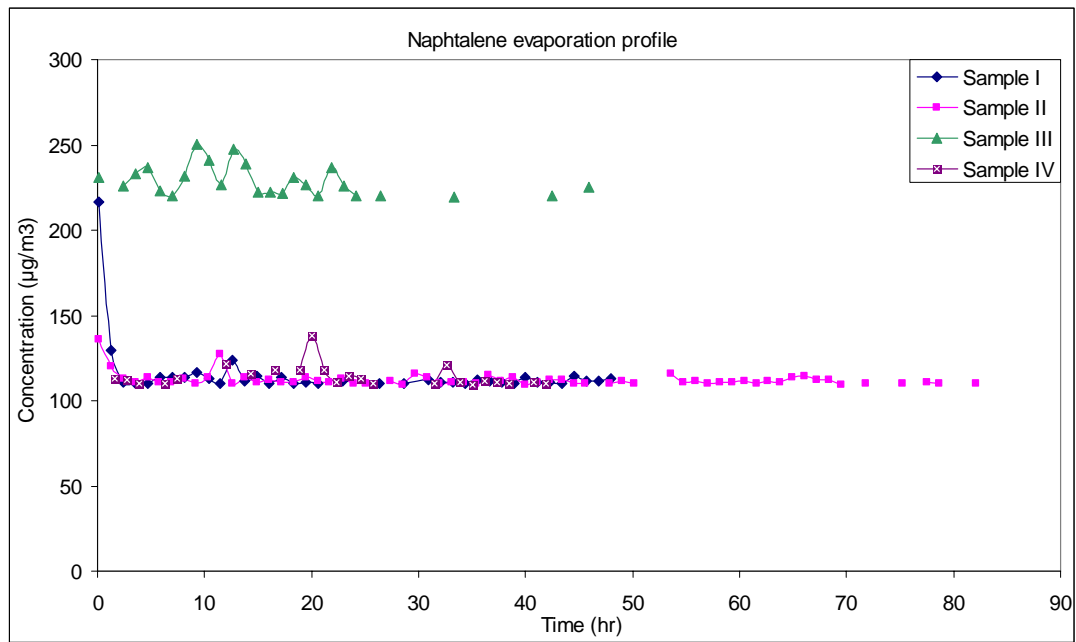


Figure 43. Concentration-time courses of naphthalene in the vapor phase during evaporation of JP-8 samples I to IV at -10°C . The detection limit for this compound is *ca* $110 \mu\text{g}/\text{m}^3$.

ANNEX I VAPOR CONCENTRATION TIME COURSES AT +20 °C, GRAPHICAL REPRESENTATIONS.

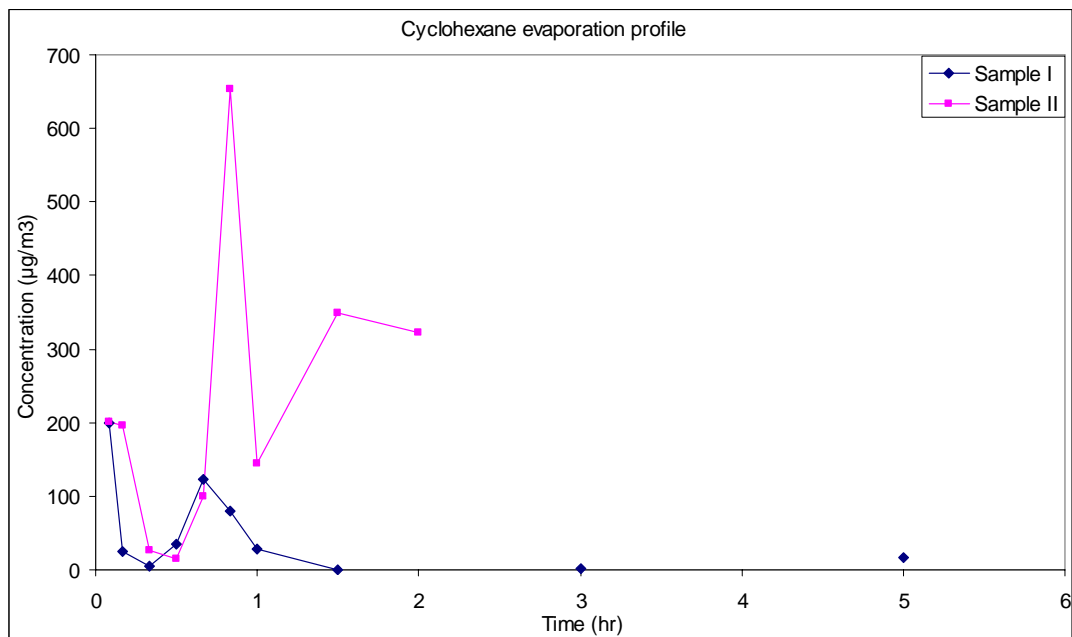


Figure 44: Concentration-time courses of cyclohexane in the vapor phase during evaporation of JP-8 samples I and II at 20 °C. The discontinuities in the measurements are due to the detection limit of the analytical configuration of *ca* 1.5 µg/m³.

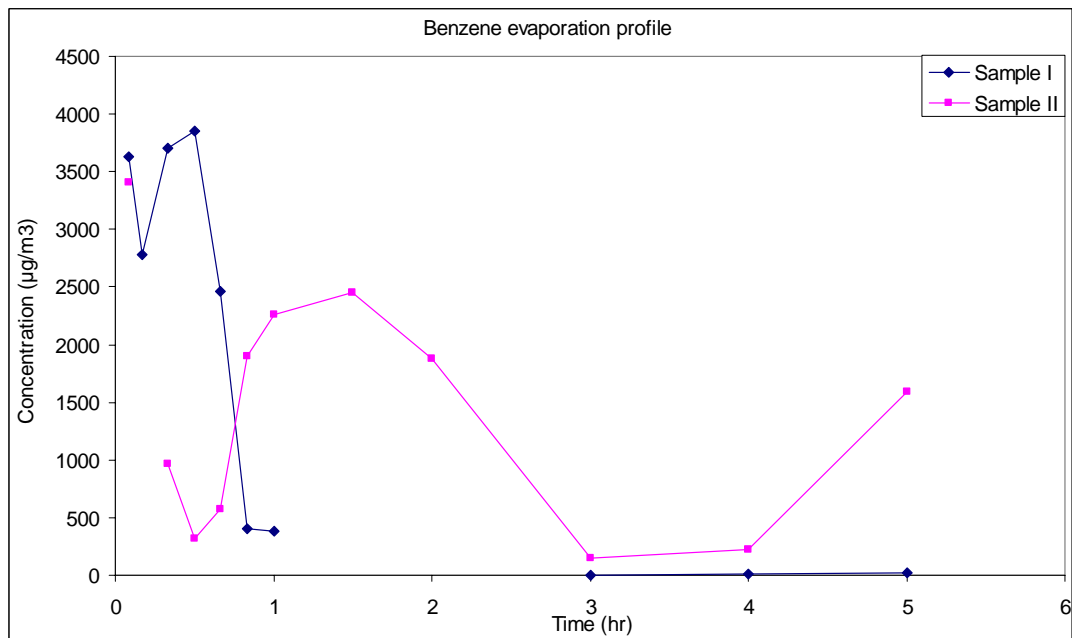


Figure 45. Concentration-time courses of benzene in the vapor phase during evaporation of JP-8 samples I and II at 20 °C. The discontinuities in the measurements are due to the detection limit of the analytical configuration of *ca* 0.2 µg/m³.

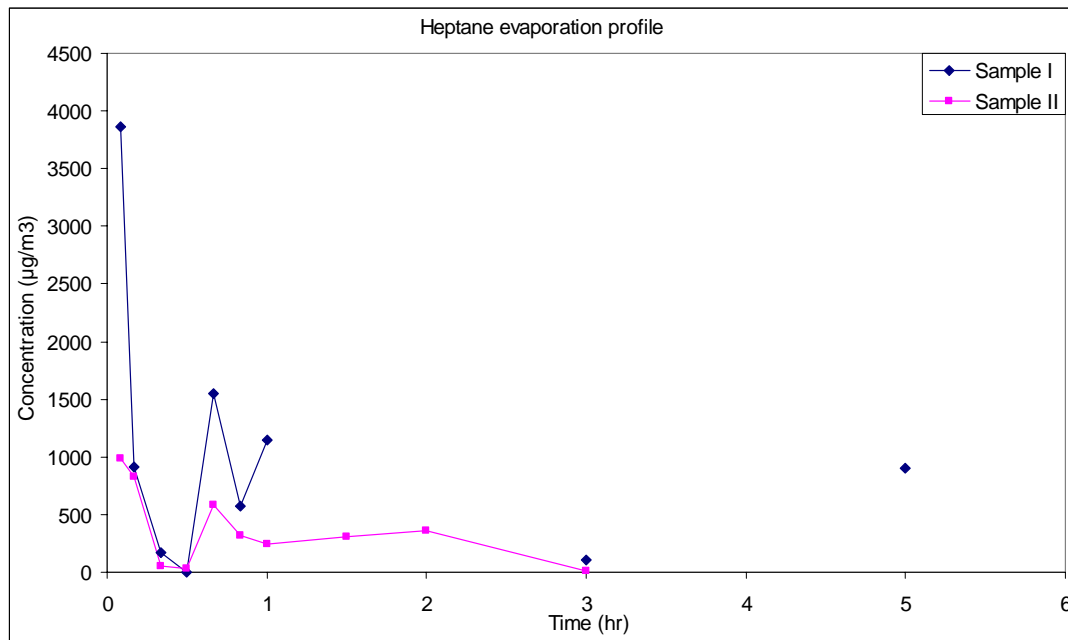


Figure 46. Concentration-time courses of heptane in the vapor phase during evaporation of JP-8 samples I and II at 20 °C. The discontinuities in the measurements are due to the detection limit of the analytical configuration of *ca* 1.5 µg/m³.

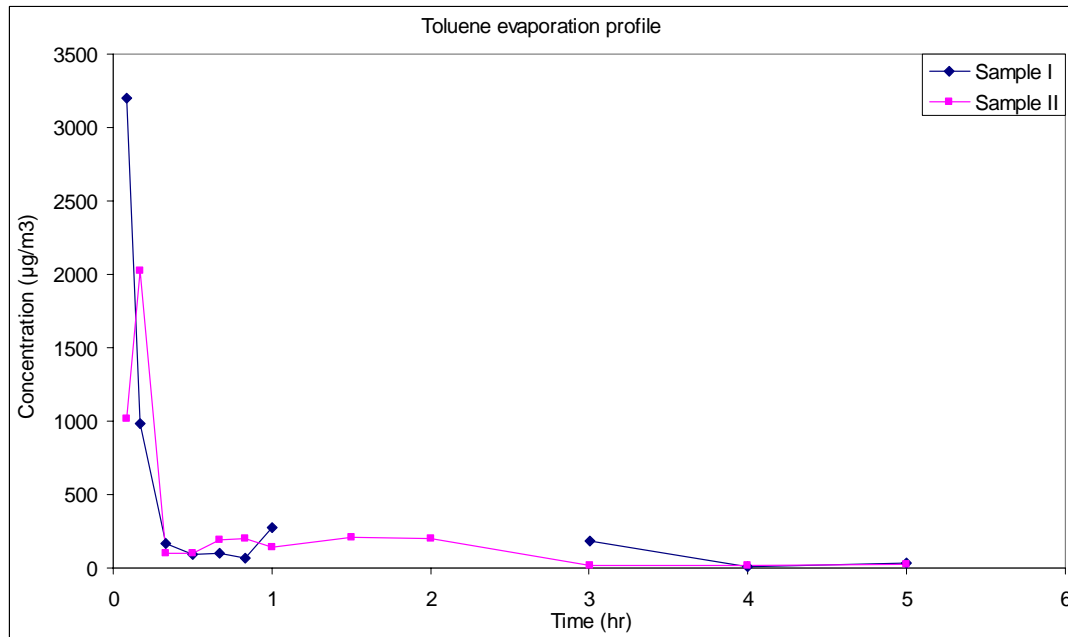


Figure 47. Concentration-time courses of toluene in the vapor phase during evaporation of JP-8 samples I and II at 20 °C. The discontinuities in the measurements are due to the detection limit of the analytical configuration of *ca* 0.5 µg/m³.

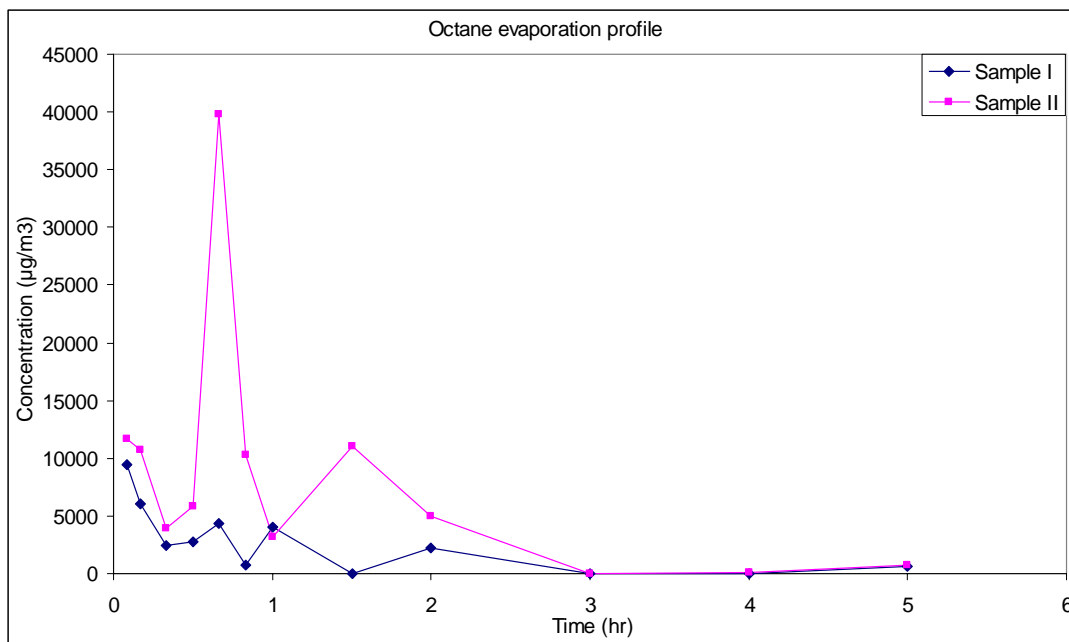


Figure 48. Concentration-time courses of octane in the vapor phase during evaporation of JP-8 samples I and II at 20 °C. The detection limit for this compound is *ca* 3 µg/m³.

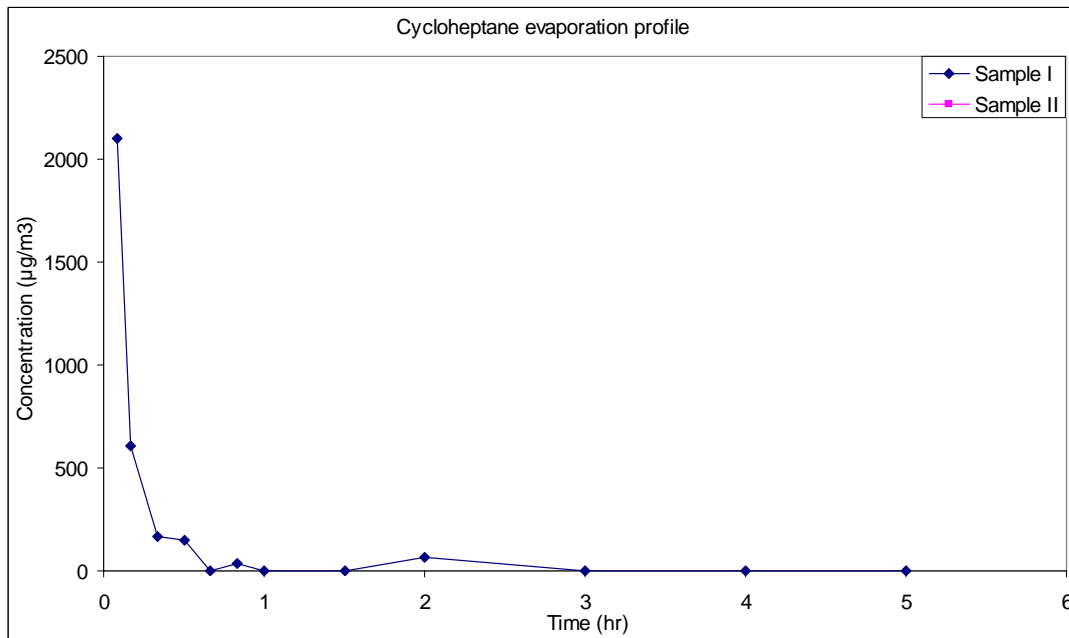


Figure 49. Concentration-time courses of cycloheptane in the vapor phase during evaporation of JP-8 samples I and II at 20 °C. The discontinuities in the measurements are due to the detection limit of the analytical configuration of *ca* 2 µg/m³. Cycloheptane could not be detected in any the vapor samples of fuel sample II.

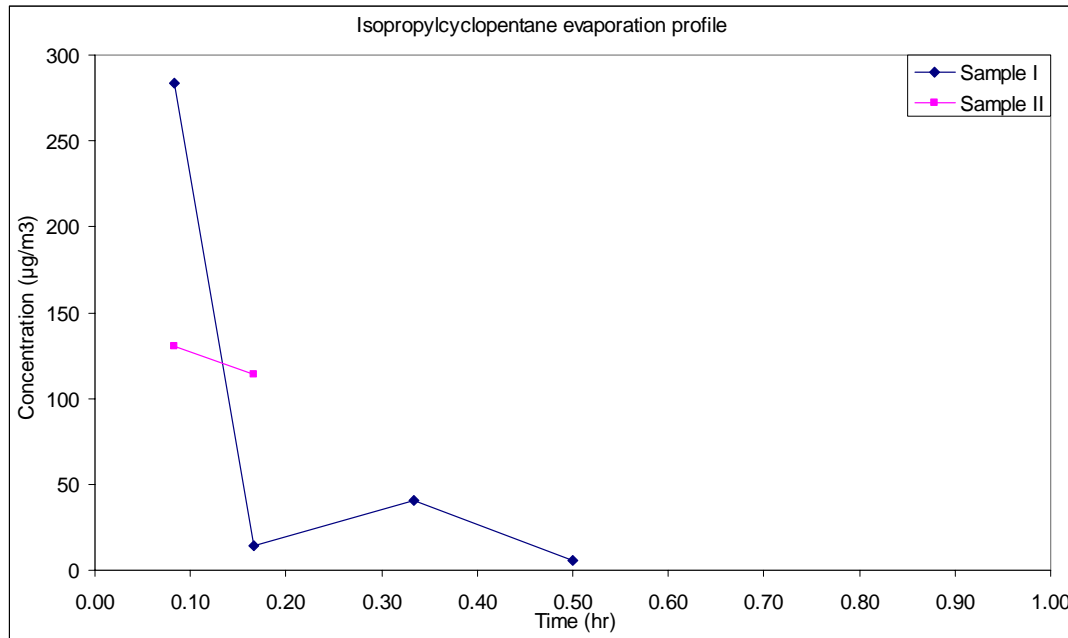


Figure 50. Concentration-time courses of isopropylcyclopentane in the vapor phase during evaporation of JP-8 samples I and II at 20 °C. In about 30 min the vapor concentration has dropped below the detection limit of the analytical configuration of *ca* 2 µg/m³.

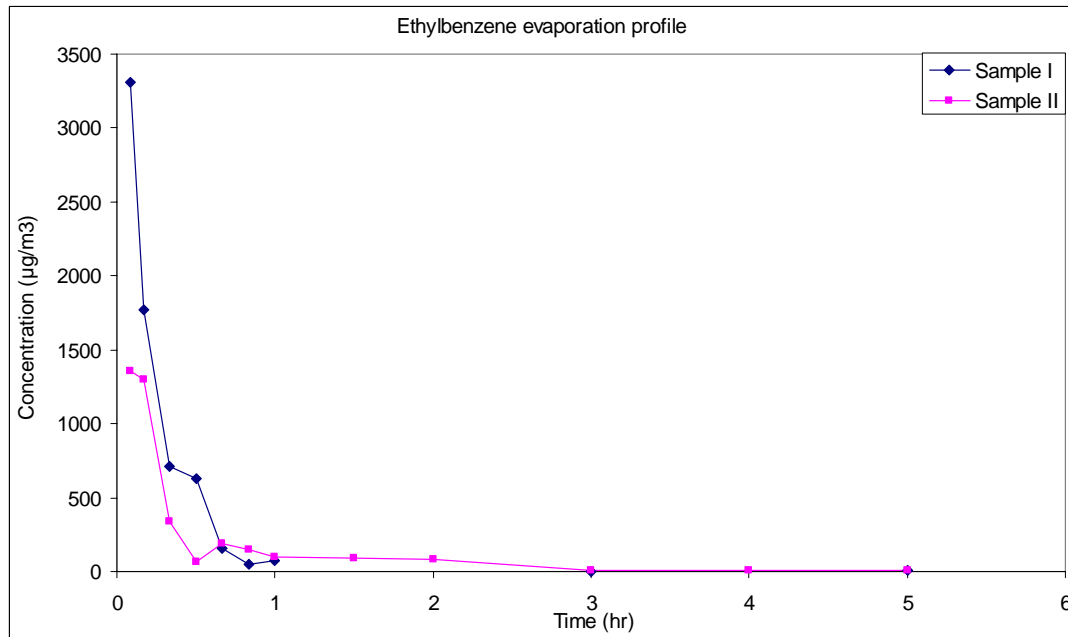


Figure 51. Concentration-time courses of ethylbenzene in the vapor phase during evaporation of JP-8 samples I and II at 20 °C. The discontinuities in the measurements are due to the detection limit of the analytical configuration of *ca* 10 µg/m³.

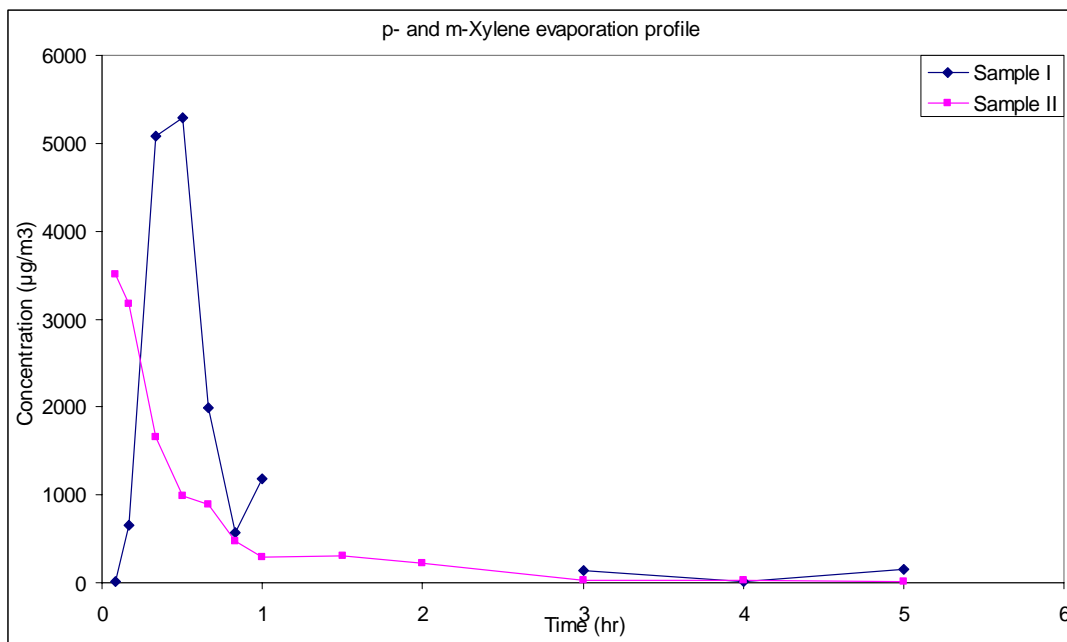


Figure 52. The summed concentration-time courses of p- and m-Xylene in the vapor phase during evaporation of JP-8 samples I and II at 20 °C. The discontinuities in the measurements are due to the detection limit of the analytical configuration of *ca* 8 μg/m³.

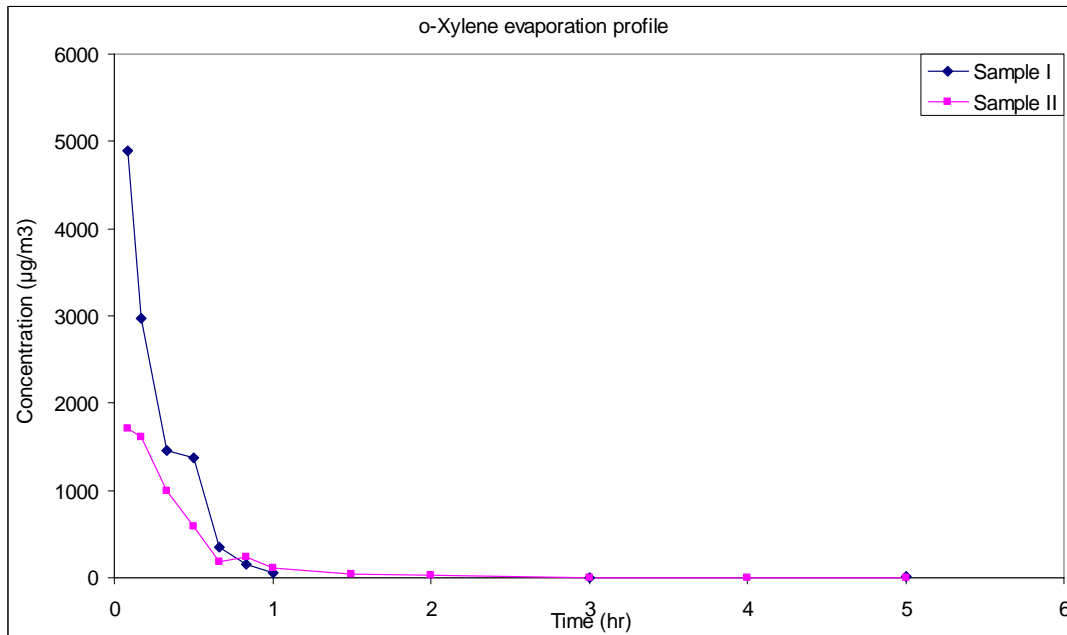


Figure 53. Concentration-time courses of o-xylene in the vapor phase during evaporation of JP-8 samples I and II at 20 °C. The detection limit for this compound is *ca* 18 μg/m³.

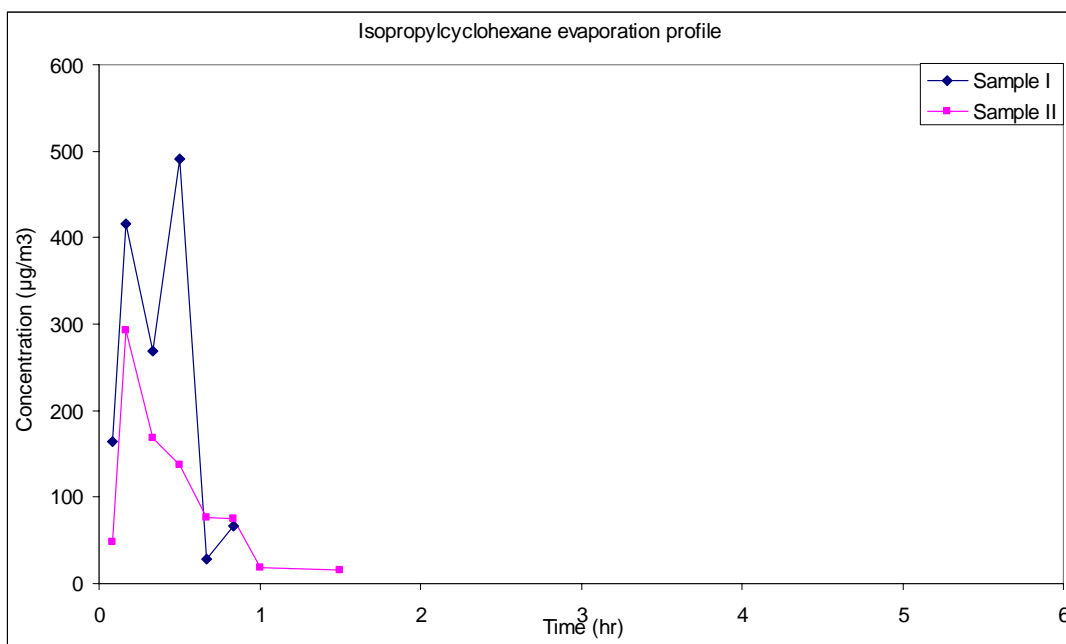


Figure 54. Concentration-time courses of isopropylcyclohexane in the vapor phase during evaporation of JP-8 samples I and II at 20 °C. The detection limit for this compound is *ca* 3 µg/m³.

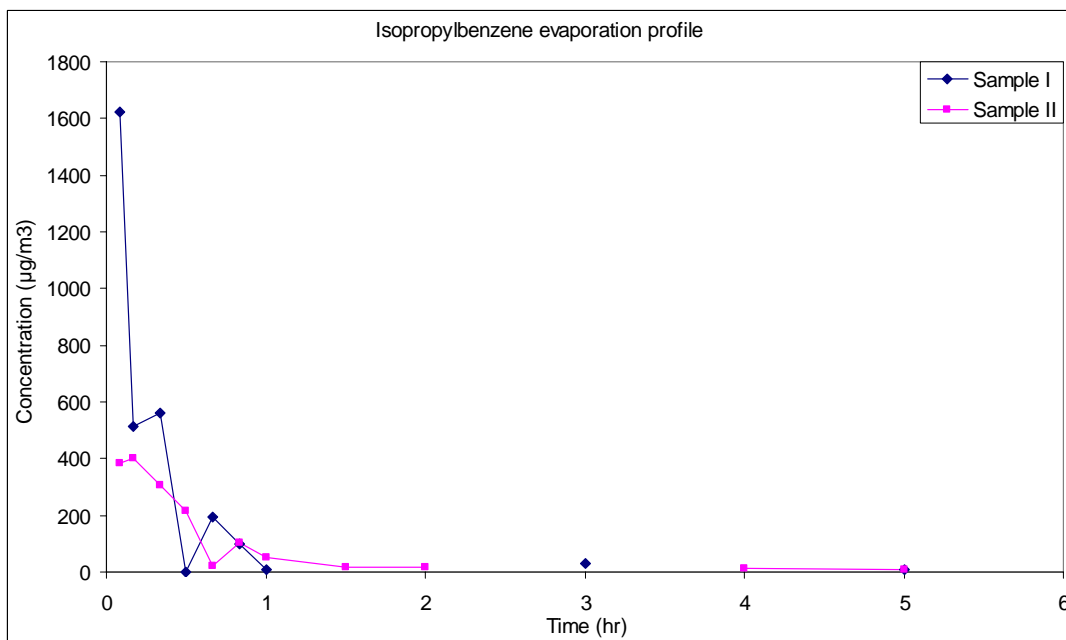


Figure 55. Concentration-time courses of isopropylbenzene in the vapor phase during evaporation of JP-8 samples I and II at 20 °C. The discontinuities in the measurements are due to the detection limit of the analytical configuration of *ca* 3.4 µg/m³.

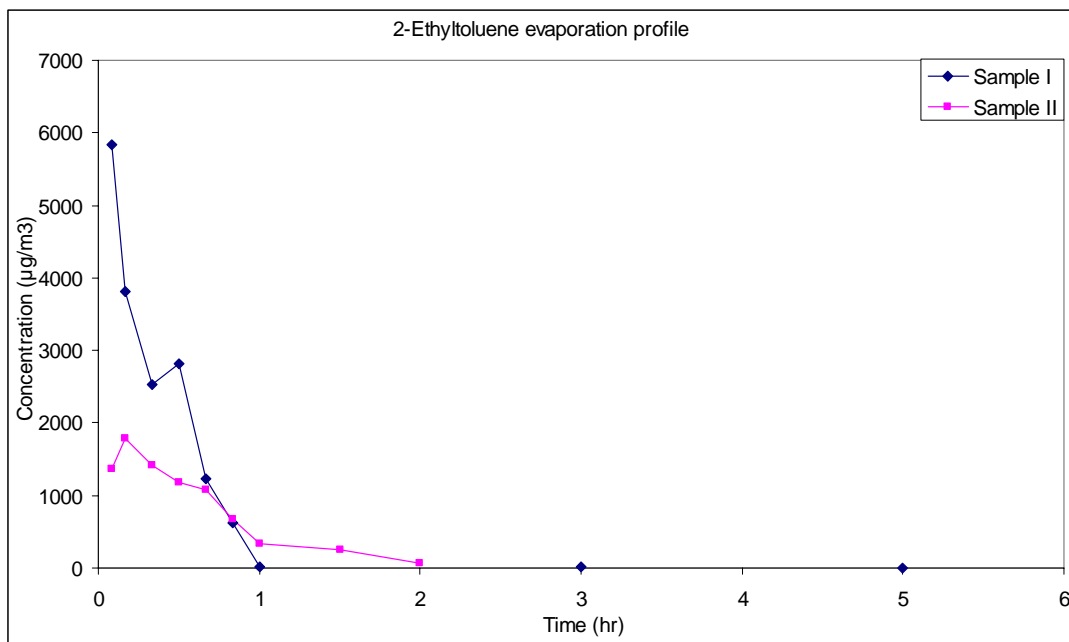


Figure 56. Concentration-time courses of 2-ethyltoluene in the vapor phase during evaporation of JP-8 samples I and II at 20 °C. The discontinuities in the measurements are due to the detection limit of the analytical configuration of *ca* 5 $\mu\text{g}/\text{m}^3$.

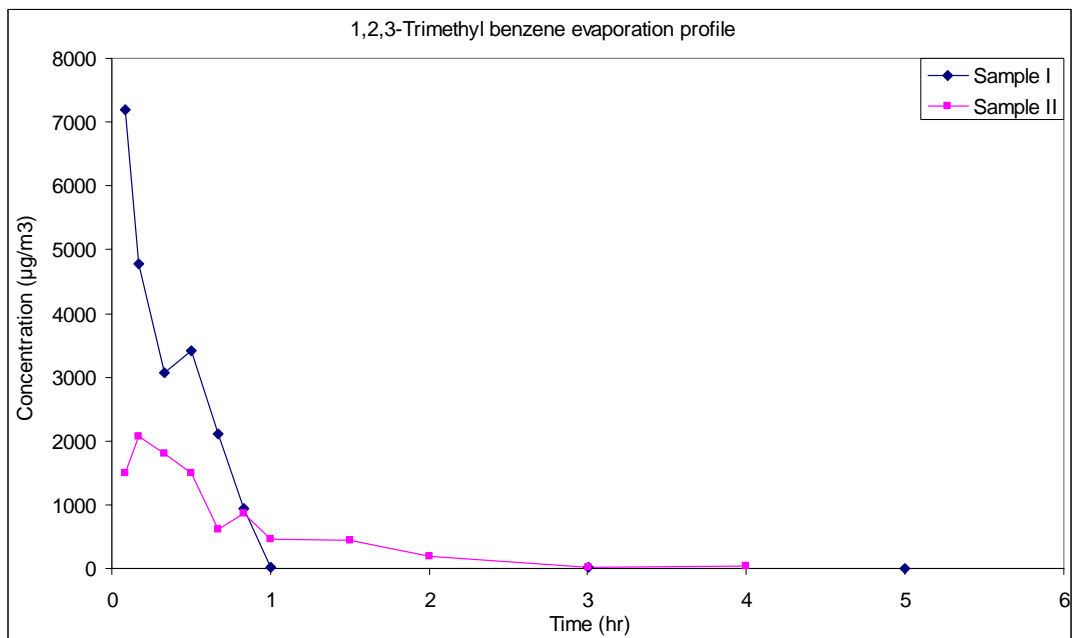


Figure 57. Concentration-time courses of 1,2,3-trimethylbenzene in the vapor phase during evaporation of JP-8 samples I and II at 20 °C. The discontinuities in the measurements are due to the detection limit of the analytical configuration of *ca* 6 $\mu\text{g}/\text{m}^3$.

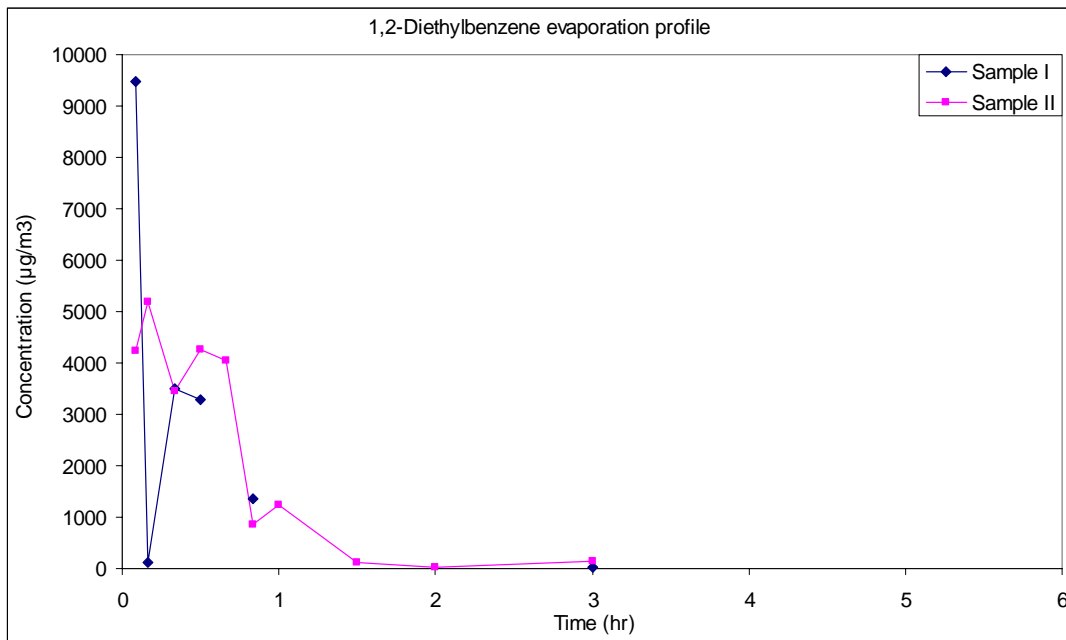


Figure 58. Concentration-time courses of 1,2-diethylbenzene in the vapor phase during evaporation of JP-8 samples I and II at 20 °C. The discontinuities in the measurements are due to the detection limit of the analytical configuration of *ca* 60 $\mu\text{g}/\text{m}^3$.

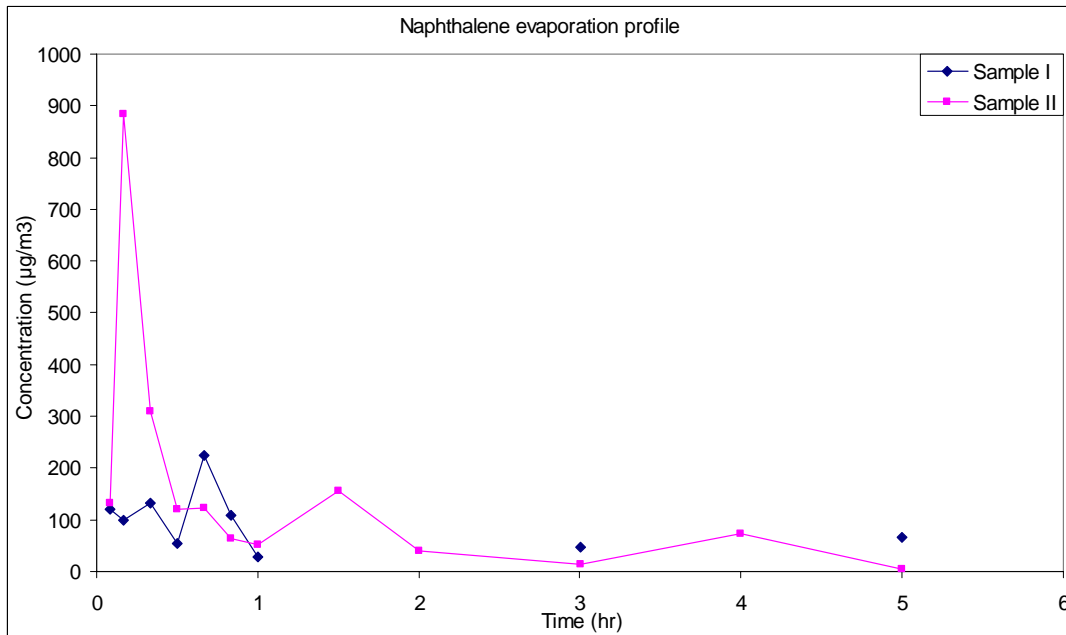


Figure 59. Concentration-time courses of naphthalene in the vapor phase during evaporation of JP-8 samples I and II at 20 °C. The discontinuities in the measurements are due to the detection limit of the analytical configuration of *ca* 110 $\mu\text{g}/\text{m}^3$.

ANNEX J ACRONYMS AND ABBREVIATIONS

Ct	Product of concentration and exposure time
FID	Flame ionization detector
GC	Gas chromatography
GCxGC	GC times GC or Comprehensive Gas chromatography
JP-8	Jet propulsion Fuel type 8
LCt50	Product of concentration and exposure time that produces 50 % mortality in a population
MEG	Military exposure guideline
MS	Mass Spectrometry
NPD	Nitrogen Phosphorus detector
PEL	Permissible exposure level
PCA	Poly Cyclic Aromatic compounds
PAH	Poly Aromatic Hydrocarbons
TLV	Threshold Limit Value
TNO	Netherlands' Organization for Applied Scientific Research
ToF-MS	Time of Flight Mass Spectrometer
USARIEM	U.S. Army Research Institute of Environmental Medicine
USAMRMC	U.S. Army Medical Research and Materiel Command